THE JOURNAL OF PHYSICAL CHEMISTRY B

Article

pubs.acs.org/JPCB

Self-Assembly in Aqueous Oppositely Charged Gemini Surfactants: A Correlation between Morphology and Solubilization Efficacy

Sneha Singh,[†] Arti Bhadoria,[†] Kushan Parikh,[‡] Sanjay Kumar Yadav,[§] Sugam Kumar,[∥] V. K. Aswal,[∥] and Sanjeev Kumar*[,†]

[†]Applied Chemistry Department, Faculty of Technology and Engineering, The Maharaja Sayajirao University of Baroda, Vadodara 390 001, India

[‡]Department of Applied Science, Faculty of Life, Health & Applied Science, ITM Vocational University, Vadodara 391 760, India

[§]Soft Material Research Laboratory, Department of Chemistry, Faculty of Science, The Maharaja Sayajirao University of Baroda, Vadodara 390 002, India

[∥]Solid State Physics Divison, Bhabha Atomic Research Centre, Trombay, Mumbai 400085, India

Supporting Information

ABSTRACT: Micellization behavior of oppositely charged gemini surfactants (anionic surfactant; phosphoric acid, *P*,*P*′-1,4-butanedieyl, *P*,*P*′-didodecylester, disodium salt (12-4-12A), and cationic surfactant; butanediyl-1,4, bis (*N*,*N*-hexadecyl ammonium) dibromide (16-4-16) or (D-isosorbate-1,4-diyl bis(*N*,*N*-dimethyl-*N*-hexadecylammonium acetoxy) dichloride (16-Isb-16)) has been studied (individually or of a gemini mixture) by conductivity and surface tension measurements. Critical micelle concentration (CMC) data show both synergistic (for 12-4-12A + 16-Isb-16) and antagonistic (for 12-4-12A + 16-4-16) interactions between the two components. Small angle neutron scattering (SANS) measurement shows formation of various aggregates, spherical (or ellipsoidal), rod-shaped, and vesicular, by changing the mole fraction (at fixed total surfactant concentration, 10 mM). Viscosity, zeta (ζ)-potential, and transmission electron microscopy (TEM) data are found in conformity of SANS results. Surprisingly, two morphologies (vesicles and rod-shaped micelles) show stability in a wide temperature range (303−343 K). The behavior has been explained on the basis of temperature induced dehydration and depletion of micellar charge. Aqueous gemini mixtures, of different morphologies, have been used for the determination of solubilization efficacy (using UV−visible spectrophotometer) toward polycyclic aromatic hydrocarbons (PAHs: anthracene; pyrene or fluorene). Molar solubilization ratio (MSR) data suggest that vesicles enhance the solubilization efficacy. SANS analysis shows that vesicle bilayer thickness increases upon PAH solubilization. The order of bilayer thickness increase is found to be anthracene > pyrene > fluorene, which is in the same order as the aqueous solubility of PAHs. This is the first report which correlates morphology to the solubilization efficacy.

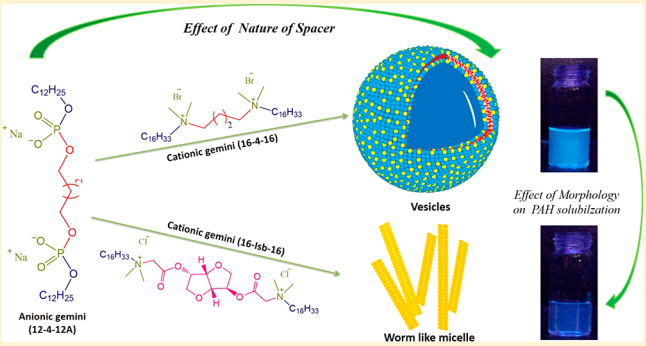

1. INTRODUCTION

In many practical applications, oppositely charged surfactant mixtures show synergistic properties (e.g., critical micelle concentration or CMC) than those attainable with the individual constituents.[1−3] Compared to conventional surfactants, gemini (or dimeric) counterparts (referred to as *m*-*s*-*m*, *m* and *s* are the number of carbon atoms in alkyl and spacer chains) show some novel solution properties.[4−7] There are many reports about the solution behavior of the mixture of gemini surfactants with their single chain analogues.[8−11] However, not many reports are available on mixtures of gemini surfactants.[1,2,12] Only in one of these studies, micellar morphology has been investigated.[2] Among gemini and single chain counterparts, the presence of a spacer is the main architectural difference and seems responsible for intriguing properties. Most of the changes with spacers are related to variation of the length of the polymethylene chain.[6,7,13−16] Few reports are also available with biocompatible spacers.[10,17−22]

Recently, cationic gemini surfactant has been regularly used as one of the components of mixed micelles to achieve the enhanced potential in solubilization, pollutant removal, or surface activity.[10,23−26] In aqueous surfactant aggregates (micelles or vesicles), solubilization of organic solutes (e.g., higher chain length alcohol or alkane) increases many fold and is responsible for a number of surfactant based applications.[27−32] It has been reported that mixing of cationic gemini (with oppositely charged single chain anionic surfactants) shows increased solubilization of polycyclic aromatic hydro-

Received: April 27, 2017
Revised: August 11, 2017
Published: August 21, 2017

DOI: 10.1021/acs.jpcb.7b03989
J. Phys. Chem. B 2017, 121, 8756−8766

Scheme 1. Schematic Representative Chemical Structures of Anionic and Cationic Gemini Surfactants with Abbreviations

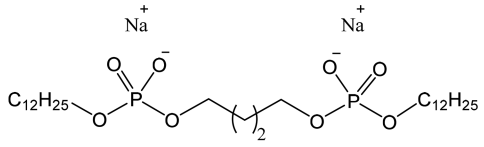

Anionic Gemini Surfactant (12-4-12A)

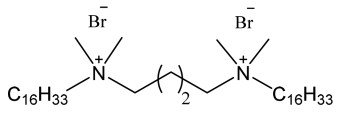

Cationic Gemini Surfactant (16-4-16)

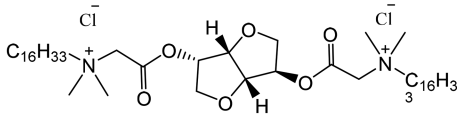

Cationic Gemini Surfactant (16-Isb-16)

carbons (PAHs).[8−11,33] Further, gemini mixtures shown better solubilization potential over constituting individual components.[34] Cationic and anionic surfactant mixtures have been reported as potential candidates for producing higher order morphologies.[3,35,36] Not a single report is available on the relation between mixed aggregate micellar morphology (spherical, rod-shaped, or vesicle) and solubilization potential.

The present study focused on oppositely charged mixed gemini surfactant systems (12-4-12A/16-4-16 and 16-Isb-16, Scheme 1) with respect to their micellization, morphologies, and solubilization efficacy (for PAHs) in aqueous medium. The investigation has been designed to determine: (i) critical micelle concentration (CMC) of single and mixed gemini; (ii) morphologies present in the system (at fixed 10 mM [gemini]) having different mole fractions ($x = 0 - 1$), (iii) comparative solubilization potential of each morphology; and (iv) size variation of mixed vesicles after solubilizing pyrene, anthracene, or fluorene. Being a first report, it is hoped to get insight about maximum exploitation of gemini mixing in construction of higher order aggregates/enhancing PAH solubility. Conductometry and tensiometry are used to determine the CMC of respective mixtures and the micellar interaction parameter (β^m). Small angle neutron scattering (SANS), viscosity, and transmission electron microscopy (TEM) are used to draw information about the morphology present in the solution. The SANS data are also supported by zeta (ζ)-potential measurements.

2. EXPERIMENTAL SECTION

2.1. Materials. Isosorbide (s = Isb) and polymethylene (s = 4) spacer based cationic and anionic gemini surfactants have been synthesized and characterized as reported earlier.[27,34] Chemical structures of gemini with abbreviations are given in Scheme 1. PAHs (anthracene, fluorene, and pyrene) were of the highest purity grade available. Freshly prepared deionized double distilled water (0.5−1.5 $\mu S \cdot cm^{-1}$) was used to prepare aqueous solutions for all of the measurements except SANS. D_2O used in the sample preparation for SANS (99.9 atom % D) was purchased from Sigma, St Louis, MO, USA.

2.2. Methods. *2.2.1. Surface Tension Measurements.* CMC values are determined from surface tension measurements using a Du-Nouy detachment tensiometer (Win − Son & Co., Kolkata) with a platinum (gold joint) ring. The tensiometer was calibrated using double distilled water. A known volume of water was added to a vessel containing stock solution (30 mL) of the single and mixed surfactant system with different mole fractions. Solutions were agitated and stirred every time carefully to avoid foaming. A set of three successive readings was recorded at each concentration (the deviation was ±0.2 mN/m).

2.2.2. Electric Conductivity Measurements. The conductivity of the oppositely charged aqueous surfactant mixture of different mole fractions was measured as a function of mixture concentration using a conductivity meter (EUTECH Cyberscan CON510, cell constant 1 cm^{-1}) with an inbuilt temperature sensor. A precalibrated cell has been used to measure the specific conductance (κ) at each concentration. A 500 μL stock solution was added in a known volume of water (thermostatted at 303 ± 0.1 K using a SCHOTT CT1650 bath). The CMC value was obtained from the intersection point of two straight lines in a plot of κ vs [gemini mixture].

2.2.3. Zeta (ζ)-Potential Measurements. Zeta (ζ)-potential measurements were performed on a SZ-100 nanoparticle size analyzer (HORIBA, Japan). This instrument is equipped with a green (5320 Å) laser and photomultiplier tube detectors. About 0.5 mL of sample solution was transferred into a dipped electrode plastic cuvette through a nylon membrane filter (0.22 μm) and placed in a sample chamber. Data are averages of five decay cycles (each decay cycle is of five runs with a 5 s interval).

2.2.4. SANS Measurements. SANS measurements were carried out using a SANS spectrometer at Dhruva Reactor, Bhabha Atomic Research Centre, Trombay, India.[37] The samples were placed in a quartz sample holder having a thickness of 2 mm, and the mole fraction/temperature was varied. The measured SANS data were corrected and normalized to an absolute scale using a standard procedure. In SANS measurements, the coherent differential scattering cross section per unit volume ($d\Sigma/d'\Omega$) as a function of scattering vector ($Q = 4\pi \sin\theta/\lambda$, where 2θ is the scattering angle and λ is the wavelength of the incoming neutrons) is measured. For a monodisperse micelle solution, it can be expressed as follows[38]

$$\frac{d\Sigma}{d\Omega} = nP(Q)S(Q) + B \quad (1)$$

where n is the number density of the micelle. $P(Q)$ is the form factor and is decided by the shape and size of the micelle. $S(Q)$ is the interparticle structure factor which depends on the intermicellar interactions. B is a constant term denoting the incoherent scattering background mainly contributed from hydrogen in the micelle. The details of data analysis and the different models used are provided in the Supporting Information.[39−43]

2.2.5. Transmission Electron Microscopy. Transmission electron microscope (TEM) images were obtained with a JEOL JEM 2100 transmission electron microscope accelerating at a

DOI: 10.1021/acs.jpcb.7b03989
J. Phys. Chem. B 2017, 121, 8756−8766

working voltage of 120 kV. A drop of mixed gemini solution was placed on the carbon-coated copper grid (200 mesh) followed by drying for a few minutes (~298 K). Then, a drop of fresh uranyl acetate solution was put on the sample. The grid was again dried at the same temperature.

2.2.6. Viscosity Measurements. The viscosity measurements were carried out using an Ubbelohde suspended level capillary viscometer thermostatted at 303 ± 0.1 K. The viscometer was cleaned and dried before each measurement. The details are reported elsewhere.[44]

2.2.7. Solubilization Experiment. The solubility of PAH has been determined in aqueous surfactant systems (single or mixed), at different mole fractions (x = 0−1, total [gemini] = 10 mM), by adding an excess amount of PAH (fluorene, anthracene, or pyrene, physical data are provided in Table S1, see the Supporting Information). Aqueous surfactant(s) + PAH mixture has been equilibrated for 48 h before centrifugation to remove excess PAH. The solubilization of PAH in micellar solutions of different morphologies (ellipsoidal or rod-shaped or vesicles) has been analyzed, at respective λ_{max}, by UV−visible spectrophotometer (Shimadzu, UV-2450, UV−visible spectrophotometer) having a quartz cell (path length 1 cm) at 303 K. The composition of the surfactant mixture was the same in both the reference and measurement cell to eliminate its effect on the UV absorbance. Concentrations of PAH are calculated by the Lambert−Beer law (using respective molar extinction coefficient (ε) values of each PAH).[45,46]

3. RESULTS AND DISCUSSION

3.1. Micellization of Pure and Mixed Gemini Surfactants. CMCs of individual gemini surfactants have been determined by the variation of surface tension (γ) or conductivity with concentration (only plots related to γ variation are shown in Figure 1). The absence of minima in

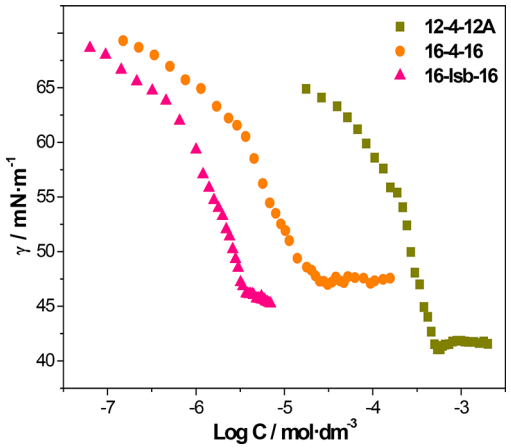

Figure 1. Plot of surface tension (γ) vs log C (logarithm of concentration) of pure gemini surfactants in aqueous solution at 303 K.

Figure 1 ensures the purity of the synthesized material. Figure 2 shows the variation of γ (Figure 2a) and κ (Figure 2b) with [mixed gemini] for 16-4-16 + 12-4-12A combinations (data related to 16-Isb-16 + 12-4-12A are shown in Figure S1; see the Supporting Information). CMC data are given in Table 1.

CMC variations with the mole fraction of added 12-4-12A, to cationic gemini surfactant (16-4-16 or 16-Isb-16), has been shown in Figure 3. A pseudo phase separation model has been applied to know how the binary gemini mixtures deviate from the ideal mixing.[47] The CMC values of mixed gemini (cmc_{exp}) were found to be lower than the CMC of 12-4-12A (cmc_1) and higher than that of 16-4-16 or 16-Isb-16 (cmc_2). For a mixture of oppositely charged surfactants, a simple relationship exists for ideal mixing[48]

$$\frac{1}{cmc_i} = \frac{x_1}{cmc_1} + \frac{x_2}{cmc_2} \quad (2)$$

where x_1 and x_2 are mole fractions of two components of the mixture. Equation 2 can be used to determine the ideal cmc (cmc_i) for ideal mixing of oppositely charged gemini. The negative or positive variations of cmc_{exp} from cmc_i indicate synergistic or antagonistic interaction in various mixtures, respectively (Table 1). On the basis of the regular solution theory, the following expression has been proposed[49]

$$\frac{[(X_1^m)^2 \ln(cmc_{exp}x_1/cmc_1X_1^m)]}{(1 - X_1^m)^2[cmc_{exp}(1 - x_1)/cmc_2(1 - X_1^m)]} = 1 \quad (3)$$

where X_1^m is the mole fraction of 12-4-12A in the mixed micelle. This value could not be determined with most of the 12-4-12A + 16-4-16 systems due to the absence of convergence of the data in the Mathematica computer program. The ideal micelle mole fraction of 12-4-12A (X_1^i) can be obtained by Motomura's approximation.[50]

$$X_1^i = \frac{x_1 cmc_2}{x_1 cmc_2 + (1 - x_1)cmc_1} \quad (4)$$

Generally, the interaction parameter (β^m) is used to characterize the nature and strength of the interactions between different surfactants using the following equation[51]

$$\beta^m = [\ln(cmc_e p_1/cmc_1X_1^m)]/(1 - X_1^m)^2 \quad (5)$$

The $+\beta^m$ value represents an antagonistic interaction between two gemini. Here, cmc_{exp} is found to be lower/higher than the cmc_i. $-\beta^m$ (synergistic effect) is the result of the packing of the individual gemini monomers in the mixed micelle and resultant cmc_{exp}. The values of cmc_{exp}, cmc_i, cmc_1, cmc_2, X_1^m, X_1^i, and β^m are compiled in Table 1. Both synergistic and antagonistic effects have been reported in recent time.[1,34]

3.2. Morphological Transitions. Oppositely charged mixed gemini can produce strong electrostatic attraction in addition to that of hydrophobic interactions among the alkyl tails. This results in the increase of hydrophobic tail volume and decrease in headgroup area.[52] The packing parameter, P ($=v/A_0l$, with v being the volume of the hydrocarbon part of the surfactant(s) molecule(s) and l and A_0 are length and effective surface area per surfactant(s) molecule(s), respectively), is related to the micellar morphology formed in the solution.[53] The presence of oppositely charged surfactants has a strong chance to get incorporated in the mixed micelle together with overcoming of electrostatic repulsion. The latter effect is responsible for the decrease in A_0, and hence, P increases. An increase in P can also be understood by considering two oppositely charged gemini components as a *single surfactant* of higher v value. In assuming a single surfactant, it should be clear that the length of such a surfactant molecule will be equivalent to the length of the individual monomer with higher carbon number (16-4-16 or 16-Isb-16) and will not be affected by the component of lower carbon number (12-4-12A). The increase in v and decrease in A_0 are responsible for the increase in P.

DOI: 10.1021/acs.jpcb.7b03989
J. Phys. Chem. B 2017, 121, 8756−8766

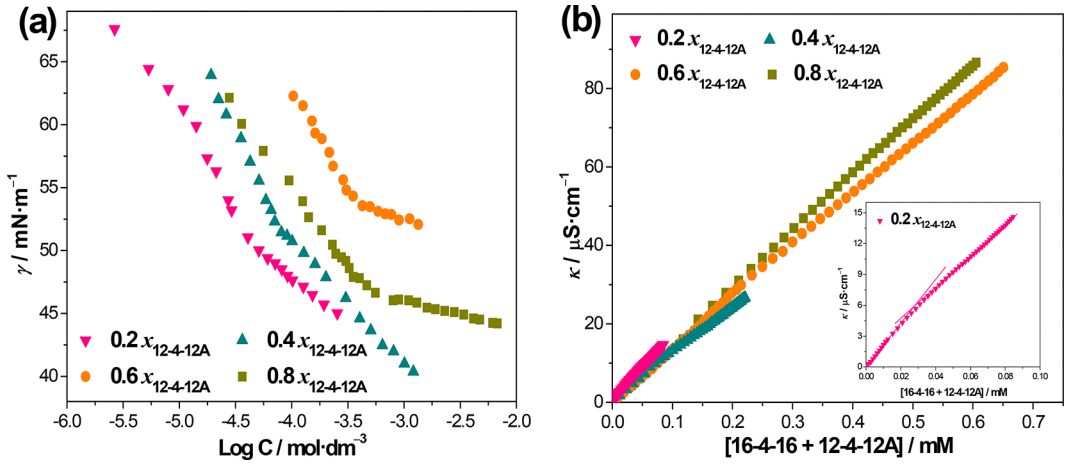

Figure 2. (a) Representative plot of surface tension (γ) vs log C (logarithm of concentration) and (b) plot of specific conductance (κ) vs [surfactants] of mixed gemini surfactants (16-4-16 + 12-4-12A) at different mole fractions of anionic gemini ($x_{12\text{-}4\text{-}12A}$) in aqueous solution at 303 K.

Table 1. Micellization Parameters (Critical Micelle Concentration, CMC) and Interaction Parameters (by Using Rubingh's Method) of Single (Pure) and Mixed (Binary) Gemini Surfactant Systems in Aqueous Solution at 303 K

	CMC_{exp} (mM)					
$x_{12\text{-}4\text{-}12A}$	conductometry	tensiometry	CMC_{ideal} (mM)	X_1^m	X_{ideal}	β^m
			16-4-16			
0.0	0.0244	0.0231				
0.2	0.0292	0.0372	0.0306	0.4400	0.0109	−11.87
0.4	0.0734	0.0758	0.0395			
0.6	0.2822	0.3691	0.0570			
0.8	0.4159	0.4508	0.1036			
1.0	0.5310	0.4790				
			16-Isb-16			
0.0	0.0027	0.0030				
0.2	0.0031	0.0034	0.0034	0.3383	0.0014	−12.96
0.4	0.0037	0.0039	0.0045	0.2460	0.0034	−7.899
0.6	0.0046	0.0055	0.0067	0.2599	0.007	−8.048
0.8	0.0099	0.0104	0.0132	0.3345	0.019	−9.798
1.0	0.5310	0.4790				

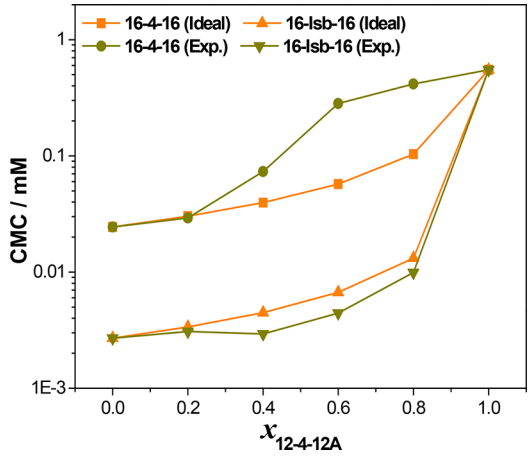

Figure 3. CMC (by conductometry) variation mixed surfactant systems (cationic−anionic) with mole fraction of anionic gemini surfactant ($x_{12\text{-}4\text{-}12A}$) in aqueous solution at 303 K. The plot represents experimental and ideal values (calculated from ideal mixing model).

Critical conditions for the formation of spherical, rod-shaped, vesicles, or inverted structures are $P \leq 1/3$, $1/3 \leq P \leq 1/2$, $1/2 \leq P \leq 1$, $P \geq 1$, respectively. Surfactants (or surfactant mixture or so-called *single surfactant*) with smaller headgroup areas and larger hydrophobic volume tend to form grown or higher order aggregates. Structural transitions into higher order aggregates have been explained on the basis of increasing P.[54] Mixing oppositely charged surfactant is an easier approach to construct a surfactant self-assembly of desired morphology.[2,3]

Figure 4 shows the variation of relative viscosity (η_r) with the mole fraction of 12-4-12A in the mixture (with 16-4-16 or 16-Isb-16). It is observed that η_r is a function of the mole fraction of 12-4-12A and is found to vary by a few orders of magnitude. On the basis of η_r variation, three different regions (I−III) can be identified. These viscosity regions indicate about morphological transitions taking place by varying the mole fractions of two components of the mixture (at fixed 10 mM [gemini(s)]). The mixing of the two gemini can cause reduction in the electrostatic repulsion between the charged head groups, in addition to increased hydrophobic interactions, facilitates micellar structural transition (may be micellar growth). Initially present spherical aggregates (or ellipsoidal) are expected to grow upon adding 12-4-12A which subsequently convert to other morphologies, as reflected in η_r variation. It has been reported that the viscosity due to a short rod-shape micelle, with an axial ratio of 4, is not different from that due to spherical micelles in the solution.[55] Therefore, η_r cannot be

DOI: 10.1021/acs.jpcb.7b03989
J. Phys. Chem. B 2017, 121, 8756−8766

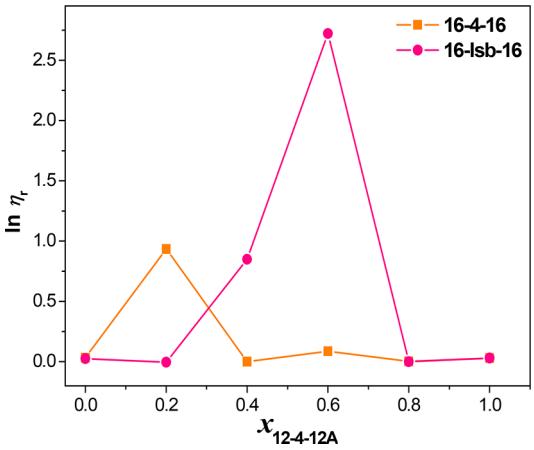

Figure 4. Relative viscosity (ln η_r) data of 10 mM mixed gemini surfactant system at different mole fractions of anionic gemini surfactant ($x_{12\text{-}4\text{-}12A}$) in aqueous solution at 303 K.

used to predict the morphologies in each region and only qualitatively distinguishes various transitions occurring in the solution (regions I–III) whose probability has already been mentioned on the basis of P (*vide supra*). The idea of electrostatic interaction variation can be conceived from zeta (ζ)-potential variation with the mole fraction of 12-4-12A (Figure 5). The change of sign of ζ from positive to negative via

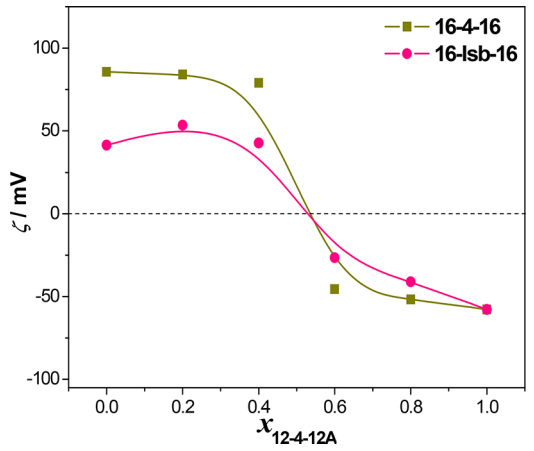

Figure 5. Zeta (ζ)-potential data of 10 mM mixed gemini surfactant aqueous system at different mole fractions of anionic gemini surfactant ($x_{12\text{-}4\text{-}12A}$) in aqueous solution at 303 K.

zero indicates that micellar surface charge is dependent on the mole fraction of each component and decides micellar surface charge which can be related to the variation of P and hence to the micellar morphology as mentioned above (*vide supra*).

Studies on the morphology of surfactant aggregates by SANS coupled with the physicochemical method highlight important links between structure and bulk physical properties.[44,56−60] Figure 6 shows SANS spectra ($d\Sigma/d\Omega$ vs Q) for 10 mM individual gemini surfactants. The data show interaction peaks correspond to charged micelle. The analyzed SANS data for pure surfactants are given in Table 2 which indicate ellipsoidal/rod-shaped micelles in the solution. The value of a has been found more for 16-4-16 than 16-Isb-16. This may be due to the polar nature of the isosorbide species which is reflected in the higher value of effective charge per monomer (α). The fitted parameters can be used to find the number density of the

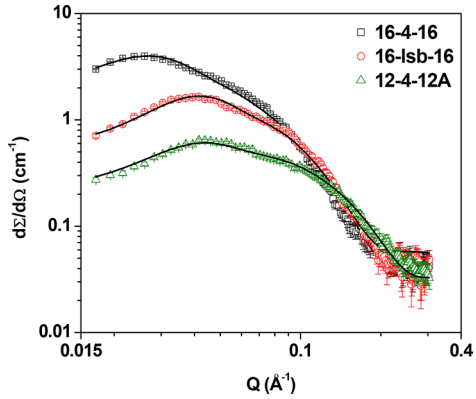

Figure 6. Representative SANS spectra of 10 mM pure gemini surfactant system in aqueous solution at 303 K.

Table 2. SANS Fitted Micellar Parameters of 10 mM Aqueous Mixed Gemini Surfactant Systems at 303 K

$x_{12\text{-}4\text{-}12A}$	semimajor axis a (Å)	semiminor axis b (Å)	fractional charge (α)	polydispersity
		16-4-16		
0.0	95.8	20.4	0.1	0.18
0.2	111.8	20.3		0.18
0.4		Vesicles with a Bilayer Thickness of 25 Å		
0.6	141.2	21.7		0.18
0.8	44.5	19.0	0.18	0.18
1.0	29.5	14.1	0.65	0.18
		16-Isb-16		
0.0	37.2	20.0	0.43	0.18
0.2	45.8	20.8	0.16	0.18
0.4	104.0	20.0		0.18
0.6	101.2	20.0		0.18
0.8	32.3	18.6	0.6	0.18
1.0	29.5	14.1	0.65	0.18

micelles and hence the average intermicellar distance (D). This can be used to back calculate the position of the expected correlation peak using equation S6 (see the Supporting Information) and is found in fairly good agreement with that of the observed one (e.g., Figure 6).

The SANS data for mixed gemini are shown in Figure 7. With the addition of oppositely charged gemini surfactant (keeping total [gemini(s)] constant, 10 mM), the interaction peak corresponding to the charged micelle starts disappearing with no plateau in the comparable mole fractions of the two components (0.4 and 0.6 or 0.6 and 0.4). At some specific mole fractions (e.g., 0.6/0.4) of two oppositely charged surfactants (e.g., 16-4/Isb-16 and 12-4-12A), the formation of large aggregates (rod-like micelles or vesicles) leads to a reduction in number density and hence an increase in intermicellar distances. These systems, therefore, behave as dilute, and no correlation peak appears in the Q range of the measurements. Also at the approximate by equimolar concentrations, there may be a near charge balance of oppositely charged surfactants making the system relatively less ionic. This restricts the determination of any $S(Q)$ parameters for these concentrations.

The data with mole fraction 0.5 could not be acquired due to the instability of both systems. A perusal of SANS spectra (Figure 7) shows an interaction peak, appearance of a plateau, disappearance of the plateau, reappearance of the plateau, and finally reappearance of the interaction peak. This behavior may

DOI: 10.1021/acs.jpcb.7b03989
J. Phys. Chem. B 2017, 121, 8756−8766

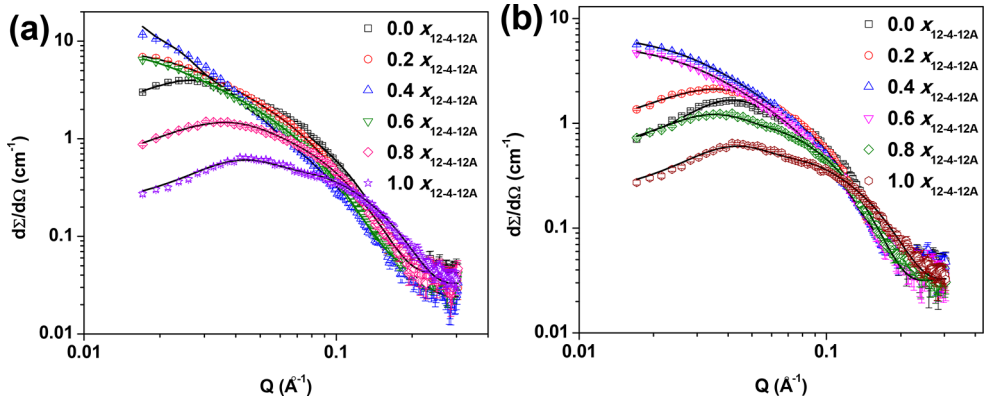

Figure 7. SANS spectra of 10 mM mixed aqueous gemini surfactant systems at different mole fractions of anionic gemini surfactant ($x_{12\text{-}4\text{-}12A}$) at 303 K: (a) 16-4-16; (b) 16-Isb-16.

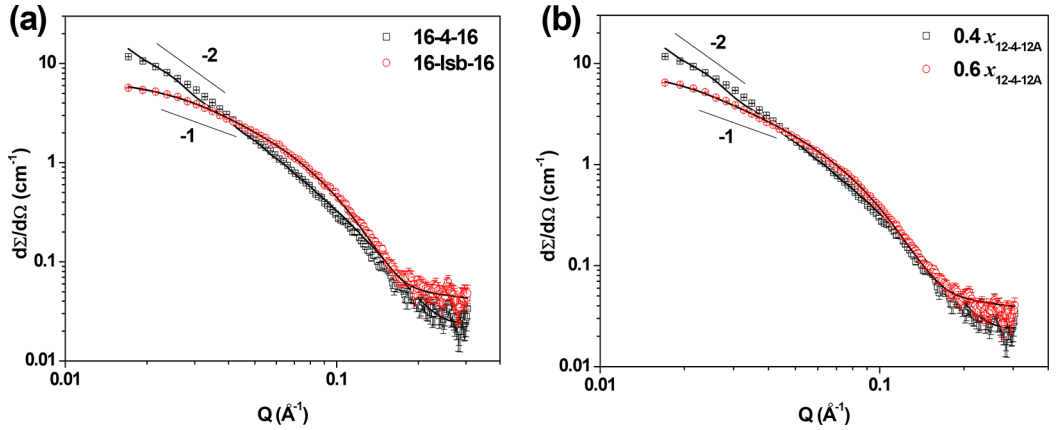

Figure 8. (a) SANS spectra of 10 mM aqueous mixed gemini surfactant system at $0.4x_{12\text{-}4\text{-}12A}$; (b) SANS spectra of 10 mM aqueous mixed gemini surfactant system (16-4-16 + 12-4-12A) at two different mole fractions of anionic gemini ($x_{12\text{-}4\text{-}12A}$).

be due to variation in α (governed by electrostatic interactions or A_0) and possible morphological transitions (driven by variation of P). The analyzed SANS data (Table 2) for 16-4-16 + 12-4-12A show the transition of rod-shaped micelle to vesicle upon increasing the mole fraction of 12-4-12 A in the mixture keeping the total surfactant concentration constant (10 mM). It may be mentioned here that bilayers are formed for only one composition (12-4-12A (x = 0.4) + 16-4-16 (x = 0.6)). The bilayers are again converted to rod-shaped micelles and then to ellipsoidal ones with the further increase of the content of 12-4-12A in the mixture. Similar transitions were observed with the mixture containing 16-Isb-16 with the deference that no vesicle formation has been found in the system (rod-shape only). For equal composition of the above two mixtures (12-4-12A (x = 0.4) + 16-4-16 or 16-Isb-16 (x = 0.6)), the formation of two different morphologies (bilayer vesicle or rod-shaped micelle) may be due to different α values and neutralization of charge by the addition of 12-4-12A (Figure 7). The polarity of the spacer has a role in the formation and shape of the final aggregate in the solution. Figure 8 (log−log plot) shows that the data follow a slope of −2 or −1 at low Q, indicative of scattering from vesicle or rod-shape micelle, respectively.[60] The vesicle bilayer thickness can be determined from the SANS data using a cross-sectional Guinier plot, and the value has been found to be 25 Å. This value is reasonably in agreement with the bilayer thickness reported for other surfactant systems.[60,61] The presence of vesicles in the $0.4x_{12\text{-}4\text{-}12A}$ + $0.6x_{16\text{-}4\text{-}16}$ system has also been confirmed by the TEM result (Figure 9). TEM observations have also been used to support DLS data regarding the formation of vesicles in the solution.[62]

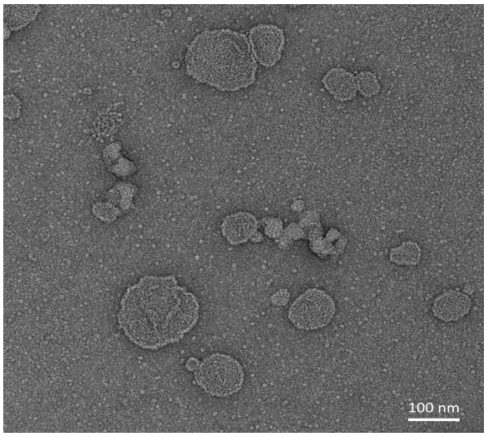

Figure 9. TEM image of 10 mM aqueous solution of $0.6x_{16\text{-}4\text{-}16}$ + $0.4x_{12\text{-}4\text{-}12A}$. The scale bar represents 100 nm.

3.3. Temperature Induced Micellar Morphologies.

SANS data has also been acquired for two mixtures (Figure 10), of equal mole fractions, formed by 12-4-12A (x = 0.4) with 16-4-16 or 16-Isb-16 at different temperatures (303−343 K). The starting morphologies were vesicles and rod-shaped micelles, respectively. The increase of temperature shows an

DOI: 10.1021/acs.jpcb.7b03989
J. Phys. Chem. B 2017, 121, 8756−8766

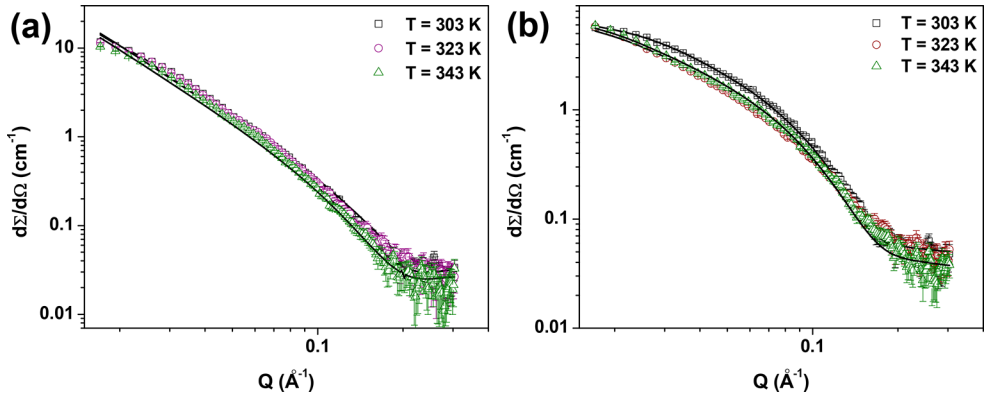

Figure 10. SANS spectra of 10 mM mixed gemini surfactant system (at $0.4x_{12\text{-}4\text{-}12A}$) at different temperatures (T, 303−343 K): (a) 16-4-16; (b) 16-Isb-16.

insignificant change in the bilayer thickness (Table 3). However, temperature induced micellar growth has been observed with the 12-4-12A + 16-Isb-16 system. In earlier studies, a vesicle to wormlike micelle transition has been reported for surfactant systems with increasing temperature or shear.[60,63,64] The transition has been explained on the basis of desorption of oppositely charged methyl salicylate ion from the cationic micellar surface on heating. The difference in the present systems, and the ones from earlier studies,[60,63,64] is the second component (12-4-12A) which forms mixed micelles instead of methyl salicylate adsorbed micelles (leading to methyl salicylate ion desorption on heating). The above desorption causes an increase in A_0 and reduction in P (derives vesicle to rod-shape micelle transition). A similar transition has also been observed with a cationic surfactant−alkanol system.[65,66] However, no such transition has been observed with the present system due to the fact that hydrophobic interaction is playing a major role in forming mixed vesicles which restrict desorption of 12-4-12A or 16-4-16 on heating. Further, heating may cause temperature driven dehydration of interacting head groups which may be responsible for increased electrostatic attraction with a concomitant decrease in A_0. The above interrelated factors are responsible for the increase in bilayer thickness (Table 3). A similar type of reasoning can be invoked for the 12-4-12A + 16-Isb-16 system where heating induces (rod-shaped) micellar growth. Recently, temperature induced micellar growth has also been reported in an aqueous mixture of cationic gemini with an anionic surfactant.[67] This observation of stability of higher order aggregates (vesicles/rod shaped micelles) on heating has been reported here for the first time in a mixed oppositely charged gemini surfactant system. Therefore, vesicles of different thermal stability can be produced at will by judicious selection of the second component in a two-component surfactant mixture. This morphological information has been used to explain PAH solubilization efficacy in different kinds of surfactant morphology formed in mixed systems.

Table 3. SANS Fitted Micellar Parameters of 10 mM Aqueous Mixed Gemini Surfactant (12-4-12A + 16-4-16 and 12-4-12A + 16-Isb-16) Systems at Different Temperatures (T)

	$0.6x_{16\text{-}4\text{-}16}$	$0.6x_{16\text{-}Isb\text{-}16}$	
T (K)	bilayer thickness (Å)	semimajor axis a (Å)	semiminor axis b (Å)
303	25.0	104.0	20.0
323	26.2	132.2	20.0
343	25.8	135.7	20.0

3.4. Solubilization in Single/Mixed Gemini. Typical plots of absorbance vs wavelength for anthracene solubilization in mixed aqueous gemini (12-4-12A + 16-4-16) at different mole fractions (x = 0−1) are shown in Figure 11 (similar plots were obtained with other PAHs but not shown). The absorbance changes are random due to the presence of different morphologies (*vide supra*) in the solution. The molar solubilization ratio (MSR) is the number of moles of the PAH solubilized per mole of the gemini(s) present in the solution.[13] MSR can be calculated by using the following equation

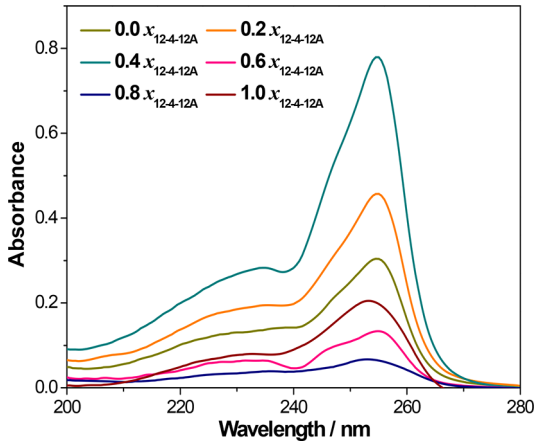

Figure 11. Representative UV−visible spectra of anthracene in 10 mM aqueous pure and mixed gemini surfactant (16-4-16 + 12-4-12A) solutions, at different mole fractions of anionic gemini ($x_{12\text{-}4\text{-}12A}$).

$$\mathrm{MSR} = \frac{(S_t - S_{cmc})}{(C_t - C_{cmc})} \tag{6}$$

where S_t is the total PAH solubility in the mixture solution at a particular total surfactant concentration C_t. S_{cmc} is the solubility of the PAH at the cmc of the mixture (C_{cmc}). The MSR data with single and binary mixtures are compiled in Table 4. Comparing MSR data obtained for single and oppositely charged mixed gemini systems, higher MSR values have been found with the latter. Higher MSR values have also been found with 16-4-16 + 12-4-12A when compared with the data obtained in an earlier study.[34] This difference may be due to the

DOI: 10.1021/acs.jpcb.7b03989
J. Phys. Chem. B 2017, 121, 8756−8766

Table 4. Solubilization Parameters (Molar Solubilization Ratio, MSR; Micelle−Aqueous Phase Partition Coefficient, ln K_m; Gibbs Free Energy, ΔG_s°) of 10 mM Single and Mixed Gemini Surfactants in Aqueous Solution at 303 K

		anthracene			pyrene			fluorene		
$x_{12\text{-}4\text{-}12A}$	morphology	MSR	ln K_m	$-\Delta G_s$ (kJ mol^{-1})	MSR	ln K_m	$-\Delta G_s$ (kJ mol^{-1})	MSR	ln K_m	$-\Delta G$ (kJ mol^{-1})
					16-4-16					
1.0	ellipsoidal	0.0261	8.861	22.33	0.0381	10.15	25.58	0.0910	10.36	26.09
0.8	rod	0.0282	8.936	22.52	0.0576	15.07	37.98	0.0711	9.82	24.74
0.6	rod	0.0276	8.913	22.46	0.0857	21.84	55.05	0.1078	10.20	25.71
0.4	vesicle	0.0321	9.060	22.83	0.1706	40.32	101.62	0.2544	10.94	27.56
0.2	rod	0.0261	8.844	22.29	0.1426	34.53	87.03	0.1486	10.49	26.42
0.0	rod	0.0257	8.84	22.29	0.1091	27.22	68.60	0.1587	10.54	26.57
					16-Isb-16					
1.0	ellipsoidal	0.0261	8.861	22.33	0.0381	10.15	25.58	0.0910	10.36	26.09
0.8	ellipsoidal	0.0132	8.182	20.62	0.064	16.64	41.94	0.1889	10.69	26.91
0.6	rod	0.0276	8.913	22.46	0.0653	16.96	42.75	0.1947	10.72	27.01
0.4	rod	0.0260	8.855	22.32	0.0840	21.44	54.04	0.1683	10.59	26.69
0.2	ellipsoidal	0.0265	8.874	22.37	0.0596	15.56	39.22	0.1125	10.24	25.80
0.0	ellipsoidal	0.0136	8.212	20.69	0.0756	19.45	49.02	0.1281	10.35	26.09

fact that an earlier study has been performed at concentrations near the CMC where, preferentially, spherical micelles were present. However, different morphologies are present (rod-shaped or vesicles) in the present case (well above the CMC (Tables 1 and 4)) and may be responsible for the differences in the MSR values. Due to the formation of large micelles (in the present mixtures), the available hydrophobic volume will be more than the micelle with single gemini surfactant. This higher hydrophobic volume will be responsible for the effective solubilization of PAH and higher MSR values. Among the gemini mixtures, the vesicle forming system (16-4-16, x = 0.6) has been found more effective than the one having other morphology. The MSR values for different morphologies (formed by mixed surfactant systems) follow the order vesicles > rod-shape micelles > ellipsoidal micelles > spherical micelles. The micelle water partition coefficient (K_m) represents the solubilization by micellar phase which can be used to determine the standard free energy change of solubilization (ΔG_s).[34] The negative value of ΔG_s (Table 4) shows that spontaneous solubilization of PAHs takes place in the mixed gemini system. Solubilization efficacy depends on the polarity and hydrophobic volume of the PAH and contributes toward the MSR value. The data show a synergistic effect of mixing of two oppositely charged gemini surfactants, at an appropriate composition, which can result in higher order aggregates (e.g., vesicles, Figure 9). Table 5 shows the comparative MSR data for PAH solubilization observed by different workers in oppositely charged surfactant systems. MSR data depicts that mixing of two surfactants, generally, enhances the solubility of PAH more than for individual ones: This trend followed even in the present study. Being a very less soluble PAH, anthracene showed the highest MSR with the vesicular system formed by $0.6x_{16\text{-}4\text{-}16}$ + $0.4x_{12\text{-}4\text{-}12A}$ compared to the ones reported in the literature[10,68−70] (Table 5). Among the PAHs, MSR follows the order fluorene > pyrene> anthracene. It may be mentioned here that the MSR for each PAH has been found highest with the system containing vesicles.

Table 5. MSR Data Reported in Various Studies for the Solubilization of PAH in Aqueous Solution at 303 K

	MSR		
system[a]	anthracene	pyrene	ref
16-E2-16 + SDS	0.0248	0.0576	10
16-E2-16 + SDBS	0.0243	0.0745	10
16-6-16 + AOT	0.0103	0.0526	69
12-E2-12 + SDS	0.0061	0.0137	70
16-4-16 (0.7) + 12-4-12A (0.3)	0.0148	0.1023	34
16-Eda-16 (0.6) + 12-4-12A (0.4)	0.0147	0.0813	34
16-4-16 (0.6) + 12-4-12A (0.4)	0.0321	0.1706	present study
16-Isb-16 (0.4) + 12-4-12A (0.6)	0.0276	0.0653	present study

[a]Mixed oppositely charged surfactant systems with x = 0.5 each (if different then mentioned in parentheses).

3.5. Vesicle Size Variation after PAH Solubilization. As mentioned above, the vesicular system formed by $0.6x_{16\text{-}4\text{-}16}$ + $0.4x_{12\text{-}4\text{-}12A}$ shows a higher solubilization efficacy with each PAH. SANS data (Figure 12) are collected in order to get an idea about the vesicle thickness variation on solubilizing PAH. Surprisingly, vesicle morphology remained similar even after PAH solubilization with a difference of bilayer thickness (Table 6). Being a hydrophobic material, PAHs are expected to partition near the central part of the bilayer. As mentioned earlier, being less soluble in water (Table S1), anthracene could be solubilized preferentially, in the central part of the bilayer rather than the region near the head groups. However, the reverse may be the case with fluorene. If this is true, bilayer

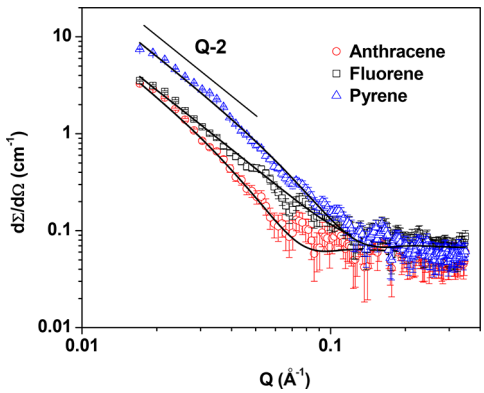

Figure 12. SANS spectra of 10 mM aqueous vesicular (mixed gemini surfactant (16-4-16 + 12-4-12A)) system at $0.4x_{12\text{-}4\text{-}12A}$ after solubilizing of the PAHs.

DOI: 10.1021/acs.jpcb.7b03989
J. Phys. Chem. B 2017, 121, 8756−8766

Table 6. Bilayer Thickness Data of Vesicles (10 mM, 16-4-16 + 12-4-12A Gemini, System) with and without Solubilization of PAH in Aqueous Solution at 303 K

$0.6x_{16\text{-}4\text{-}16}$	bilayer thickness (Å)
without PAH	25.0
fluorene	32.5
pyrene	38.7
anthracene	55.4

thickness should increase more in the case of anthracene than fluorene (or pyrene). This indeed was observed from our SANS results (Table 6). A working scheme has been proposed to show the solubilization of PAHs in a typical vesicle which is formed by the mixing of two oppositely charged gemini surfactants (Scheme 2). In order to exploit the full potential of the above systems, more work is needed to understand the morphological transitions after self-assembly solubilization of various hydrophobic molecules such as PAH, dyes, drugs, etc.

4. CONCLUSION

CMC data show that mixing of oppositely charged gemini surfactants produces both synergistic and antagonistic effects. The interaction parameter (ß) is a quantitative measure of the interaction between the two components (the sign of ß represents synergistic or antagonistic interaction). The mixing increases the surfactant packing parameter (P) of the so-called *single surfactant* (cationic + anionic gemini). Zeta potential data show the formation of aggregates of lower charge together with charge reversal. Variations in P and |charge| decide the type of the aggregate. SANS data, for mixtures (containing $0.4x_{12\text{-}4\text{-}12A}$), revealed the presence of vesicles (also supported by TEM image, Figure 9) with 16-4-16 and long cylindrical micelles with 16-Isb-16. Heating, of the above two systems, shows aggregate growth governed by the dehydration of the aggregate. A mixture, containing vesicular aggregates, has been found to be more efficient over the other morphologies regarding PAH solubilization. The solubilization of PAH causes an increase in bilayer thickness (or hydrophobic volume, Table 6). The increased volume can be utilized for further solubilization (sequential, competitive, or simultaneous) of an appropriate hydrophobic molecule (or another PAH).[71,72] The study provides a clear corelation between morphology and solubilization efficacy.[26] The correlation, of selecting binary mixtures for the surfactant based technologies involving solubilization, could serve as a basis for the wide spectrum of applications (from industrial to nano- to biological).[29,73,74]

■ ASSOCIATED CONTENT

Supporting Information

The Supporting Information is available free of charge on the ACS Publications website at DOI: 10.1021/acs.jpcb.7b03989.

Tables S1 and S2: (i) structural formula and properties of PAHs; (ii) surfactant systems and their scattering length densities. Equations S1−S6 SANS. Equations S7 and S8 scattering length density calculation. Figure S1: (i) representative plots of surface tension vs log C; (ii) specific conductance vs [surfactant] of mixed gemini surfactants at 303 K. (PDF)

■ AUTHOR INFORMATION

Corresponding Author

*Phone: +91-265-2434188 (Ext. 212). M. No.: +91-9427453243. E-mail: drksanjeev@gmail.com.

ORCID

V. K. Aswal: 0000-0002-2020-9026

Sanjeev Kumar: 0000-0001-8696-0982

Notes

The authors declare no competing financial interest.

■ ACKNOWLEDGMENTS

Authors are thankful to UGC-DAE CSR, Mumbai, India (CRS−M−204), for financial support. Ms. Sneha Singh is thankful for the project fellowship. The Head, Applied Chemistry Department, Faculty of Tech. & Engg., The Maharaja Sayajirao University of Baroda, Vadodara, India, is gratefully acknowledged for research facilities.

■ REFERENCES

(1) Liu, Z.; Fan, Y.; Tian, M.; Wang, R.; Han, Y.; Wang, Y. Surfactant Selection Principle for Reducing Critical Micelle Concentration in Mixtures of Oppositely Charged Gemini Surfactants. *Langmuir* **2014**, *30*, 7968−7976.

(2) Pei, X.; Zhao, J.; Wei, X. Wormlike Micelles Formed by Mixed Cationic and Anionic Gemini Surfactants in Aqueous Solution. *J. Colloid Interface Sci.* **2011**, *356*, 176−181.

(3) Yin, H.; Zhou, Z.; Huang, J.; Zheng, R.; Zhang, Y. Temperature-Induced Micelle to Vesicle Transition in the Sodium Dodecylsulfate/Dodecyltriethylammonium bromide System. *Angew. Chem., Int. Ed.* **2003**, *42*, 2188−2191.

(4) Oda, R.; Huc, I.; Schmutz, M.; Candau, S. J.; MacKintosh, F. C. Tuning Bilayer Twist using Chiral Counterions. *Nature* **1999**, *399*, 566−569.

(5) Menger, F. M.; Keiper, J. S. Gemini Surfactants. *Angew. Chem., Int. Ed.* **2000**, *39*, 1906−1920.

Scheme 2. Schematic Representative PAH Solubilization Site in Vesicle Bilayer

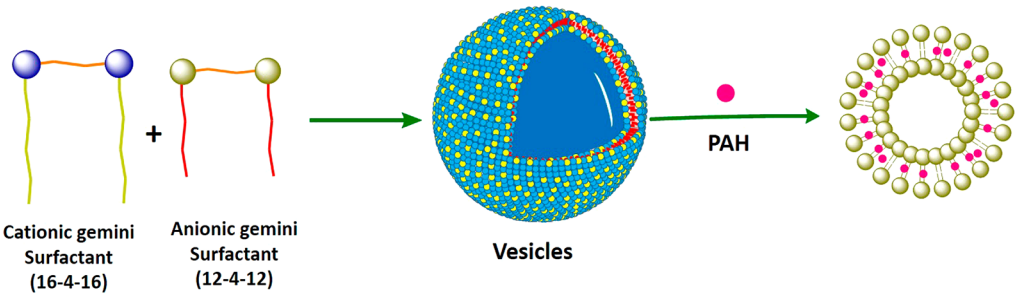

DOI: 10.1021/acs.jpcb.7b03989
J. Phys. Chem. B 2017, 121, 8756−8766

(6) Zana, R. Dimeric and Oligomeric Surfactants Behavior at Interfaces and in Aqueous Solution: A Review. *Adv. Colloid Interface Sci.* **2002**, *97*, 205−253.
(7) Han, Y.; Wang, Y. Aggregation Behavior of Gemini Surfactants and their Interaction with Macromolecules in Aqueous Solution. *Phys. Chem. Chem. Phys.* **2011**, *13*, 1939−1956.
(8) Fatma, N.; Panda, M.; Ansari, W. H. Solubility Enhancement of Anthracene and Pyrene in the Mixtures of a Cleavable Cationic Gemini Surfactant with Conventional Surfactants of Different Polarities. *Colloids Surf., A* **2015**, *467*, 9−17.
(9) Wei, J.; Huang, G.; An, C.; Yu, H. Investigation on the Solubilization of Polycyclic Aromatic Hydrocarbons in the Presence of Single and Mixed Gemini Surfactants. *J. Hazard. Mater.* **2011**, *190*, 840−847.
(10) Ansari, W. H.; Fatma, N.; Panda, M. Kabir-ud-Din. Solubilization of Polycyclic Aromatic Hydrocarbons by Novel Biodegradable Cationic Gemini Surfactant Ethane-1, 2-Diyl Bis (N, N-Dimethyl-N-Hexadecylammoniumacetoxy) Dichloride and its Binary Mixtures with Conventional Surfactants. *Soft Matter* **2013**, *9*, 1478−1487.
(11) Tsubone, K. The Interaction of an Anionic Gemini Surfactant with Conventional Anionic Surfactant. *J. Colloid Interface Sci.* **2003**, *261*, 524−528.
(12) Xu, H.; Liu, B.; Kang, P.; Bao, X. Properties of a Binary System Containing Anionic and Cationic Gemini Surfactants. *J. Surfactants Deterg.* **2015**, *18*, 297−302.
(13) Rosen, M. J. Gemini: A New Generation of Surfactants: These Materials have Better Properties than Conventional Ionic Surfactants as well as Positive Synergistic Effects with Non-Ionics. *CHEMTECH* **1993**, *23*, 30−33.
(14) Lu, T.; Lan, Y.; Liu, C.; Huang, J.; Wang, Y. Surface Properties, Aggregation Behavior and Micellization Thermodynamics of a Class of Gemini Surfactants with Ethyl Ammonium Headgroups. *J. Colloid Interface Sci.* **2012**, *377*, 222−230.
(15) Rodríguez, A.; del Mar Graciani, M.; Munoz, M.; Robina, I.; Moya, M. L. Effects of Ethylene Glycol Addition on the Aggregation and Micellar Growth of Gemini Surfactants. *Langmuir* **2006**, *22*, 9519−9525.
(16) Sikiric, M.; Smit, I.; Tusek-Bozic, L.; Tomasic, V.; Pucic, I.; Primozic, I.; Filipovic-Vincekovic, N. Effect of the Spacer Length on the Solid Phase Transitions of Dissymmetric Gemini Surfactants. *Langmuir* **2003**, *19*, 10044−10053.
(17) Zhang, Z.; Zheng, P.; Guo, Y.; Yang, Y.; Chen, Z.; Wang, X.; An, X.; Shen, W. The Effect of the Spacer Rigidity on the Aggregation Behavior of Two Ester-Containing Gemini Surfactants. *J. Colloid Interface Sci.* **2012**, *379*, 64−71.
(18) Yaseen, Z.; Rehman, S. U.; Tabish, M. Interaction Between DNA and Cationic Diester-Bonded Gemini Surfactants. *J. Mol. Liq.* **2014**, *197*, 322−327.
(19) Sakai, K.; Umezawa, S.; Tamura, M.; Takamatsu, Y.; Tsuchiya, K.; Torigoe, K.; Ohkubo, T.; Yoshimura, T.; Esumi, K.; Sakai, H.; Abe, M. Adsorbtion and Micellization Behaviour of Novel Gluconamide-type Gemini Surfactants. *J. Colloid Interface Sci.* **2008**, *318*, 440−448.
(20) Bombelli, C.; Giansanti, L.; Luciani, P.; Mancini, G. Gemini Surfactant based Carriers in Gene and Drug Delivery. *Curr. Med. Chem.* **2009**, *16*, 171−183.
(21) Parikh, K.; Mistry, B.; Jana, S.; Gajaria, T.; Gupta, S.; Devkar, R. V.; Kumar, S. Isosorbide Spacer Containing Gemini Surfactants: Surface and Biochemical Study. *Colloid Polym. Sci.* **2015**, *293*, 1437−1446.
(22) Kumar, S.; Parikh, K. Influence of Spacer on Association Behavior and Thermodynamic Parameters of Dimeric Cationic Surfactants. *J. Surfactants Deterg.* **2013**, *16*, 739−749.
(23) Siddiqui, U. S.; Kumar, S. Kabir-ud-Din. Structural Transition of Bifunctional Surfactants. *Monatsh. Chem.* **2009**, *140*, 457−462.
(24) Rosen, M. J.; Tracy, D. J. Gemini Surfactants. *J. Surfactants Deterg.* **1998**, *1*, 547−554.
(25) Kabir-ud-Din; Shafi, M.; Bhat, P. A.; Dar, A. A. Solubilization Capabilities of Mixture of Cationic Gemini Surfactant with Conventional Cationic, Nonionic and Anionic Surfactants Towards Polycyclic Aromatic Hydrocarbons. *J. Hazard. Mater.* **2009**, *167*, 575−581.
(26) Nagarajan, R. Solubilization by Amphiphilar Aggregates. *Curr. Opin. Colloid Interface Sci.* **1997**, *2*, 282−293.
(27) Wenk, M. R.; Fahr, A.; Reszka, R.; Seelig, J. Paclitaxel Partitioning into Lipid Bilayers. *J. Pharm. Sci.* **1996**, *85*, 228−231.
(28) Cape, J. L.; Monnard, P. A.; Boncella, J. M. Prebiotically Relevant Mixed Fatty Acid Vesicles Support Anionic Solutes Encapsulation and Photochemically Catalysed Trans-Membrane Charge Transport. *Chem. Sci.* **2011**, *2*, 661−671.
(29) Shah, A.; Shahzad, S.; Munir, A.; Nadagouda, M. N.; Khan, G. S.; Shams, D. F.; Rana, U. A. Micelles as Soil and Water Decontamination Agents. *Chem. Rev.* **2016**, *116*, 6042−6074.
(30) Lu, T.; Li, Z.; Huang, J.; Fu, H. Aqueous Surfactant Two-Phase Systems in a Mixture of Cationic Gemini and Anionic Surfactants. *Langmuir* **2008**, *24*, 10723−10728.
(31) Prevost, S.; Wattebled, L.; Laschewsky, A.; Gradzielski, M. Formation of Monodisperse Charged Vesicles in Mixtures of Cationic Gemini Surfactants and Anionic SDS. *Langmuir* **2011**, *27*, 582−591.
(32) Brito, R. O.; Marques, E. F.; Gomes, P.; Falcao, S.; Soderman, O. Self-Assembly in a Catanionic Mixture with an Aminoacid-Derived Surfactant: From Mixed Micelles to Spontaneous Vesicles. *J. Phys. Chem. B* **2006**, *110*, 18158−18165.
(33) Yoshimura, T.; Ohno, A.; Esumi, K. Mixed Micellar Properties of Cationic Trimeric-Type Quaternary Ammonium Salts and Anionic Sodium n-Octyl Sulfate Surfactants. *J. Colloid Interface Sci.* **2004**, *272*, 191−196.
(34) Yadav, S. K.; Parikh, K.; Kumar, S. Solubilization Potentials of Single and Mixed Oppositely Charged Gemini Surfactants: A Case of Polycyclic Aromatic Hydrocarbons. *Colloids Surf., A* **2017**, *514*, 47−55.
(35) Shrestha, R. G.; Shrestha, L. K.; Aramaki, K. Formation of Wormlike Micelle in a Mixed Amino-Acid Based Anionic Surfactant and Cationic Surfactant Systems. *J. Colloid Interface Sci.* **2007**, *311*, 276−284.
(36) Kumar, S.; Patel, H. Morphological Transitions in Aqueous CTAB−NaDC System: Macroscopic and Microscopic Studies. *J. Mol. Liq.* **2014**, *190*, 74−80.
(37) Aswal, V. K.; Goyal, P. S. Small-Angle Neutron Scattering Diffractometer at Dhruva Reactor. *Curr. Sci.* **2000**, *79*, 947−953.
(38) Svergun, D. I.; Koch, M. H. J. Small-Angle Scattering Studies of Biological Macromolecules in Solution. *Rep. Prog. Phys.* **2003**, *66*, 1735−1782.
(39) Pedersen, J. S. Analysis of Small-Angle Scattering Data from Colloids and Polymer Solutions: Modeling and Least-Squares Fitting. *Adv. Colloid Interface Sci.* **1997**, *70*, 171−210.
(40) Hayter, J. B.; Penfold, J. An Analytic Structure Factor for Macroion Solutions. *Mol. Phys.* **1981**, *42*, 109−118.
(41) Chen, S. H.; Sheu, E. Y.; Kalus, J.; Hoffmann, H. Small-Angle Neutron Scattering Investigation of Correlations in Charged Macromolecular and Supramolecular Solutions. *J. Appl. Crystallogr.* **1988**, *21*, 751−769.
(42) Bressler, I.; Kohlbrecher, J.; Thunemann, A. F. SASfit: A Tool for Small-Angle Scattering Data Analysis using a Library of Analytical Expressions. *J. Appl. Crystallogr.* **2015**, *48*, 1587−1598.
(43) Kaur, R.; Kumar, S.; Aswal, V. K.; Mahajan, R. K. Influence of Headgroup on the Aggregation and Interactional Behavior of Twin-Tailed Cationic Surfactants with Pluronics. *Langmuir* **2013**, *29*, 11821−11833.
(44) Kabir-ud-Din; Kumar, S.; Aswal, V. K.; Goyal, P. S. Effect of the Addition of n-alkylamines on the Growth of Sodium Dodecyl Sulfate Micelles. *J. Chem. Soc., Faraday Trans.* **1996**, *92*, 2413−2415.
(45) Moroi, Y.; Mitsunobu, K.; Morisue, T.; Kadobayashi, Y.; Sakai, M. Solubilization of Benzene, Naphthalene, Anthracene, and Pyrene in 1-dodecanesulfonic Acid Micelle. *J. Phys. Chem.* **1995**, *99*, 2372−2376.
(46) Friedel, R. A.; Orchin, M. *Ultraviolet Spectra of Aromatic Compounds*; Wiley Press: New York, 1951.
(47) Holland, P. M.; Rubingh, D. N. Non-ideal Multicomponent Mixed Micelle Model. *J. Phys. Chem.* **1983**, *87*, 1984−1990.

DOI: 10.1021/acs.jpcb.7b03989
J. Phys. Chem. B 2017, 121, 8756−8766

(48) Clint, J. H. Micellization of Mixed Nonionic Surface Active Agents. *J. Chem. Soc., Faraday Trans. 1* **1975**, *71*, 1327−1334.
(49) Rubingh, D. N.; Mittal, K. L. *Solution Chemistry of Surfactants*; Plenum Press: New York, 1979; Vol. *1*, p 337.
(50) Motomura, K.; Yamanaka, M.; Aratono, M. Thermodynamic Consideration of the Mixed Micelle of Surfactants. *Colloid Polym. Sci.* **1984**, *262*, 948−955.
(51) Liu, L.; Rosen, M. J. The Interaction of Some Novel Diquaternary Gemini Surfactants with Anionic Surfactants. *J. Colloid Interface Sci.* **1996**, *179*, 454−459.
(52) Brasher, L. L.; Herrington, K. L.; Kaler, E. W. Electrostatic Effects on the Phase-Behavior of Aqueous Cetyltrimethylammonium Bromide and Sodium Octyl Sulfate Mixtures with Added Sodium-bromide. *Langmuir* **1995**, *11*, 4267−4277.
(53) Israelachvili, J. N.; Mitchell, D. J; Ninham, B. W. J. Theory of Self-Assembly of Hydrocarbon Amphiphile in to Micelles and Bilayers. *J. Chem. Soc., Faraday Trans. 2* **1976**, *72*, 1525−1568.
(54) Lin, Z.; Cai, J. J.; Scriven, L. E.; Davis, H. T. Spherical-to-Wormlike Micelle Transition in CTAB Solutions. *J. Phys. Chem.* **1994**, *98*, 5984−5993.
(55) Kohler, H. H.; Strnad, J. Evaluation of Viscosity Measurements of Dilute Solutions of Ionic Surfactants Forming Rod-Shaped Micelles. *J. Phys. Chem.* **1990**, *94*, 7628−7634.
(56) Kumar, S.; Parveen, N. Kabir-ud-Din. Effect of Urea Addition on Micellization and the Related Phenomena. *J. Phys. Chem. B* **2004**, *108*, 9588−9592.
(57) Bergstrom, M.; Pedersen, J. S. A Small-Angle Neutron Scattering Study of Surfactant Aggregates Formed in Aqueous Mixtures of Sodium dodecyl sulfate and Dodecyldimethylammonium bromide. *J. Phys. Chem. B* **2000**, *104*, 4155−4163.
(58) Kumar, S.; Bhadoria, A.; Patel, H.; Aswal, V. K. Morphologies Near Cloud Point in Aqueous Ionic Surfactant: Scattering and NMR Studies. *J. Phys. Chem. B* **2012**, *116*, 3699−3703.
(59) Bhadoria, A.; Kumar, S.; Aswal, V. K.; Kumar, S. Mechanistic Approach on Heat Induced Growth of Anionic Surfactants: A Clouding Phenomenon. *RSC Adv.* **2015**, *5*, 23778−23786.
(60) Davies, T. S.; Ketner, A. M.; Raghavan, S. R. Self-Assembly of Surfactant Vesicles that Transform into Viscoelastic Wormlike Micelles Upon Heating. *J. Am. Chem. Soc.* **2006**, *128*, 6669−6675.
(61) Jung, H. T.; Coldren, B.; Zasadzinski, J. A.; Iampietro, D. J.; Kaler, E. W. The Origins of Stability of Spontaneous Vesicles. *Proc. Natl. Acad. Sci. U. S. A.* **2001**, *98*, 1353−1357.
(62) Zhang, Q.; Gao, Z.; Xu, F.; Tai, S.; Liu, X.; Mo, S.; Nui, F. Surface Tension and Aggregation Properties of Novel Cationic Gemini Surfactants with Diethylammonium Head Groups and Diamido Spacer. *Langmuir* **2012**, *28*, 11979−11987.
(63) Buwalda, R. T.; Stuart, M. C.; Engberts, J. B. Wormlike Micellar and Vesicular Phases in Aqueous Solutions of Single-tailed Surfactants with Aromatic Counter-ions. *Langmuir* **2000**, *16*, 6780−6786.
(64) Zheng, Y.; Ln, Z.; Zakin, J. L; Talmon, Y.; Davis, H. T.; Scriven, L. E. Cryo-TEM Imaging the Flow-Induced Transition from Vesicles to Threadlike Micelles. *J. Phys. Chem. B* **2000**, *104*, 5263−5271.
(65) Karayil, J.; Kumar, S.; Hassan, P. A.; Talmond, Y.; Sreejith, L. Microstructural Transition of Aqueous CTA B Micelles in the Presence of Long Chain Alcohols. *RSC Adv.* **2015**, *5*, 12434−12441.
(66) Sreejith, L.; Parathakkat, S.; Nair, S. M.; Kumar, S.; Varma, G.; Hassan, P. A.; Talmon, Y. Octanol-Triggered Self-Assemblies of the CTAB/KBr System: A Microstructural Study. *J. Phys. Chem. B* **2011**, *115*, 464−470.
(67) Ji, X.; Tian, M.; Wang, Y. Temperature-Induced Aggregate Transitions in Mixtures of Cationic Ammonium Gemini Surfactant with Anionic Glutamic Acid Surfactant in Aqueous Solution. *Langmuir* **2016**, *32*, 972−981.
(68) Kabir-ud-Din; Shafi, M.; Bhat, P. A.; Dar, A. A. Solubilization Capabilities of Mixtures of Cationic Gemini Surfactant with Conventional Cationic, Nonionic and Anionic Surfactants towards Polycyclic Aromatic Hydrocarbons. *J. Hazard. Mater.* **2009**, *167*, 575−581.
(69) Panda, M. Study of Surface and Solution Properties of Gemini-Conventional Surfactant Mixtures and their Effects on Solubilization of Polycyclic Aromatic Hydrocarbons. *J. Mol. Liq.* **2011**, *163*, 93−98.
(70) Fatma, N.; Panda, M.; Ansari, W. H. Solubility Enhancement of Anthracene and Pyrene in the Mixtures of a Cleavable Cationic Gemini Surfactant with Conventional Surfactants of Different Polarities. *Colloids Surf., A* **2015**, *467*, 9−17.
(71) Masrat, R.; Maswal, M.; Dar, A. A. Competitive Solubilization of Naphthalene and Pyrene in Various Micellar Systems. *J. Hazard. Mater.* **2013**, *244*−*245*, 662−670.
(72) Liang, X.; Zhang, M.; Guo, C.; Abel, S.; Yi, X.; Lu, G.; Yang, C.; Dang, Z. Competitive Solubilization of Low-Molecular-Weight Polycyclic Aromatic Hydrocarbons Mixtures in Single and Binary Surfactant Micelles. *Chem. Eng. J.* **2014**, *244*, 522−530.
(73) Wei, J.; Huang, G.; An, C.; Yu, H. Investigation on the Solubilization of Polyaromatic Hydrocarbons in the Presence of Single and Mixed Gemini Surfactants. *J. Hazard. Mater.* **2011**, *190*, 840−847.
(74) Sales, P. S.; Fernandez, M. A. Synergism in the Desorption of Polycyclic Aromatic Hydrocarbons from Soil Models by Mixed Surfactant Solutions. *Environ. Sci. Pollut. Res.* **2016**, *23*, 10158−10164.

DOI: 10.1021/acs.jpcb.7b03989
J. Phys. Chem. B 2017, 121, 8756−8766

Journal of Molecular Liquids 279 (2019) 108–119

Contents lists available at ScienceDirect

Journal of Molecular Liquids

journal homepage: www.elsevier.com/locate/molliq

Spacer nature and composition as key factors for structural tailoring of anionic/cationic mixed gemini micelles: Interaction and solubilization studies

Sneha Singh [a], Kushan Parikh [b], Sugam Kumar [c], V.K. Aswal [c], Sanjeev Kumar [a,*]

[a] Applied Chemistry Department, Faculty of Technology and Engineering, The Maharaja Sayajirao University of Baroda, Vadodara 390 002, India
[b] Department of Industrial Chemistry, Faculty of Life, Health & Allied Science, ITM Vocational University, Vadodara 391 760, India
[c] Solid State Physics Division, Bhabha Atomic Research Centre, Trombay, Mumbai 400085, India

ARTICLE INFO

Article history:
Received 30 November 2018
Received in revised form 8 January 2019
Accepted 19 January 2019
Available online 25 January 2019

Keywords:
Gemini surfactant
Critical micelle concentration
Vesicles
Bilayer thickness
Zeta-potential
Solubilization

ABSTRACT

Strategies (composition, morphology and spacer nature variations) are reported for aqueous solubility enhancement of hydrophobic material. Critical micelle concentration (cmc) of mixed oppositely charged gemini surfactants has been studied conductometrically. *Phosphoric acid, P, P′-1,4-butanedieyl, P, P′ didodecylester, disodium salt* is used as an anionic component while cationic geminis, with different spacers (polymethylene, ethylenediamine, isosorbide, and ethylene glycol), are used as another component. Based on micellar interaction parameter (βm), both synergistic and antagonistic interactions are observed. Zeta-potential shows variation in charge (or charge reversal) of the mixed aggregate. Small angle neutron scattering, dynamic light scattering and transmission electron microscopy show spacer nature dependent formation of micelles/vesicles. Molar solubilization ratio, of polycyclic aromatic hydrocarbon (PAH), suggests higher solubilization in vesicles. Solubilization depends on the vesicle electrostatics and bi-layer thickness. Potential key factors of the process seem bi-layer polarity and interaction with individual PAHs. Approach might be employed to enhance aqueous solubility/bioavailability of other hydrophobic materials such as drugs, dyes or pesticides.

1. Introduction

Self-assembly of molecules plays a decisive role in physico-biochemical processes [1]. One of such examples is photosynthesis which involves self-assembly responsible for photophosphorylation [2]. The self-assembly can be considered as a first step for the physical synthesis of an organized structure such as *vesicles*. They have been considered as precursors of the living cell [3,4]. A rich diversity of amphiphilic molecules (*e.g.* Surfactant) and ways of interaction among them result in self-assembled aggregates like micelles, reverse micelles, vesicles, gels among others [5]. Vesicles have been of interest due to their utility in diverse technologies [6–10] Nature of surfactant molecules is one of the governing factors for the formation of vesicles [11,12].

In recent years, much attention has been paid to cationic surfactants due to their high affinity to negatively charged hydrophobic solutes (nucleotides units of DNA, cell membrane and drugs) [13,14]. It has been reported that catanionic vesicles (formed by the mixing of oppositely charged surfactants) have various advantages over conventional lipid vesicles [11,15,16]. Vesicle formation has also been reported when a single/double chain [17,18] cationic surfactant (with simple salt) has been mixed to a certain medium to higher chain length alcohols [19–21]. Cationic surfactant gives vesicular aggregates in presence of oppositely charged hydrotropic ions which converts into other morphologies on varying the composition [22].

With the ever-increasing demand of chemical technologies, a renewed interest for better performing amphiphilic systems is growing. Solubilization of hydrophobic material into micellar aggregates has been studied for industrial, medicinal and environmental applications. The solubilization efficacy decides the optimality of the surfactant system. Mixed surfactant systems have been proved superior from the solubilization point of view over individual components of the mixture [23–25]. A polycyclic aromatic hydrocarbon (PAH) contaminates the environment and remains present in the atmosphere owing to their low aqueous solubility. Aqueous mixed surfactant systems have been known to decontaminate the PAH polluted sites. Much of the research is now shifted towards mixing of surfactants over single ones [26]. Gemini surfactants are known for better properties such as lower critical micelle concentration (cmc), higher surface activity, and unusual rheology [27–29]. Generally, gemini and conventional surfactants are similar, but spacer group that links both surfactant moieties around the head group could be hydrophilic or hydrophobic, rigid or flexible, longer or shorter

* Corresponding author at: Department of Applied Chemistry, Faculty of Technology & Engineering, The Maharaja Sayajirao University of Baroda, Vadodara 390 002, Gujarat, India.
E-mail address: drksanjeev@gmail.com (S. Kumar).

https://doi.org/10.1016/j.molliq.2019.01.097
0167-7322/

[30–32]. However, only a few reports are available related to the influence of nature of spacer on the applications and solution behavior of gemini surfactants [23,33–36]. Recently, studies related to solubilization of PAHs are reported in aqueous cationic gemini mixtures [37,38]. However, solubilization efficacy of oppositely charged gemini mixtures has been studied only a few times [24,39]. In one of these studies, it has been reported that mixing composition affects the micellar morphology with a concomitant influence on solubilization efficacy [39]. To the best of our knowledge, no attempt has been made to correlate the nature of the gemini spacer, resulting morphology and PAH solubilization efficacy in order to develop a structure-property relationship. Further, mixed vesicles are, probably, not utilized for the solubilization behavior of PAHs. No report has been found on co-solubilization of PAHs in vesicles and its effect on size/shape of the aggregates.

The prime objective of the work is to correlate PAH solubilization with surfactant morphology formed by oppositely charged gemini mixtures (containing cationic geminis with various spacers, Scheme 1). The study constitutes physicochemical characterization of gemini mixtures, correlation of structure of mixed assemblies with the nature of the spacer/composition, aggregate charge and consequences on aqueous solubility of hydrophobic molecules (*e.g.*, PAH). CMC measurements are performed conductometrically while structural information is collected from dynamic light scattering (DLS), transmission electron microscopy (TEM) and small angle neutron scattering (SANS). PAH solubilization data were acquired spectrophotometrically.

2. Experimental section

2.1. Materials

Cationic and anionic gemini surfactants are synthesized and characterized as reported earlier [24,34]. PAHs (anthracene, fluorene, phenanthrene, and pyrene) were of highest purity grade available. Chemical structures of geminis and PAHs (with abbreviations) are given in Scheme 1 (and see Table S3). De-ionized double distilled water (0.5–1.5μS·cm^{-1}) was used to prepare the solution throughout the study except for SANS measurements. D_2O was used in the sample preparation for the SANS study (99.9 atom % D, purchased from Sigma, St Louis, USA).

2.2. Methods

2.2.1. Electric conductivity measurements

The conductivity of the aqueous gemini mixture (of different mole fractions) was measured as a function of mixture concentration using a conductivity meter (EUTECH Cyberscan CON510, cell constant 1 cm^{-1}) with an inbuilt temperature sensor. A pre-calibrated cell has been used to measure specific conductance (κ) at each concentration. 500 μl stock solution was added in a known volume of water (thermostated at 303 ± 0.1 K using SCHOTT CT1650 bath). The CMC value was obtained from the intersection point of two straight lines in a plot of κ *vs* [mixture].

2.2.2. Dynamic light scattering (DLS)/zeta (ζ)-potential measurements

Average hydrodynamic diameter (D_h) and zeta (ζ) - potential measurements were performed on a SZ-100 nanoparticle size analyzer (HORIBA, Japan). This instrument is equipped with a green (5320 Å) laser and photomultiplier tube detectors. The measurement is based on the time-dependent fluctuation in the intensity of scattered light through dispersion of particles under random motion. The analysis allows computing diffusion coefficients which are used in Stokes-Einstein equation for the determination of D_h. 0.5 ml of surfactant (s) solution was transferred into dipped electrode plastic cuvette through a nylon membrane filter (0.22 μm) and placed in a sample

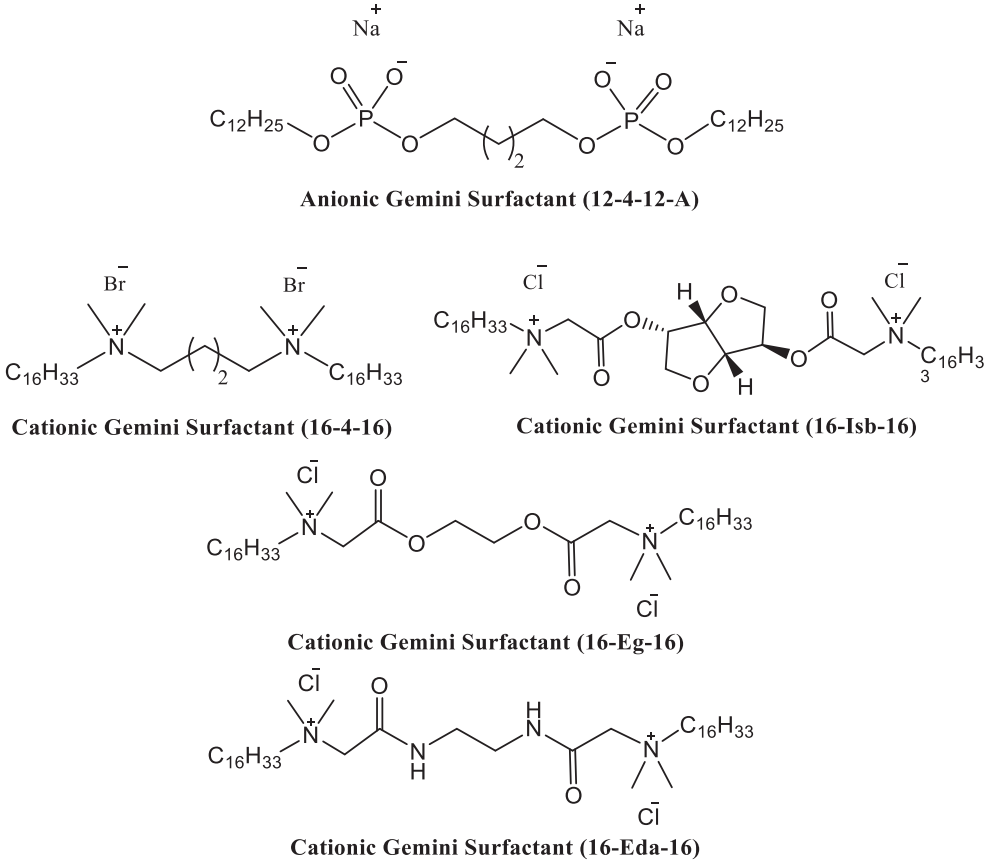

Scheme 1. Schematic representative chemical structures of anionic and cationic gemini surfactants with abbreviations.

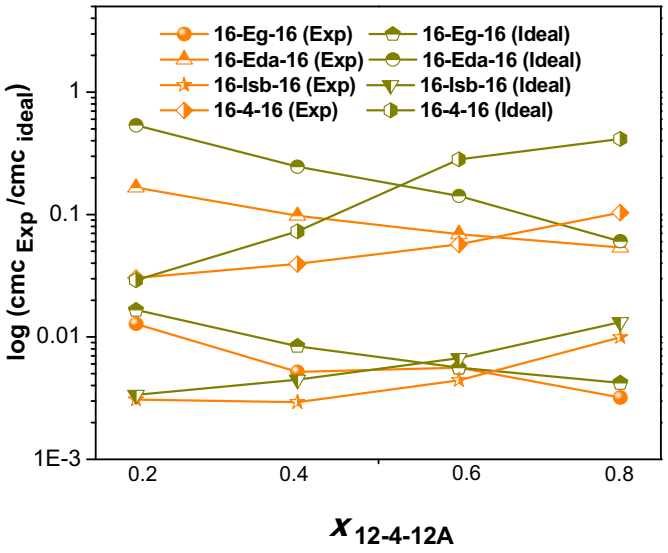

Fig. 1. Critical micelle concentration ($cmc_{exp\ or\ ideal}$) variation with a mole fraction of anionic gemini ($x_{12\text{-}4\text{-}12\text{-}A}$) in mixed gemini surfactant systems in aqueous solution at 303 K.

chamber. Data are average of 5 decay cycles (each decay cycle is of 5 runs with a 5 s interval).

2.2.3. SANS measurements

SANS measurements were carried out using a SANS spectrometer at Dhruva Reactor, Bhabha Atomic Research Centre, Trombay, India [40]. The samples were placed in a quartz cuvette having a thickness of 2 mm and measurements were performed at different compositions/temperatures. Data were treated to an absolute scale as reported elsewhere [39]. Coherent differential scattering cross-section per unit volume ($d\Sigma/d\Omega$), as a function of scattering vector ($Q = 4\pi\sin\theta/\lambda$, where 2θ is the scattering angle and λ is the wavelength of the incoming neutrons), has been measured. For a mono-disperse particle, $d\Sigma/d\Omega$ can be given as [41].

$$\frac{d\sum}{d\Omega} = nP(Q)S(Q) + B \tag{1}$$

where n is the particle number density. P(Q) is the form factor and is decided by the shape and size of the particle. S(Q) is the inter-particle structure factor govern by the inter-micellar interactions. B denotes the incoherent scattering background mainly resulted from the hydrogen-containing moieties in the aggregates. Details of the models involved in the data analysis are separately given in the supplementary information [42–46].

2.2.4. TEM studies

Transmission electron microscopy (TEM) images were obtained with a JEOL JEM 2100 transmission electron microscope accelerating at a working voltage of 120 kV. A drop of the sample solution was placed on the carbon-coated copper grid (200 mesh) followed by drying for a few minutes (~298 K). Later on, a drop of fresh uranyl acetate solution was put on the grid having the dried sample. The grid was again dried at the same temperature.

2.2.5. PAH solubilization study

The solubility of PAH has been determined in aqueous gemini systems (single or mixed), at different mole fractions ($x = 0$–1, total [gemini] = 10 mM) by adding an excess amount of PAH (fluorene, anthracene, phenanthrene or pyrene). Aqueous gemini(s) + PAH mixture has been equilibrated for 48 h before centrifugation to remove excess PAH. The solubilization of PAH in micellar solutions, containing different morphologies, has been analyzed, at respective $\lambda_{max,}$ by UV–visible spectrophotometer (Shimadzu, UV-2450) having a quartz cell (path length 1 cm) at 303 K. The composition of gemini mixture was same in both reference and measurement cuvettes to eliminate its effect on the UV-absorbance. Solubility (or concentration) of PAH was calculated by Lambert-Beer law (using respective molar extinction coefficient, ε) [47,48] The molar solubilization ratio (MSR) is the ratio of the molar solubility of the PAH in micelles to the total[gemini(s)] in the micellar form [28]. MSR can be computed by the following expression,

$$\mathrm{MSR} = \frac{(S_t - S_{cmc})}{(C_t - C_{cmc})} \tag{2}$$

where, S_t is the total PAH molar solubility in the aqueous gemini mixture at fixed [surfactant] (C_t=10 mM). S_{cmc} is the solubility of the PAH corresponding to the cmc of the gemini mixture (C_{cmc}). Same procedure has been adopted in the co-solubilization experiment where more than one PAHs were solubilized simultaneously.

3. Results and discussion

3.1. Micellization studies

Conductometry has been used to determine the cmc of all the gemini surfactants (cmc data given in Table S1 of supplementary information). Anionic gemini (12-4-12A) shows higher cmc due to having lower alkyl chain length. Cationic geminis show different cmc values though they have same carbon chain length (hexadecyl). This deference may be due to two factors: 1) nature of the spacer and 2) nature of the counter-ion. Even for same counter ion, the cmc values were different for different gemini surfactant. This indicates that the spacer nature has a decisive effect on the micellization process [36,49]. Interaction, of various combinations of oppositely charged gemini surfactants, has been studied using various solution theory.

cmc variations with a mole fraction of added 12-4-12A, to cationic gemini surfactant (16-Eda-16 or 16-Eg-16), has been shown in Fig. 1. Pseudo phase separation model has been applied to understand how the micellization behavior of gemini mixtures deviates from the ideal mixing [50]. Experimental cmc (cmc_{exp}) of each mixture was found lower than the cmc of 12-4-12A (cmc_1) and higher than 16-Eda-16 or

Table 1
Micellization parameters (cmc_{exp} and cmc_{ideal}) and interaction parameter (β^m, by Rubingh's method) of mixed gemini surfactant systems in aqueous solution at 303 K.

$x_{12\text{-}4\text{-}12A}$	16-4-16			16-Isb-16			16-Eda-16			16-Eg-16		
	cmc_{exp}	cmc_{ideal}	β^m	cmc_{exp}	cmc_{ideal}	β^m	cmc_{exp}	cmc_{ideal}	β^m	cmc_{exp}	cmc_{ideal}	β^m
	(mM)			(mM)			(mM)			(mM)		
0.0	0.0244	–	–	0.0027	–	–	0.044	–	–	0.0034		
0.2	0.0292	0.0306	-11.87	0.0031	0.0034	-12.96	0.059	0.0538	–	0.0128	0.0042	–
0.4	0.0734	0.0395	–	0.0037	0.0045	-7.90	0.141	0.0695	–	0.0052	0.0056	-0.08
0.6	0.2822	0.0570	–	0.0046	0.0067	-8.05	0.265	0.0978	–	0.0056	0.0084	-0.42
0.8	0.4159	0.1036	–	0.0099	0.0132	-9.80	0.518	0.165	–	0.003	0.0165	-7.13
1.0	0.5310	–		0.5310	–	–	0.531	–	–	0.531		

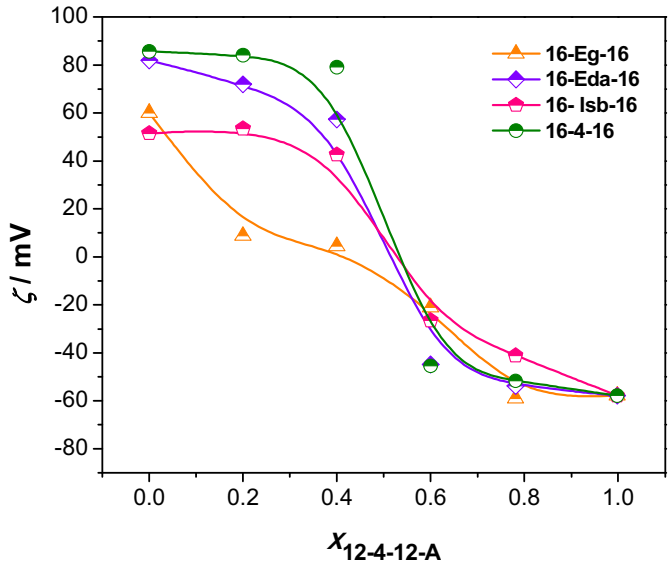

Fig. 2. Zeta (ζ) – potential data of 10 mM mixed gemini surfactant aqueous systems at a different mole fraction of anionic gemini surfactant ($x_{12\text{-}4\text{-}12A}$) in aqueous solution at 303 K.

16-Eg-16 (cmc_2). Similar behavior has been observed in the earlier study where different combinations of oppositely charged gemini surfactants were mixed [39]. For a mixture of oppositely charged surfactants, a simple relationship exists for ideal mixing [51–53] (cmc data treatment is given in supplementary information).

Mostly, the micellar interaction parameter (β^m) has been used to understand the nature and strength of the interactions between different amphiphilic gemini molecules (constituting the mixture) and can be obtained by applying Eq. (3) [54].

$$\beta^m = [\ \ln(cmc_e x_1/cmc_1 X_1^m)]/(1-X_1^m)^2 \quad (3)$$

As cmc_{exp} has been found lower than the cmc_i, β^m values are expected to be negative in each case (synergistic interaction). This indeed was observed (Table 1). The behavior is the result of the packing of each component in the mixed micelle (and the resultant cmc_{exp}). The data related to cmc_{exp}, cmc_i, cmc_1, cmc_2, X_1^m, X_1^i and β^m are tabulated in Table 1. Interaction among the two geminis in the mixed micelle is associated with the decrease of energy which is denoted in terms of β^m. β^m is a measure of the degree of interaction between two gemini component of the mixed micelle and accounts for deviation from ideal mixing. The higher the negative magnitude of β^m, stronger is the synergistic interaction between the two gemini components. The perusal of data of Table 1 indicates that β^m shows a dependency on the nature of the spacer present in the cationic gemini surfactant and hints towards stronger attractive interactions with 16-Isb-16. It has been reported for similar charged (cationic) gemini mixtures that β^m decreases as the chain length of the spacer decreases. However, this trend was not observed when one of the components of the mixture was a non-ionic surfactant (Brij 58) [55]. Moreover, chain length increase in cationic gemini has nearly no effect on β^m when mixed with the Brij 58 [23,56]. In the case of ester spacer based cationic (12-Eg-12) sodium dodecyl sulfate (SDS) shows higher - β^m than sodiumdodecylbenzo sulphonate (SDBS) [56]. Above discussion shows that β^m is governed by the nature of the charge of the surfactants constituting a binary mixture. In this context, β^m data of Table 1 shows not only the charge, spacer length but nature of the spacer can also be one of the governing factors deciding the strength of interaction between the components of gemini mixtures.

3.2. Structural evolutions

Mixing of anionic/cationic geminis, in aqueous solution, results in strong columbic attraction together with hydrophobic interactions among the hydrocarbon tails. The coulombic effects causes decrease in area of the head group(s) while hydrophobic interactions may cause increase in volume of the alkyl tail part (of the resulting surfactant moiety produced due the mixing of two gemini components) [57] Surfactant

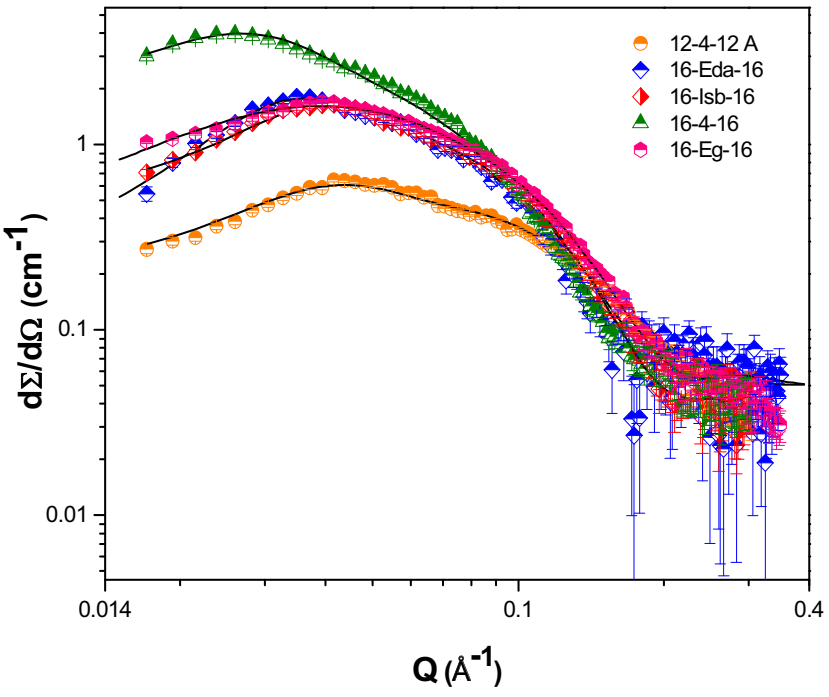

Fig. 3. SANS spectra of 10 mM pure gemini surfactants at 303 K.

Table 2
Micellar dimensions and charge (α) for 10 mM aqueous gemini surfactant at 303 K.

Surfactant	Semi-major axis *a* (Å)	Semi-minor axis *b* (Å)	Fractional charge (α)	*a*/*b*	Morphology
16-4-16	95.8	20.4	0.10	4.7	Ellipsoidal
16-Isb-16	37.2	20.0	0.43	1.9	Ellipsoidal
16-Eda-16	35.0	20.5	0.21	1.7	Ellipsoidal
16-Eg-16	34.7	17.9	0.09	1.9	Ellipsoidal
12-4-12A	29.5	14.1	0.65	2.1	Ellipsoidal

parameter, P ($= v/A_0 l$, v is the volume of the hydrocarbon part of the surfactant(s) molecule(s), l and A_0 are lengths and effective surface area per surfactant(s) molecule(s), respectively), can be related to aggregate morphology [58]. The presence of oppositely charged surfactants has a strong chance to get incorporated in the mixed micelle together with overcoming of electrostatic repulsion. Columbic attraction can be responsible for the lowering of A_0 with a concomitant increase in P. Another contribution of the increase in P comes from by considering two gemini surfactant components of the mixture as a *single amphiphilic moiety* of higher alkyl tail volume (v). Various morphological transitions have been explained on the basis of the *P* value [59]. Mixing oppositely charged amphiphilic molecules is a promising strategy for the physical synthesis of self -assembly of desired morphology [16,22].

The idea of columbic attraction variation can be taken from zeta (ζ) – potential profile obtained with the variation of the composition of the mixture. (Fig. 2) The crossover of sign (from positive to negative) of ζ hints in the variation of micellar surface charge (as well as *A* value) which can be correlated with the P value and the resulting micellar structure produced in the solution is dependent on the mole fraction of each component and decides micellar surface charge which can be related to the variation of P and hence to the micellar morphology as mentioned above.

SANS spectra ($d\Sigma/d\Omega$ *vs* Q) for 10 mM gemini surfactant solution are depicted in Fig. 3. Fig. 3 shows the interaction peak in all cases which is an indication of the presence of charged micelle in the solution. The related analyzed micellar parameter data for each gemini surfactants are compiled in Table 2. SANS analysis shows that ellipsoidal micelles are present in the solution with every gemini surfactant except 16-4-16. With the dodecyl chain in 12-4-12A, it is obvious that micelles of higher sphericity will form as reported with another ionic surfactant of the dodecyl chain [60]. For equal alkyl tail length (16 C-atom) gemini with polymethylene spacer of (4 C atom) forms rod-shaped micelles while ellipsoidal morphology observed with geminis having other spacers this clearly indicates that spacer has a decisive role to dictate the type of morphology a gemini will form in the solution. Since polymethylene spacer gemini (16-4-16) is distinctly hydrophobic in comparison to other geminis and, therefore, one can expect increased hydrophobic interactions and aggregate of higher morphology. This indeed was observed from the present study (Table 2). Analyzed data can be used to compute number density of the micelles and hence the average intermicellar distance (D). This can be used to back-calculate the position of the expected correlation peak using Eq. S6 and is found in fairly good agreement with that of experimental one (Fig. 3).

The SANS spectra for various compositions of mixed geminis are shown in Fig. 4. With the addition of anionic 12-4-12A to cationic 16-Eda-16 or 16-Eg-16 (keeping total [gemini(s)] constant, 10 mM), interaction peak corresponding to the charged micelle starts disappearing with no plateau in the comparable mole fractions of the two components (0.4 and 0.6, 0.5 and 0.5 or 0.6 and 0.4). At some specific mole fractions (*e.g.* 0.6/0.4 or 0.4/0.6) of oppositely charged surfactants (*e.g.* 16-Eg/Eda-16 and 12-4-12A), the formation of large aggregates (rod-like micelles or vesicles) leads to a reduction in number density and hence increase in inter micellar distance. These systems, therefore, behave as dilute and no correlation peak appears in the Q range of the measurements. Also, at the approximate by equimolar concentrations,

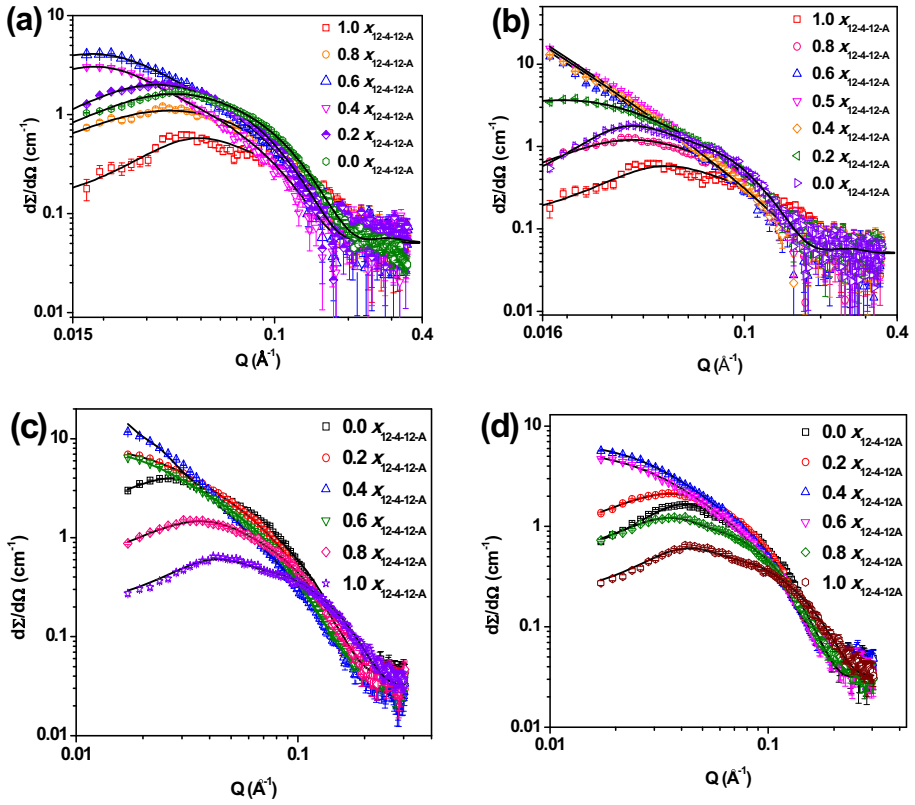

Fig. 4. SANS spectra of 10 mM mixed aqueous gemini surfactant systems at different mole fraction of anionic gemini surfactant ($x_{12\text{-}4\text{-}12A}$) at 303 K: (a) 16-Eg-16; (b) 16-Eda-16 (c) 16-4-16 and (d) 16-Isb-16.

Table 3
SANS fitted micellar parameters of 10 mM aqueous mixed gemini surfactant systems at 303 K.

$x_{12\text{-}4\text{-}12A}$	Semi-major axis a (Å)	Semi-minor axis b (Å)	Fractional charge (α)	Aggregation number
16-Eda-16				
0.0	35.0	20.5	0.21	67
0.2	89.3	20.3	0.04	171
0.4	**Vesicles with a bi-layer thickness of 23 Å.**			
0.5	**Vesicles with a bi-layer thickness of 25 Å.**			
0.6	**Vesicles with a bi-layer thickness of 22 Å.**			
0.8	36.5	20.5	0.10	86
1.0	29.5	14.1	0.65	35
16-Eg-16				
0.0	34.7	17.9	0.09	66
0.2	43.7	20.3	0.09	86
0.4	112.4	20.3	0.04	234
0.6	124.3	20.4	0.03	258
0.8	37.9	16.6	0.10	59
1.0	29.5	14.1	0.65	35
16-4-16				
0.0	95.8	20.4	0.1	182
0.2	111.8	20.3	–	191
0.4	**Vesicles with a bi-layer thickness of 25 Å**			
0.6	141.2	21.7	–	354
0.8	44.5	19.0	0.18	90
1.0	29.5	14.1	0.65	35
16-Isb-16				
0.0	37.2	20.0	0.43	68
0.2	45.8	20.8	0.16	95
0.4	104.0	20.0	–	210
0.6	101.2	20.0	–	215
0.8	32.3	18.6	0.6	63
1.0	29.5	14.1	0.65	35

Bold represents in Table 3 about vesicle formation and its bi-layer thickness.

there may be near charge balance of oppositely charged surfactants making the system nearly pseudo nonionic (as observed by zeta potential data, Fig. 2). This restricts the determination of any S(Q) parameters for these concentrations. The similar mixing effect was observed for other combinations of oppositely charged gemini surfactants [39]. On combining the SANS spectra of present and earlier studies (Fig. 4), it is clearly observed that the nature of spacer has a distinct effect on the SANS spectra of mixed oppositely charged gemini surfactants. The trend of data with 16-Isb-16 (in the mixture) matches with 16-Eg-16 (in the mixture) while the data of 16-4-16 are similar with the data of 16-Eda-16. In all the above-mentioned mixture components are more or less similar to the difference of the nature of the spacer. 16-Isb/Eg-16 and 16-4/Eda-16 fall into two separate groups of forming different kind of morphologies at an individual same composition (ellipsoidal/rod and rod/vesicles). Isb or Eg are distinctly polar spacers than Eda or polymethylene (hydrophobic spacers). Therefore, the polarity of the spacer has a role to play in deciding the self-assembly to be formed in aqueous oppositely charged gemini mixture.

The analyzed SANS data (Table 3) show the morphological transition on increasing the mole fraction of 12-4-12 A in the mixtures keeping constant [gemini(s)] (10 mM). It may be mentioned here that bi-layers are formed for various compositions (of the mixtures) having nearly equal mole fractions (0.4 or 0.6) and hydrophobic spacer(s). However, similar compositions gave nearly rod-shaped morphologies for hydrophilic spacers (Isb/Eg).

The bi-layers are again converted to rod-shaped micelles and then to ellipsoidal ones with the further increase of the content of 12-4-12A in the mixture containing 16-4-16 or 16-Eda-16. Similar transitions were observed with the mixture containing 16-Eg-16 or 16-Isb-16 with the difference that here transition is taking place from rod-shaped morphologies. Data of Fig. 5 (log-log plot) show the characteristic Q decay for vesicles and rod-shaped micelles (a slope of −2 or −1), indicative of the role of the spacer [22]. The vesicle bi-layer thickness can be determined from the SANS data using a cross-sectional Guinier plot and the value has been found in between 22-25 Å for the two spacers, namely polymethylene and Eda. The values are in good agreement with other reported surfactant systems [22,61]. To confirm the morphology of the aggregate, observed by SANS, DLS and TEM were also used. Fig. 6a, b and c depicts the variation of hydrodynamic diameter (D_h) with the composition of the different mixed gemini systems. The aggregate has an average D_h value ~ 15 nm for all the individual gemini surfactants. Composition variation in the mixture of any two geminis from 0.2 to 0.8-mole fraction results in structural transitions as observed from the SANS study (*vide supra*). In the composition range (0.4 to 0.6), the D_h value of the aggregate is ~65 ± 5 nm. However, the above size range was not observed (Fig. 6c) when the mixture contains gemini having -Eg- spacer. The magnitude of D_h in the composition range of 0.4 to 0.6 together with the bluish color of the mixture indicates that the aggregates are vesicles whereas mixture with -Eg- spacer gemini contains ellipsoidal micelles. However, a single major peak indicates the presence of one kind of aggregates in the system (vesicles or mixed micelles). Data distinctly show the maximum change in D_h when the mixture contains nearly equal mole fractions of the two components. Overall DLS data are in consonance with SANS results and confirm the presence of higher order aggregates *e.g.*, Vesicles.

TEM observations have also been used to support the information, regarding the formation of vesicles in the solution, obtained from SANS and DLS studies. Figs. 7 & 8 show TEM micrographs (negatively stained) of different gemini mixtures. For gemini with polymethylene, spacer exhibits both formation of open (0.4 $x_{16\text{-}4\text{-}16}$) and closed (0.6

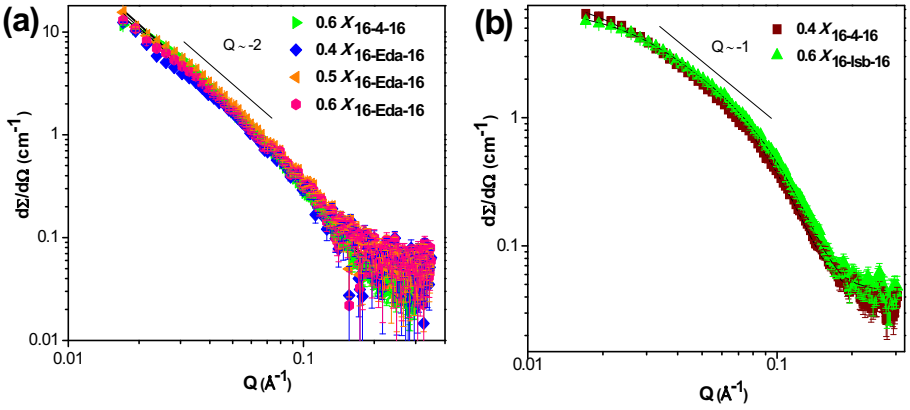

Fig. 5. (a) SANS spectra of 10 mM aqueous mixed gemini surfactant system showing vesicular aggregates and (b) SANS spectra of 10 mM aqueous mixed gemini surfactant system having rod-shaped micelles.

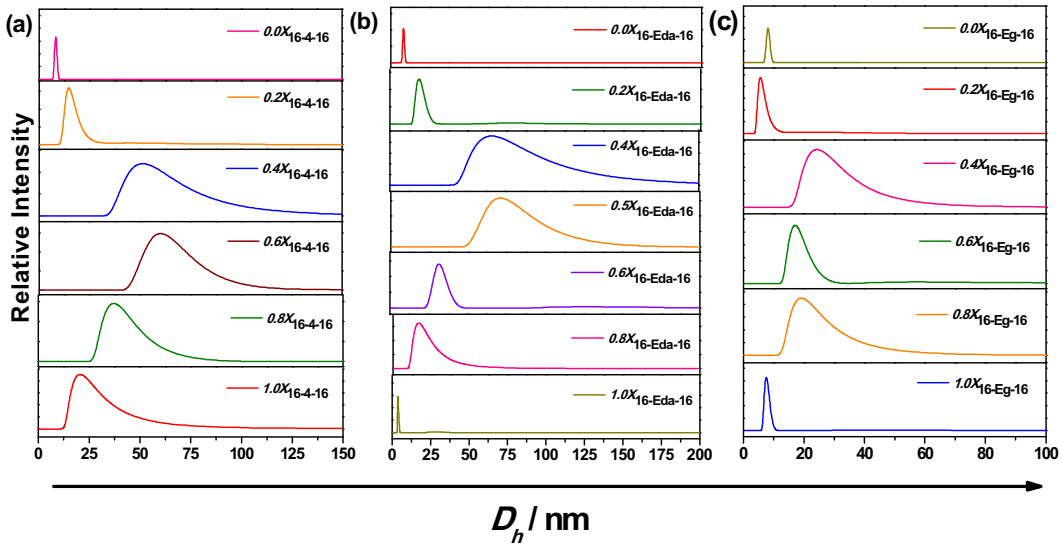

Fig. 6. DLS data of 10 mM aqueous mixed gemini surfactant system at different mole fractions of anionic gemini surfactant ($x_{12\text{-}4\text{-}12A}$) at 303 K: (a) 16-4-16; (b) 16-Eda-16 and (c) 16-Eg-16.

$x_{16\text{-}4\text{-}16}$) vesicles in the aqueous mixture. Due to above morphologies, SANS and DLS data were found different for the above to composition. However, gemini with Eda spacer, in the mixture, shows the formation of closed vesicles with both the compositions (0.4 or 0.5 $x_{16\text{-}Eda\text{-}16}$). Above data clearly, indicate that vesicle formation is dependent on both the composition and nature of the spacer. It is fair to mention here that other two cationic gemini with spacers -Isb- and -Eg- are failed to produce vesicles in the similar composition range of the mixture. TEM images corroborate the idea of vesicle formation proposed on the basis of SANS data and DLS results.

3.3. Temperature influence on micellar morphologies

It has been observed that certain gemini mixtures contain vesicles at room temperature. SANS data are also acquired at different temperatures (303–343 K) for a few mixtures (Fig. 9). Overall bi-layer thickness data (Table 4) show that system with polymethylene spacer (*i.e.* 16-4-16) gives relatively stable vesicles over Eda spacer system (16-Eda-16) at equal composition. The similar insensitivity of the heating for the vesicular system has been reported recently [62]. However, a hydrophilic spacer (*e.g.* Eda) may bind with background water which may

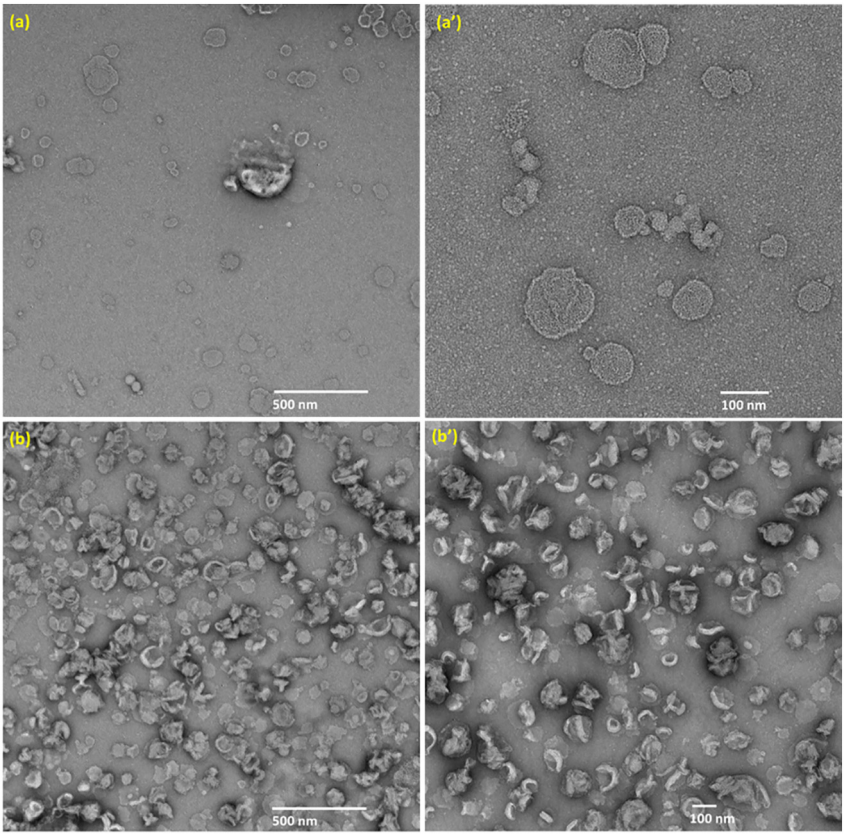

Fig. 7. Negative stained TEM images of 10 mM mixed gemini surfactant system of 16-4-16 + 12-4-12 A (a, a′) 0.6 $x_{16\text{-}4\text{-}16}$ and (b, b′) 0.4 $x_{16\text{-}4\text{-}16}$ at scale 500 and 100 nm, respectively.

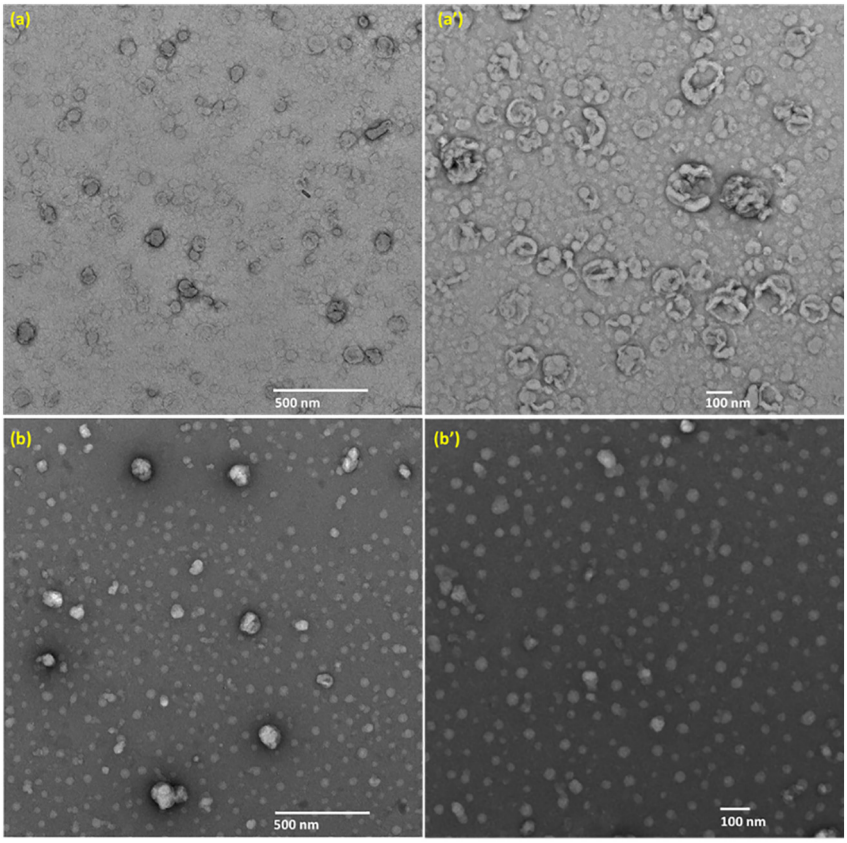

Fig. 8. Negative stained TEM images of 10 mM mixed gemini surfactant system of 16-Eda-16 + 12-4-12 A (a, a′) 0.6 $x_{16\text{-Eda-}16}$ and (b, b′) 0.4 $x_{16\text{-Eda-}16}$ at scale 500 and 100 nm, respectively.

release on heating and responsible for compact bilayer. In earlier studies, the morphological transition has been reported for surfactant systems with increasing temperature or shear [22,63,64]. The transition has been explained on the basis of the release of oppositely charged hydrotropic counter ion from the cationic micellar surface on heating. The difference in present systems and the ones from earlier studies, [22,63,64] is the second component, (12-4-12A) which forms mixed vesicles instead of methyl salicylate bind vesicles. A similar transition has also been observed with a cationic surfactant – alkanol system [20,21]. However, no such transition has been observed with the present system due to the fact that hydrophobic interactions are playing a decisive role in the formation of vesicles which check the disintegration of 12-4-12A on heating. Recently, temperature induced micellar growth has also been reported in an aqueous mixture of cationic gemini with an anionic surfactant [65]. This observation of the stability of higher order aggregates on heating has not been reported many times. Our results of semi-major axis (b), observed with -Isb- spacer gemini in the mixture (0.6 $x_{16\text{-Isb-}16}$), show an increase with temperature. With heating, gradual dehydration of the oppositely charged head groups takes place which facilitates coulombic attraction. This causes a reduction in the average area of head group A^0 (of resulting pseudo gemini surfactant) with a net effect of an increase in surfactant parameter value (Rp) and micellar growth [58]. Therefore, aggregates of different thermal stability can be produced at will by judicious selection of the second component as well as with an appropriate gemini spacer in two components aqueous gemini mixture. The structural information's are used to explain PAH solubilization in the solutions of different morphologies.

3.4. Solubilization in single/mixed geminis

The absorbance variation has been found to be dependent on the aqueous morphologies (*vide supra*) present in the solution (relevant

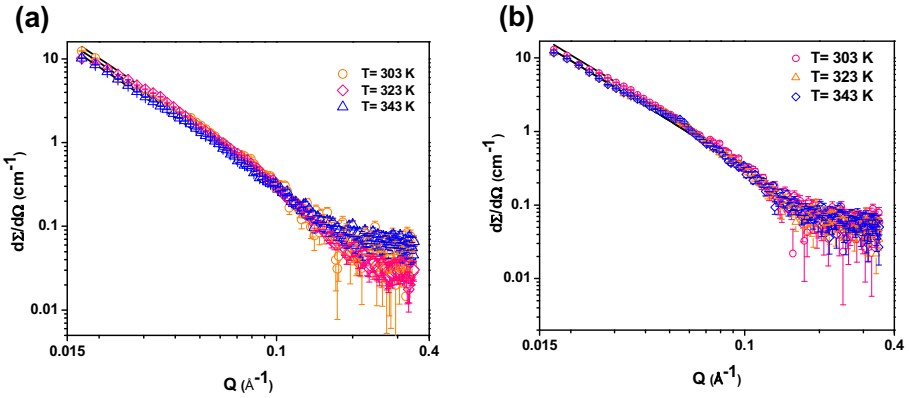

Fig. 9. SANS spectra of 10 mM aqueous mixed gemini surfactant system (16-Eda-16 + 12-4-12A) at different mole fractions and temperature: (a) 0.4 $x_{16\text{-Eda-}16}$ (b) 0.6 $x_{16\text{-Eda-}16}$.

Table 4
SANS fitted micellar parameters of 10 mM aqueous mixed gemini surfactant systems at different temperatures (T).

T	0.4 $x_{16\text{-}Eda\text{-}16}$	0.6 $x_{16\text{-}Eda\text{-}16}$	0.6 $x_{16\text{-}4\text{-}16}$	0.6 $x_{16\text{-}Isb\text{-}16}$	
K	Bi-layer thickness (Å)			Semi-major axis a (Å)	Semi-minor axis b (Å)
303	22.0	23.0	25.0	104.0	20.0
323	20.3	20.7	26.2	132.2	20.0
343	17.8	21.2	25.8	137.5	20.0

typical data are depicted in supplementary information, Fig. S1). MSR data with individual and binary gemini systems are tabulated in Table 5. MSR data show higher values with oppositely charged mixed gemini systems over individual components of the mixture. This is in consonance with the reported trend observed in an earlier study [24]. However, differences in MSR values may be due to the fact that the earlier study has been conducted at just above the CMC where, predominantly, spherical micelles would have been present. Different concentration range, as well as a change in the morphology (rod-shaped or vesicles), are responsible for the differences in the MSR data. Large aggregates (in the present study), with higher hydrophobic volume than the individual gemini surfactant micelles, are responsible for the effective solubilization of PAH and higher MSR values (Table 5). Among all gemini mixtures, vesicular systems have been found more effective than the one having other morphologies. MSR follows the order: vesicles > rod-shaped- > ellipsoidal- > spherical micelles. This reveals a synergistic effect of mixing of two oppositely charged gemini surfactant (of optimum composition), with an appropriate spacer, resulting vesicular aggregates. Among different PAHs, MSR has been found to be dependent on the polarity and geometrical size of an individual PAH.

The aqueous solubility of various PAHs follows the order: Flu > Phen > Pyr > Anth (Table S3). However, the maximum MSR (or solubility, Table 5) has been found in most cases when the composition of the two components of the mixture was in the mole fraction range of 0.4 to 0.6 (vesicles or rod-shaped micelles). Therefore, composition/morphology plays a decisive role in solubilizing the PAHs. Apart from the above factors (composition, nature of PAHs and structure of the spacer), solubilization sites of each PAH have equal importance in overall solubilization phenomenon [39,56,66]. It may be mentioned here that a typical micellar aggregate can be considered as made up of various layers of different polarities (highly polar- *head group region* to highly nonpolar-*micellar core*) [67–69]. This polarity variation can be affected by the hydrocarbon tail length, nature of the head group as well as the nature of the spacer. Probably, most of the factors are contributing in the present PAH solubilization in the aqueous mixture of oppositely charged gemini surfactants as reported for other similar systems [70,71]. MSR data

Table 5
Molar solubilization ratio (MSR) of 10 mM (single and mixed) gemini surfactants in aqueous solution with varying mole fraction of 12-4-12A ($x_{12\text{-}4\text{-}12\text{-}A}$) at 303 K.

$x_{12\text{-}4\text{-}12\text{-}A}$	Morphology	MSR			
		Anthracene	Fluorene	Pyrene	Phenanthrene
16-Eda-16					
1.0	Ellipsoidal	0.026	0.091	0.038	0.049
0.8	Rod	0.010	0.131	0.041	0.076
0.6	Vesicles	0.022	0.180	0.096	0.236
0.5	Vesicles	**0.031**	**0.316**	**0.170**	**0.334**
0.4	Vesicles	0.016	0.200	0.102	0.261
0.2	Ellipsoidal	0.011	0.060	0.062	0.088
0.0	Ellipsoidal	0.009	0.099	0.057	0.179
16-Eg-16					
0.8	Ellipsoidal	0.0012	0.106	0.011	**0.260**
0.6	Rod	**0.0154**	0.089	0.008	0.125
0.4	Rod	0.0051	**0.121**	**0.032**	0.109
0.2	Ellipsoidal	0.0038	0.050	0.007	0.114
0.0	Ellipsoidal	0.0032	0.101	0.016	0.176
16-4-16					
0.8	Ellipsoidal	0.0282	0.0711	0.058	0.152
0.6	Rod	0.0276	0.1078	0.086	0.223
0.4	Vesicle	**0.0321**	**0.2544**	**0.171**	**0.233**
0.2	Rod	0.0261	0.1486	0.143	0.081
0.0	Rod	0.0257	0.1587	0.109	0.190
16-Isb-16					
0.8	Ellipsoidal	0.0132	0.1889	0.064	0.045
0.6	Rod	**0.0276**	**0.1947**	0.065	**0.142**
0.4	Rod	0.0260	0.1683	**0.084**	0.096
0.2	Ellipsoidal	0.0265	0.1125	0.060	0.072
0.0	Ellipsoidal	0.0136	0.1281	0.076	0.079

Bold means maximum MSR in a typical mixed system.

Table 6
Comparative MSR data available from various studies for the solubilization of Anthracene and Pyrene in mixed oppositely charged surfactant systems in aqueous medium.

System[a]	MSR		Ref.
	Anthracene	Pyrene	
16-Eda-16 + SDS	0.0248	0.0576	[23]
16-Eda-16 + SDBS	0.0243	0.0745	
16-4-16 + AOT	0.016	0.047	[55]
16-5-16 + AOT	0.0119	0.0323	
16-6-16 + AOT	0.0103	0.0526	
12-Eda-12 + SDS	0.0061	0.0137	[56]
12-Eda-12 + SDBS	0.0049	0.0112	
16-4-16 (0.7) + 12-4-12A (0.3)	0.0148	0.1023	[24]
16-Eda-16 (0.6) + 12-4-12A (0.4)	0.0147	0.0813	
12-4-12 + SC	0.002	0.014	
14-4-14 + SC	0.004	0.021	
16-4-16 + SC	0.005	0.030	
12-Eda-12 + SC	0.002	0.011	
14-Eda-14 + SC	0.003	0.016	
16-Eda-16 + SC	0.004	0.023	[25]
12-4-12 + SDC	0.002	0.013	
14-4-14 + SDC	0.003	0.020	
16-4-16 + SDC	0.005	0.029	
12-Eda-12 + SDC	0.002	0.011	
14-Eda-14 + SDC	0.003	0.015	
16-Eda-16 + SDC	0.004	0.023	
16-4-16 (0.6) + 12-4-12A (0.4)	**0.0321**	**0.1706**	[39]
16-Isb-16 (0.4) + 12-4-12A (0.6)	0.0276	0.0853 (0.4 $x_{12\text{-}4\text{-}12A}$)	
16-Eda-16 + 12-4-12A	**0.031**	**0.170**	[Present study]
16-Eg-16 (0.4) + 12-4-12A (0.6)	0.0154	0.032 (0.4 $x_{12\text{-}4\text{-}12A}$)	

Table 7
MSR values of anthracene and pyrene individually and their mutual presence at various mole fractions of gemini mixtures.

$x_{12\text{-}4\text{-}12\text{-}A}$	Morphology	MSR			
		Anth	Anth-Pyr	Pyr	Pyr-Anth
16-Eda-16					
0.8	Ellipsoidal	0.010	0.013	0.041	0.062
0.6	Vesicles	0.022	0.026	0.096	0.058
0.5	Vesicles	**0.031**	**0.049**	**0.170**	**0.171**
0.4	Vesicles	0.016	0.023	0.102	0.044
0.2	Ellipsoidal	0.011	0.013	0.062	0.048
0.0	Ellipsoidal	0.009	0.011	0.057	0.035
16-Eg-16					
0.8	Ellipsoidal	0.0012	0.009	0.011	0.014
0.6	Ellipsoidal	**0.0154**	**0.018**	0.008	0.019
0.4	Ellipsoidal	0.0051	**0.015**	**0.032**	0.046
0.2	Ellipsoidal	0.0038	0.016	0.007	0.039
0.0	Ellipsoidal	0.0032	0.011	0.016	0.040

Bold means maximum MSR in a typical mixed system.

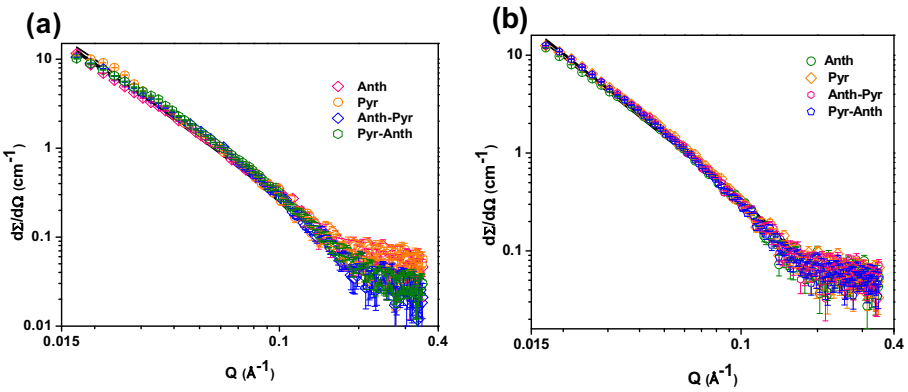

Fig. 10. SANS spectra of 10 mM aqueous mixed gemini surfactant system (16-Eda-16 + 12-4-12A) after solubilizing PAHs (a) 0.4 $x_{16\text{-Eda-}16}$ (b) 0.6 $x_{16\text{-Eda-}16}$.

reported for typical PAH (anthracene or pyrene) have been compiled and compared with the present surfactant systems (Table 6) [23–25,39,55,56]. Moreover, one of the systems (having 16-Eda-16 + 12-4-12A) shown similar efficacy (towards vesicle formation as well as MSR) though it contains a biodegradable spacer (-Eda-) [23]. This indicates that less biodegradable spacer containing gemini can be replaced by the above system without losing the efficacy towards hydrophobic molecule solubilization. To get insight regarding the site of solubilization, co solubilization (solubilization of one PAH in presence of other) experiment has also been performed and the data are discussed.

3.5. Co-solubilization of PAHs in the mixed gemini surfactant system

Co-solubilization of a pair of PAHs (pyrene and anthracene) are performed in two gemini mixtures (one each from polymethylene/Eda and Isb/Eg). The co-solubilization data are compiled in Table 7. Data show that solubilization of an individual PAH can increase or decrease on co-solubilization of another PAHs. As mentioned earlier, the solubilization site of a particular PAH has a role to play in the co-solubilization of more than one PAH. If the solubilization site is common for the PAHs in the pair, the solubilization content of one of them may decrease. However, if the two PAHs has different micellar solubilization sites, their mutual presence may increase solubilization content due to increased hydrophobic interactions caused by the presence of PAHs. This indeed was observed in Table 7. Here, MSR values of anthracene increase in presence of pyrene. Additionally, pyrene solubilization (singly or with anthracene) shows increase or decrease depending upon system composition. However, the vesicular system shows a significant increase in MSR of anthracene in presence of pyrene. Contrary to this, MSR of pyrene shows composition dependence in presence of anthracene. A detailed study is needed to get further insight.

3.6. Vesicles size variation after PAH solubilization

As mentioned above, vesicular systems show higher solubilization efficacy with each PAH. SANS data (Fig. 10) are collected in order to get an idea about the vesicle thickness variation on solubilizing PAH.

Table 8
PAH(s) solubilization effect on Bi-layer thickness of vesicles in aqueous solution at 303 K.

System		Bi-layer thickness (Å)				
	Zeta-potential	Without PAH	Anth	Pyr	Anth-Pyr	Pyr-Anth
0.4 $x_{16\text{-Eda-}16}$	−44.8	22.0	21.7	22	22.3	21.8
0.6 $x_{16\text{-Eda-}16}$	+57.3	23.0	19.7	62.5	22.5	21.2
0.6 $x_{16\text{-4-}16}$	+79.4	25.0	55.4	38.7	–	–

Data of Table 8 show that vesicles forming system have charges of the different signs (+ or −). The negative vesicles show nearly no change in bilayer thickness due to the solubilization of anthracene or pyrene. However, positively charged vesicles show significant changes in bilayer thickness with the solubilization of anthracene or pyrene. This may be due to electrostatic repulsion between electron cloud of PAH and head group charge of the mixed vesicles. In the former case (0.4 $x_{16\text{-eda-}16}$) this repulsion in the vesicular interior has less effect on bilayer thickness as indeed observed. On the other side in case of positive vesicles, one can expect electrostatic attraction between the vesicular head and electron cloud of a typical PAH. This may predominant hydrophobic interaction and responsible for higher bilayer thickness. However, when one PAH is added in presence of another bilayer thickness shows a significant reduction. More data are needed to generalize the trend. It may be mentioned here that electrostatic interaction (repulsion or attraction) may change the polarity of the vesicular aggregates and hence interaction and solubilization site of the PAH. Therefore, aggregate (vesicles or micelle) electrostatics is needed before optimizing the solubilization process for a typical hydrophobic solubilizate. A combined effect of all the above factors seems responsible for the trend shown by the data of Table 7.

4. Conclusion

The study was designed to exploit the nature of the spacer (and composition), in a typical cationic gemini surfactant (one of the components of the oppositely charged gemini mixture), in producing aggregates of varied solubilization efficacies. Both synergistic (−ß) and antagonistic (+ß) interactions are noticed. Zeta (ζ)-potential data show the aggregates of varied electrostatics. However, composition between 0.4 and 0.6 (mole-fraction) shows the formation of vesicles with moderate charge. Heating causes marginal changes in the bi-layer thickness of the vesicular aggregates. Enhanced PAH solubilization has been found in vesicles (tailored by spacer nature/composition). Non-biodegradable spacer containing gemini can be replaced by biodegradable spacer one without affecting solubilization efficacy. MSR (of co-solubilized PAHs) data also show the variation of solubility in simultaneous presence of PAHs as reported earlier [66]. Strategies can be extended for the enhanced solubilization of other hydrophobic materials such as dyes, drugs or pesticides [72–74].

Acknowledgment

Authors are thankful to UGC DAE CSR, Mumbai, India (CRS–M–204), for financial support. Ms. Sneha Singh is thankful for the project fellowship. The Head, Applied Chemistry Department, Faculty of Tech. & Engg., The Maharaja Sayajirao University of Baroda, Vadodara, India, is gratefully acknowledged for research facilities.

Appendix A. Supplementary data

Supplementary data to this article can be found online at https://doi.org/10.1016/j.molliq.2019.01.097.

References

[1] N. Kundu, D. Banik, N. Sarkar, Self-assembly of amphiphiles into vesicles and fibrils: investigation of structure and dynamics using spectroscopy and microscopy techniques, Langmuir 34 (39) (2018) 11637–11654.
[2] P.D. Boyer, B. Chance, L. Ernster, P. Mitchell, E. Racker, E.C. Slater, Oxidative phosphorylation and photophosphorylation, Annu. Rev. Biochem. 46 (1) (1977) 955–966.
[3] D.W. Deamer, The first living systems: a bioenergetic perspective, Microbiol. Mol. Biol. Rev. 61 (2) (1997) 239–261.
[4] P.L. Luisi, P. Walde, T. Oberholzer, Lipid vesicles as possible intermediates in the origin of life, Curr. Opin. Colloid Interface Sci. 4 (1) (1999) 33–39.
[5] S. Fleming, R.V. Ulijn, Design of nanostructures based on aromatic peptide amphiphiles, Chem. Soc. Rev. 43 (23) (2014) 8150–8177.
[6] B. György, M.E. Hung, X.O. Breakefield, J.N. Leonard, Therapeutic applications of extracellular vesicles: clinical promise and open questions, Annu. Rev. Pharmacol. Toxicol. 55 (2015) 439–464.
[7] T.-Han Chou, S.K. Sahoo, Curr. Pharm. Biotechnol. 16 (12) (2015).
[8] L.Y. Zakharova, R.R. Kashapov, T.N. Pashirova, A.B. Mirgorodskaya, O.G. Sinyashin, Self-assembly strategy for the design of soft nanocontainers with controlled properties, Mendeleev Commun. 26 (6) (2016) 457–468.
[9] P. Yark, R. Dimova, Biomimetic Based Applications, Nanoparticle Synthesis in Vesicles Microreactors, InTech, 2011.
[10] P. Tanner, P. Baumann, R. Enea, O. Onaca, C. Palivan, W. Meier, Polymeric vesicles: from drug carriers to nanoreactors and artificial organelles, Acc. Chem. Res. 44 (10) (2011) 1039–1049.
[11] E.W. Kaler, A.K. Murthy, B.E. Rodriguez, J. Zasadzinski, Spontaneous vesicle formation in aqueous mixtures of single-tailed surfactants, Science 245 (4924) (1989) 1371–1374.
[12] E.J. Danoff, X. Wang, S.-H. Tung, N.A. Sinkov, A.M. Kemme, S.R. Raghavan, D.S. English, Surfactant vesicles for high-efficiency capture and separation of charged organic solutes, Langmuir 23 (17) (2007) 8965–8971.
[13] X. Wang, E.J. Danoff, N.A. Sinkov, J.-H. Lee, S.R. Raghavan, D.S. English, Highly efficient capture and long-term encapsulation of dye by catanionic surfactant vesicles, Langmuir 22 (15) (2006) 6461–6464.
[14] L.Y. Zakhrova, A.B. Mirgorodskaya, G.A. Gayanamova, R.R. Kashapov, T.N. Pashirova, E.A. Vasilieva, Yu F. Zuev, O.G. Synyashin, in: A.M. Grumezecu (Ed.), In Encapsulations, 295, Academic Press, London, 2016.
[15] E.W. Kaler, K.L. Herrington, A.K. Murthy, J.A. Zasadzinski, Phase behavior and structures of mixtures of anionic and cationic surfactants, J. Phys. Chem. 96 (16) (1992) 6698–6707.
[16] H. Yin, Z. Zhou, J. Huang, R. Zheng, Y. Zhang, Temperature-induced micelle to vesicle transition in the sodium dodecyl sulfate/dodecyl triethylammonium bromide system, Angew. Chem. Int. Ed. 42 (19) (2003) 2188–2191.
[17] W.R. Hargreaves, D.W. Deamer, Liposomes from ionic, single-chain amphiphiles, Biochemistry 17 (18) (1978) 3759–3768.
[18] J. Gebicki, M. Hicks, Ufasomes are stable particles surrounded by unsaturated fatty acid membranes, Nature 243 (5404) (1973) 232.
[19] Harsha Patel, Studies on Solution Behavior of Surfactants in Presence of Additives, PhD Thesis The Maharaja Sayajirao University of Baroda, 2015.
[20] L. Sreejith, S. Parathakkat, S.M. Nair, S. Kumar, G. Varma, P.A. Hassan, Y. Talmon, Octanol-triggered self-assemblies of the CTAB/KBr system: a microstructural study, J. Phys. Chem. B 115 (3) (2010) 464–470.
[21] J. Karayil, S. Kumar, P. Hassan, Y. Talmon, L. Sreejith, Microstructural transition of aqueous CTAB micelles in the presence of long chain alcohols, RSC Adv. 5 (16) (2015) 12434–12441.
[22] T.S. Davies, A.M. Ketner, S.R. Raghavan, Self-assembly of surfactant vesicles that transform into viscoelastic wormlike micelles upon heating, J. Am. Chem. Soc. 128 (20) (2006) 6669–6675.
[23] W.H. Ansari, N. Fatma, M. Panda, Solubilization of polycyclic aromatic hydrocarbons by novel biodegradable cationic gemini surfactant ethane-1, 2-diyl bis (N, N-dimethyl-N-hexadecylammoniumacetoxy) dichloride and its binary mixtures with conventional surfactants, Soft Matter 9 (5) (2013) 1478–1487.
[24] S.K. Yadav, K. Parikh, S. Kumar, Solubilization potentials of single and mixed oppositely charged gemini surfactants: a case of polycyclic aromatic hydrocarbons, Colloids Surf. A Physicochem. Eng. Asp. 514 (2017) 47–55.
[25] S.K. Yadav, K. Parikh, S. Kumar, Mixed micelle formation of cationic gemini surfactant with anionic bile salt: a PAH solubilization study, Colloids Surf. A Physicochem. Eng. Asp. 522 (2017) 105–112.
[26] S. Lamichhane, K.B. Krishna, R. Sarukkalige, Surfactant-enhanced remediation of polycyclic aromatic hydrocarbons: a review, J. Environ. Manag. 199 (2017) 46–61.
[27] R. Zana, Dimeric and oligomeric surfactants. Behavior at interfaces and in aqueous solution: a review, Adv. Colloid Interf. Sci. 97 (1–3) (2002) 205–253.
[28] a) M.J. Rosen, Gemini: a new generation of surfactants, J. Chemtech. (1993) 30.
b) F.M. Menger, J.S. Keiper, Gemini surfactants, Angew. Chem. Int. Ed. 39 (2000) 1906–1920.
[29] a) D. Kumar, N. Azum, M.A. Rub, A.M. Asiri, Aggregation behavior of sodium salt of ibuprofen with conventional and gemini surfactant, J. Mol. Liq. 262 (2018) 86–96;
b) M.A. Rub, N. Azum, F. Khan, A.M. Asiri, Aggregation of sodium salt of ibuprofen and sodium taurocholate mixture in different media: a tensiometry and fluorometry study, J. Chem. Thermodyn. 121 (2018) 199–210;
c) N. Azum, M.A. Rub, A.M. Asiri, Interaction of triblock-copolymer with cationic gemini and conventional surfactants: a physicochemical study, J. Dispers. Sci. Technol. 38 (2017) 1785–1791;
d) M.A. Rub, N. Azum, A.M. Asiri, Binary mixtures of sodium salt of ibuprofen and selected bile salts: interface, micellar, thermodynamic, and spectroscopic study, J. Chem. Eng. Data 62 (2017) 3216–3228;
e) N. Azum, M.A. Rub, A.M. Asiri, Self-association and micro-environmental properties of sodium salt of ibuprofen with BRIJ-56 under the influence of aqueous/urea solution, J. Dispers. Sci. Technol. 38 (2017) 96–104.
[30] Z. Wang, Y. Li, X.-H. Dong, X. Yu, K. Guo, H. Su, K. Yue, C. Wesdemiotis, S.Z. Cheng, W.-B. Zhang, Giant gemini surfactants based on polystyrene–hydrophilic polyhedral oligomeric silsesquioxane shape amphiphiles: sequential "click" chemistry and solution self-assembly, Chem. Sci. 4 (3) (2013) 1345–1352.
[31] R. Atkin, V. Craig, E.J. Wanless, S. Biggs, Adsorption of 12-s-12 gemini surfactants at the silica-aqueous solution interface, J. Phys. Chem. B 107 (13) (2003) 2978–2985.
[32] J. Wei, G. Huang, S. Wang, S. Zhao, Y. Yao, Improved solubilities of PAHs by multicomponent Gemini surfactant systems with different spacer lengths, Colloids Surf. A Physicochem. Eng. Asp. 423 (2013) 50–57.
[33] A.R. Tehrani-Bagha, H. Oskarsson, C. Van Ginkel, K. Holmberg, Cationic ester-containing gemini surfactants: chemical hydrolysis and biodegradation, J. Colloid Interface Sci. 312 (2) (2007) 444–452.
[34] K. Parikh, B. Mistry, S. Jana, S. Gupta, R.V. Devkar, S. Kumar, Physicochemical studies on cationic gemini surfactants: role of spacer, J. Mol. Liq. 206 (2015) 19–28.
[35] H. Nakahara, H. Nishizaka, K. Iwasaki, Y. Otsuji, M. Sato, K. Matsuoka, O. Shibata, Role of the spacer of Gemini surfactants in solubilization into their micelles, J. Mol. Liq. 244 (2017) 499–505.
[36] F.M. Menger, B.N. Mbadugha, Gemini surfactants with a disaccharide spacer, J. Am. Chem. Soc. 123 (5) (2001) 875–885.
[37] M. Panda, N. Fatma, Enhanced aqueous solubility of polycyclic aromatic hydrocarbons by green diester-linked cationic gemini surfactants and their binary solutions, J. Mol. Struct. 1115 (2016) 109–116.
[38] J. Wei, G. Huang, C. An, H. Yu, Investigation on the solubilization of polycyclic aromatic hydrocarbons in the presence of single and mixed Gemini surfactants, J. Hazard. Mater. 190 (1–3) (2011) 840–847.
[39] S. Singh, A. Bhadoria, K. Parikh, S.K. Yadav, S. Kumar, V.K. Aswal, S. Kumar, Self-assembly in aqueous oppositely charged gemini surfactants: a correlation between morphology and solubilization efficacy, J. Phys. Chem. B 121 (37) (2017) 8756–8766.
[40] V. Aswal, P. Goyal, Small-angle neutron scattering diffractometer at Dhruva reactor, Curr. Sci. 79 (7) (2000) 947–953.
[41] D.I. Svergun, M.H. Koch, Small-angle scattering studies of biological macromolecules in solution, Rep. Prog. Phys. 66 (10) (2003) 1735.
[42] J.S. Pedersen, Analysis of small-angle scattering data from colloids and polymer solutions: modeling and least-squares fitting, Adv. Colloid Interf. Sci. 70 (1997) 171–210.
[43] J.B. Hayter, J. Penfold, An analytic structure factor for macroion solutions, Mol. Phys. 42 (1) (1981) 109–118.
[44] S. Chen, E.Y. Sheu, J. Kalus, H. Hoffman, Small-angle neutron scattering investigation of correlations in charged macromolecular and supramolecular solutions, J. Appl. Crystallogr. 21 (6) (1988) 751–769.
[45] I. Breßler, J. Kohlbrecher, A.F. Thünemann, SASfit: a tool for small-angle scattering data analysis using a library of analytical expressions, J. Appl. Crystallogr. 48 (5) (2015) 1587–1598.
[46] R. Kaur, S. Kumar, V.K. Aswal, R.K. Mahajan, Influence of headgroup on the aggregation and interactional behavior of twin-tailed cationic surfactants with pluronics, Langmuir 29 (38) (2013) 11821–11833.
[47] Y. Moroi, K. Mitsunobu, T. Morisue, Y. Kadobayashi, M. Sakai, Solubilization of benzene, naphthalene, anthracene, and pyrene in 1-dodecane sulfonic acid micelle, J. Phys. Chem. 99 (8) (1995) 2372–2376.
[48] R.A. Friedel, M. Orchin, Ultraviolet Spectra of Aromatic Compounds, Wiley, New York, 1951.
[49] Z. Yaseen, S.U. Rehman, M. Tabish, Interaction between DNA and cationic diester-bonded Gemini surfactants, J. Mol. Liq. 197 (2014) 322–327.
[50] P. Holland, D. Rubingh, Nonideal multicomponent mixed micelle model, J. Phys. Chem. 87 (11) (1983) 1984–1990.
[51] J.H. Clint, Micellization of mixed nonionic surface active agents, J. Chem. Soc. Faraday Trans. 1 Phys. Chem. Condens. Phase 71 (1975) 1327–1334.
[52] D.N. Rubingh, Mixed micelle solutions, Solution Chemistry of Surfactants, Springer 1979, pp. 337–354.
[53] K. Motomura, M. Yamanaka, M. Aratono, Thermodynamic consideration of the mixed micelle of surfactants, Colloid Polym. Sci. 262 (12) (1984) 948–955.
[54] L. Liu, M.J. Rosen, The interaction of some novel diquaternary gemini surfactants with anionic surfactants, J. Colloid Interface Sci. 179 (2) (1996) 454–459.
[55] M. Panda, Solubilization of polycyclic aromatic hydrocarbons by gemini–conventional mixed surfactant systems, J. Mol. Liq. 187 (2013) 106–113.
[56] N. Fatma, M. Panda, W.H. Ansari, Solubility enhancement of anthracene and pyrene in the mixtures of a cleavable cationic gemini surfactant with conventional surfactants of different polarities, Colloid Surf. A 467 (2015) 9–17.
[57] L.L. Brasher, K.L. Herrington, E.W. Kaler, Electrostatic effects on the phase behavior of aqueous cetyltrimethylammonium bromide and sodium octyl sulfate mixtures with added sodium bromide, Langmuir 11 (11) (1995) 4267–4277.

[58] J.N. Israelachvili, D.J. Mitchell, B.W. Ninham, Theory of self-assembly of hydrocarbon amphiphiles into micelles and bilayers, J. Chem. Soc. Faraday Trans. 2: Mol. Chem. Phys. 72 (1976) 1525–1568.
[59] Z. Lin, J. Cai, L. Scriven, H. Davis, Spherical-to-wormlike micelle transition in CTAB solutions, J. Phys. Chem. 98 (23) (1994) 5984–5993.
[60] S. Kumar, V. Aswal, H. Singh, P. Goyal, Growth of sodium dodecyl sulfate micelles in the presence of n-octylamine, Langmuir 10 (11) (1994) 4069–4072.
[61] H. Jung, B. Coldren, J. Zasadzinski, D. Iampietro, E. Kaler, The origins of stability of spontaneous vesicles, Proc. Natl. Acad. Sci. 98 (4) (2001) 1353–1357.
[62] S. Rajkhowa, S. Mahiuddin, J. Dey, S. Kumar, V. Aswal, R. Biswas, J. Kohlbrecher, K. Ismail, The effect of temperature, composition and alcohols on the microstructures of catanionic mixtures of sodium dodecylsulfate and cetyltrimethylammonium bromide in water, Soft Matter 13 (19) (2017) 3556–3567.
[63] R.T. Buwalda, M.C. Stuart, J.B. Engberts, Wormlike micellar and vesicular phases in aqueous solutions of single-tailed surfactants with aromatic counterions, Langmuir 16 (17) (2000) 6780–6786.
[64] Y. Zheng, Z. Lin, J. Zakin, Y. Talmon, H. Davis, L. Scriven, Cryo-TEM imaging the flow-induced transition from vesicles to threadlike micelles, J. Phys. Chem. B 104 (22) (2000) 5263–5271.
[65] X. Ji, M. Tian, Y. Wang, Temperature-induced aggregate transitions in mixtures of cationic ammonium Gemini surfactant with anionic glutamic acid surfactant in aqueous solution, Langmuir 32 (4) (2016) 972–981.
[66] R. Masrat, M. Maswal, A.A. Dar, Competitive solubilization of naphthalene and pyrene in various micellar systems, J. Hazard. Mater. 244 (2013) 662–670.
[67] R. Nagarajan, Solubilization by amphiphilar aggregates, Curr. Opin. Colloid Interface Sci. 2 (3) (1997) 282–293.
[68] C.V. Teixeira, R. Itri, L.Q. do Amaral, Micellar shape transformation induced by decanol: a study by small-angle x-ray scattering (SAXS), Langmuir 16 (15) (2000) 6102–6109.
[69] G. Cerichelli, G. Mancini, Role of counterions in the solubilization of benzene by cetyltrimethylammonium aggregates. A multinuclear NMR investigation, Langmuir 16 (1) (2000) 182–187.
[70] X. Liang, C. Guo, S. Liu, Z. Dang, Y. Wei, X. Yi, S. Abel, Cosolubilization of phenanthrene and pyrene in surfactant micelles: experimental and atomistic simulations studies, J. Mol. Liq. 263 (2018) 1–9.
[71] S. Singh, S.K. Yadav, K. Parikh, A. Desai, S. Dixit, S. Kumar, Mixed micellization/clouding assisted solubilization of polycyclic aromatic hydrocarbon: potential in environmental remediation, J. Mol. Liq. 272 (2018) 413–422.
[72] H. Uchiyama, A. Srivastava, M. Fujimori, K. Tomoo, A. Nakanishi, M. Tandia, K. Kadota, Y. Tozuka, Investigation of physiological properties of transglycosylated stevia with cationic surfactant and its application to enhance the solubility of rebamipide, J. Phys. Chem. B (2018)https://doi.org/10.1021/acs.jpcb.8b07515.
[73] A. Shah, S. Shahzad, A. Munir, M.N. Nadagouda, G.S. Khan, D.F. Shams, D.D. Dionysiou, U.A. Rana, Micelles as soil and water decontaminations, Chem. Rev. 116 (2016) 6042–6074.
[74] H. Sun, J. Jiang, Y. Xioa, J. Du, Efficient removal of polycyclic aromatic hydrocarbons, dyes, and heavy metal ions by a homopolymer vesicle, ACS Appl. Mater. Interfaces 10 (2018) 713–722.

Journal of Molecular Liquids 272 (2018) 413–422

Contents lists available at ScienceDirect

Journal of Molecular Liquids

journal homepage: www.elsevier.com/locate/molliq

Mixed micellization/clouding assisted solubilization of polycyclic aromatic hydrocarbon: Potential in environmental remediation

Sneha Singh [a], Sanjay Kumar Yadav [b], Kushan Parikh [c], Arpita Desai [b], Sandhya Dixit [a], Sanjeev Kumar [a,*]

[a] Department of Applied Chemistry, Faculty of Technology & Engineering, The Maharaja Sayajirao University of Baroda, Vadodara 390 001, India
[b] Department of Chemistry, Faculty of Science, The Maharaja Sayajirao University of Baroda, Vadodara 390 002, India
[c] Department of Industrial Chemistry, Faculty of Life, Health & Allied Science, ITM Vocational University, Vadodara 391 760, India

ARTICLE INFO

Article history:
Received 3 July 2018
Received in revised form 31 August 2018
Accepted 4 September 2018
Available online 06 September 2018

ABSTRACT

Micellization and clouding behaviors of an anionic gemini surfactant, *phosphoric acid*, P, P′ *1,4 butanedieyl* P, P ′ *didodecyl ester*, *disodium salt* (12-4-12A), in aqueous solution, have been investigated in the presence of a surface active ionic liquid (SAIL), *tetra n pentylammonium bromide* (TPeAB). Critical micelle concentration and ^{1}H NMR data show synergistic interactions/intercalation of *n* pentyl chain between the 12-4-12A monomers constituting the micelle, respectively. 12-4-12A + TPeAB system showed the cloud point (CP) at distinctly lower [12-4-12A]. Amino acid/cyclodextrin has been used to tune the CP. DLS and TEM data suggest the formation of *n* pentyl chain (of the SAIL) mediated linked aggregates whose size decreases with lowering [TPeAB] while compactness increases by β-CD. POM data showed that larger aggregates are formed near the CP. This may be due to increased hydrophobic interactions (between dodecyl chains of the gemini and pentyl chains of the TPeAB) and decreased electrostatic repulsion (as indicated by lowering zeta-potential value at CP). Mixtures, with or without β-CD, are used for solubilization/*co* solubilization of polyaromatic hydrocarbon (PAHs-anthracene, pyrene or fluorene). Molar solubilization ratio (MSR) has been computed using UV–Visible spectrophotometry. The percentage MSR value increases in order: Anthracene > Pyrene > Fluorene in comparison to pure 12-4-12A. Cloud point extraction of anthracene shows that it concentrates ~93% in surfactant rich phase (SRP). However, anthracene content decreases (~80%) when the system contains β-CD. $GZrO_2$ nanocomposite has shown nearly complete adsorption of anthracene. Strategies, like mixed micellization, tuning of clouding and co-solubilization, can enhance solubility/bioavailability, extraction and subsequent degradation of PAHs from the aquatic/soil environment.

1. Introduction

Micellization, clouding, and solubilization represent among the three important phenomena shown by surfactants (above their critical micellar concentration, *cmc*) in aqueous solution. Mixing oppositely charged amphiphilic molecules in aqueous solution generates self-assembly with the feature of heating response. In various applications, oppositely charged surfactant mixtures produce a synergistic effect (*e.g.*, decrease in *cmc* [1]). Many reports are available regarding the solution behavior of the mixing of conventional surfactants with gemini or dimeric ones [2]. However, mixing of surface active ionic liquids with conventional or gemini surfactants has not been studied many times [3–6].

Most non-ionic surfactant solutions turn cloudy at a specific temperature known as *cloud point*, CP. For ionic surfactants, the phenomenon occasionally occurs, presumably due the presence of electrostatic repulsions which prevents micelles to come close to each other [7]. Moreover, addition of a few symmetrical and unsymmetrical quaternary salts (ionic liquids) to the anionic surfactant solution causes CP phenomenon under certain range of concentration [8,9]. The phenomenon has also been reported in surfactants systems where tetra-n-butyl ammonium/phosphonium (TBA^+/TBP^+) was part (counter ion) of the anionic surfactant molecule [10–13].

The above intriguing clouding behavior of ionic surfactant solution has been explained in terms of Van der Waals and electrostatic attractions, penetration effect of alkyl/phenyl chains/rings (of quaternary counter-ion) and solvation/hydration [12]. The alkyl chains of quaternary counter-ion may get penetrate between monomers of the micelle due to hydrophobic interactions. However, geometric constants make it difficult for all alkyl chains (of the salt) to penetrate the micellar surface. Two directions may be chosen for partitioning of alkyl chains: one is towards bulk aqueous phase and the other towards micellar interior

* Corresponding author at: Department of Applied Chemistry, Faculty of Technology & Engineering, The Maharaja Sayajirao University of Baroda, Vadodara 390 001, Gujarat, India.
E-mail address: sanjeevkumar-appchem@msubaroda.ac.in (S. Kumar).

https://doi.org/10.1016/j.molliq.2018.09.022
0167-7322/

[14]. Alkyl chains towards bulk water may produce a temporary hydrophobic region at the micellar surface [15]. This temporary region may be utilized as an additional site to enhance solubilization potential of the hydrophobic material [16]. The above clouding behavior (of the water-based system) seems more biocompatible and greener than the routinely used hazardous organic solvent-based extraction [17]. However, additive could provide a further control on the CP, and enhance the potential of clouding phenomenon using charged micellar solution [18].

Polycyclic aromatic hydrocarbons (PAHs) are persistent organic matter present in the soil sediments and aquatic environment [19]. Significant interest has been shown by various groups to remove them from the contaminated site [20]. The micellar system has a hydrophobic region which can accumulate PAH with a concomitant increase in water solubility and can be a potential method in solubilizing and removing PAHs [21–24].

Gemini or dimeric surfactant, with special molecular architecture, [25] may bring out a few novel solution behaviors including clouding phenomenon. Gemini micelle can strongly bind with counter-ion which can facilitate requirement of clouding phenomenon according to Kalur and Raghavan [26]. Further, presence of spacer can provide additional interaction features with another amphiphilic molecule or additive [27,28]. These factors may facilitate clouding phenomenon, however, only a few reports are available on clouding phenomenon in ionic gemini surfactant solution having oppositely charged surfactant or ionic liquid [5,27,29]. In one of the above studies, [5] surface active ionic liquid (tetra *n* propyl ammonium bromide) is required in large excess (~500 mM) to achieve the CP with anionic gemini surfactant.

In another study [27], the phenomenon was observed during the morphological transitions, in aqueous oppositely charged ionic surfactants, and clouding was not the focus of the study. The work reported here is, therefore, relevant not only to increase the understanding of mixed micellization or clouding phenomenon but also to improve the utilization of gemini based systems (with surface active ionic liquid with or without additives) for the solubilization (and hence increased bio-availability) of hydrophobic compound (*e.g.*, PAH).

This study is aimed at the mixing of anionic gemini surfactant, *phosphoric acid*, P,P′ *1,4 butanedieyl* P,P′ *didodecyl ester*, *disodium salt* (12-4-12A) with surface active ionic liquid (SAIL, *tetra n pentylammonium bromide*, TPeAB) with respect to their micellization, interaction, clouding (with and without additives) and solubilization potential. The investigations have been performed to determine: i) *cmc* of single and mixed systems, ii) CP – [gemini]/[TPeAB] correlation, iii) influence of additive (amino acid or cyclodextrin) on CP, iv) molar solubilization ratio (MSR) with individual and their simultaneous presence (in pairs) at 30 °C or just below the CP (40 °C), v) CP extraction of anthracene in surfactant rich phase (SRP) and vi) adsorption of extracted anthracene from the SRP to graphene-Zirconium Oxide ($GZrO_2$-NC) nanocomposite. Recently, cyclodextrin solutions have also been used for the extraction of various PAHs from the contaminated soil [30]. Being among first few reports, it is desirable to get insight into the synergistic exploitation of oppositely charged amphiphilic system (anionic gemini + SAIL with or without additive) which shows clouding. The system has been found to facilitate PAH solubilization in the single or binary state (co-solubilization). Clouding at low temperature/concentration may find use in cloud point extraction/purification of various charged/neutral and thermally labile hydrophobic molecules (*e.g.*, biomolecules) [18,31,32].

2. Experimental section

2.1. Materials

Synthesis and characterization of diphosphate anionic gemini surfactant (12-4-12A) has been reported elsewhere [22]. The purity of 12-4-12A was ensured by the absence of minimum in surface tension (γ) *vs* log [12-4-12A] (Fig. S1. see supplementary information). TPeAB

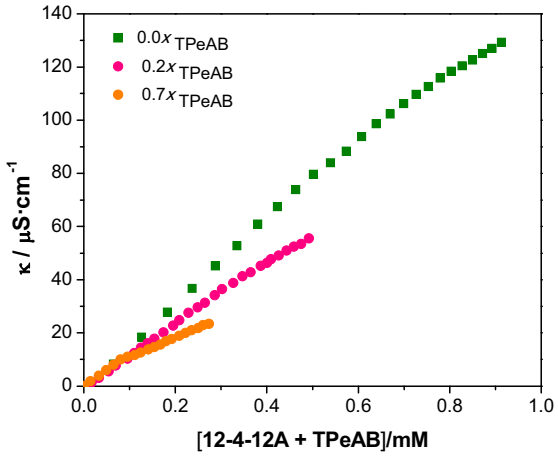

Fig. 1. Plot of specific conductance (κ) *vs* concentration of pure 12-4-12A and representative12-4-12A+ TPeAB mixed systems at two different mole fractions of surface active ionic liquid (x_{TPeAB}) in aqueous solution at 30 °C.

(≥99%, Sigma-Aldrich, St. Louis, MO, USA), Glycine (≥99%, Sigma-Aldrich, St. Louis, MO, USA), L-leucine (≥98%, Sigma-Aldrich, St. Louis, MO, USA), L phenylalanine (≥99%, Sigma-Aldrich, St. Louis, MO, USA), α cyclodextrin (98%, Spectrochem, Mumbai, India), β cyclodextrin (99%, Spectrochem, Mumbai, India), Graphite fine powder extra pure and Zirconium acetate [Zr $(CH_3COO)_2$] purchased from Loba Chemie Pvt. Ltd., Mumbai, India. The water, used in preparing the sample solution, was double-distilled in an all-glass distillation setup (specific conductivity within 1–2 $\mu S \cdot cm^{-1}$). Various surfactant + quaternary salt solutions were prepared by taking requisite amounts of surfactant and quaternary salt and making up the volumes with distilled water.

Graphene-Zirconium oxide nanocomposite ($GZrO_2$-NC) has been synthesized and characterized as reported earlier [33].

2.2. Methods

2.2.1. Conductivity measurement

Conductometric measurements are performed by a conductivity meter (EUTECH cyber scan CON510 (cell constant 1 cm^{-1})) with an in-built temperature sensor. A pre-calibrated conductivity cell was used to get specific conductance at an appropriate concentration range. The sample temperature has been precisely maintained by a SCHOTT CT 1650 thermostat with an accuracy of ±0.1 °C. The cell with an appropriate amount of water (in a vessel) is thermostat for at least 30 min before starting the measurement. The conductivity runs were carried out by adding a concentrated surfactant solution to the water. The *cmc* values for the 12-4-12A and TPeAB (Fig. S1(b)) are determined from the intersection point of two straight lines (in the plot of the specific conductance (κ) *vs* [surfactant]) and the ratio of the slopes of the post-micellar to that of the pre-micellar portions of the plot, respectively.

2.2.2. Surface tension measurement

cmc values are also determined from surface tension measurements (at 30 ± 0.1 °C) using a Du-Nouy detachment tensiometer (Win – Son & Co., Kolkata) with a platinum (gold joint) ring. The tensiometer was calibrated using double distilled water. A known volume of water was

Table 1
Critical micelle concentration (*cmc*) of anionic gemini surfactant (12-4-12A) and surface active ionic liquid (TPeAB).

Surfactants	*cmc* (mM)	
	Conductometry	Tensiometry
12-4-12A	0.55	0.50
TPeAB	20.5	20.6

Table 2
Micellization parameters (critical micelle concentration, *cmc*, by conductometrically) and interaction parameters (by using Rubingh's method) of mixed system (12-4-12A and TPeAB) at different mole fraction (x) in aqueous solution at 30 °C.

x_{TPeAB}	cmc_{exp} (mM)	cmc_{ideal} (mM)	X_1^m	X_{ideal}	β^m
0.0	0.55	–	–	–	–
0.2	0.30	1.46	0.743	0.993	−8.10
0.33	0.12	1.23	0.651	0.987	−12.39
0.5	0.10	0.93	0.619	0.974	−13.19
0.6	0.08	0.76	0.598	0.961	−14.41
0.71	0.07	0.56	0.578	0.939	−15.46
1.0	20.5	–	–	–	–

added to a vessel containing a stock solution (30 ml) of 12-4-12A or TPeAB. Solutions were stirred every time carefully to check the foaming. Set of three successive observations was recorded at each concentration (deviation was ±0.2 mN/m).

2.2.3. NMR measurement

^{1}H NMR spectra were obtained with Bruker NMR spectrometer with a proton resonance frequency of 400.15 MHz at 298 K. The experimental details are given elsewhere [12].

2.2.4. Cloud point (CP) measurement

Cloud point (CP) data are acquired by placing samples containing 12-4-12A solutions, with a fixed concentration of SAIL, into a temperature-controlling thermostat (SCHOTT CT 1650). The temperature of the sample solution was precisely controlled with an accuracy of ±0.1 °C. Temperatures at onset and disappearance of turbidity (visual observation) have been noted (by adopting heating-cooling cycle). The average of above two temperatures was taken as the CP. The measurement was repeated for the same sample and nearly two concurrent values (within ±0.1 °C) were considered as the final CP. Similar CP measurements were made on different fixed concentrations of 12-4-12A and varying the [TPeAB]. The method was also adopted to get CPs in the presence of amino acid/cyclodextrin.

2.2.5. Dynamic light scattering (DLS) and zeta (ζ)-potential measurements

Average hydrodynamic diameter (D_h) and Zeta (ζ) - potential measurements were performed on a SZ-100 nanoparticle size analyzer (HORIBA, Japan). This instrument is equipped with a green (5320 Å) laser and photomultiplier tube detectors. The technique is based on the time dependent fluctuation in the intensity of scattered light through a suspension of particles under random motion. Analysis of intensity fluctuation allows to compute diffusion coefficients which are used in Storks-Einstein for the determination of the D_h. About 0.5 ml of sample solution was transferred into dipped electrode plastic cuvette through nylon membrane filter (0.22 μm) and placed in a sample chamber. Data are average of 5 decay cycles (each decay cycle is of 5 runs with a 5 s interval).

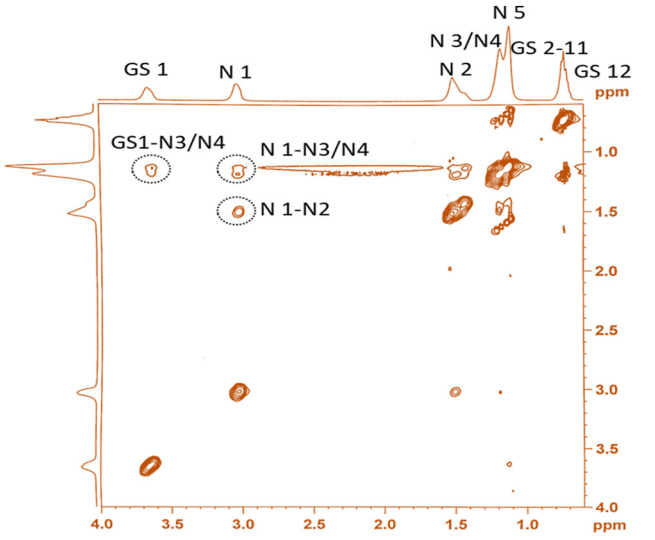

Fig. 3. 2D NOESY ^{1}H NMR spectra of mixed system (2 mM 12-4-12 A + 2 mM TPeAB) in D_2O.

2.2.6. Transmission electron microscopy (TEM)

TEM images were obtained with a JEOL JEM 2100 transmission electron microscope accelerating at a voltage of 120 kV. Other experimental details are same as reported elsewhere [23].

2.2.7. Polarizing optical microscopy

To visualize the aggregates and their transformation at higher temperature (~CP), Polarizing optical microscope (POM), Nikon eclipse Ci POL microscope fitted with Linkem heating stage was used.

2.2.8. Solubilization experiment

The solubility of PAHs has been determined in aqueous surfactant + ionic liquid system (single or mixed) by adding an excess amount of PAH (fluorene; Flu, anthracene; Anth or pyrene; Pyr: physical data are provided in Table S1, see the Supplementary Information). Aqueous 12-4-12A + PAH (or 12-4-12A with TPeAB + PAH) mixture has been

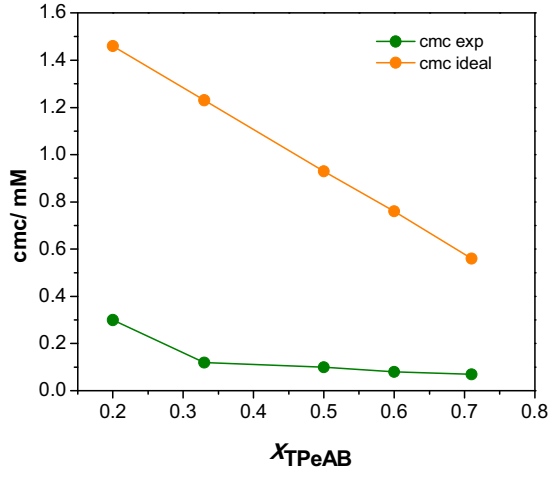

Fig. 2. Critical micelle concentration (*cmc*, by conductometrically) variation of mixed system (12-4-12A + TPeAB) with mole fraction of TPeAB (x_{TPeAB}) in aqueous solution at 30 °C. The plot represents experimental and ideal values (calculated from Clint model).

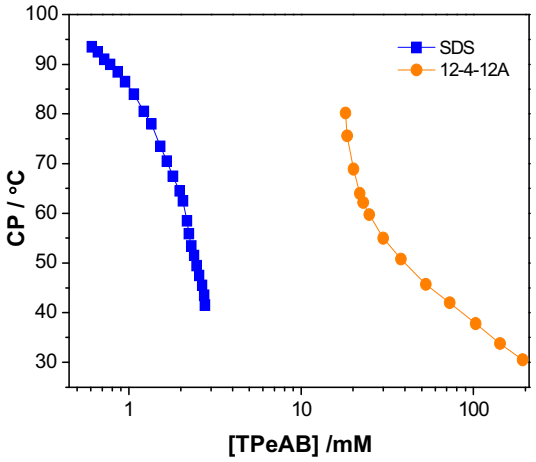

Fig. 4. Cloud Point (CP) of anionic conventional (sodium dodecylsulfate, SDS) and gemini surfactant (12-4-12A) as function of concentration of TPeAB.

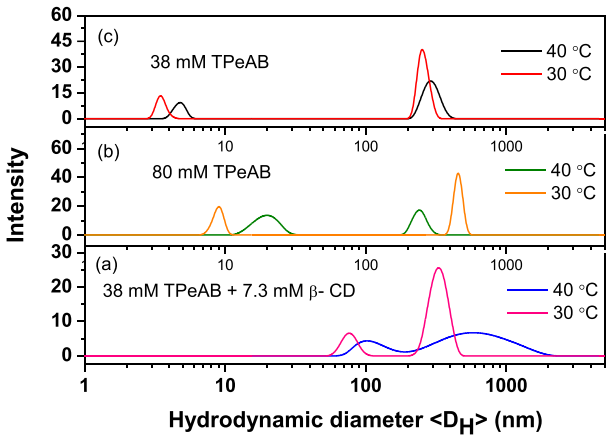

Fig. 5. DLS data for 2 mM 12-4-12A + 38 mM (or 80 mM) TPeAB with (a) and without β-CD (b, c).

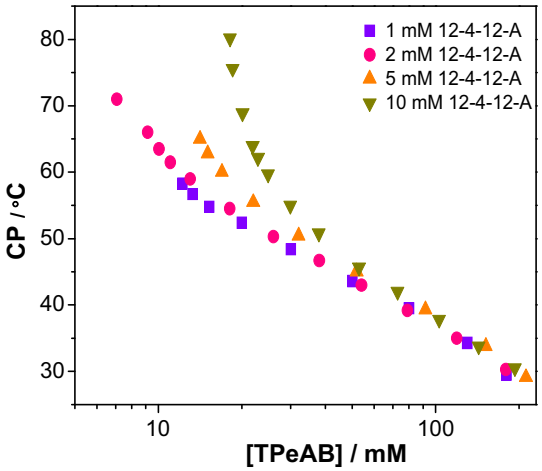

Fig. 6. Cloud point (CP) variations, for different concentrations of 12-4-12-A, with [TPeAB].

equilibrated for 48 h before centrifugation to remove excess PAH. The solubilization of PAH in micellar solution has been analyzed, at respective λ_{max}, by UV–Visible spectrophotometer (Shimadzu, UV-2450) having a quartz cell (path length 1 cm) at 303 K. The composition of the surfactant (or mixture) was the same in both reference and measurement cell to remove its effect on the UV-absorbance. Concentrations of PAH are calculated by Lambert-Beer law (using respective molar extinction coefficients (ε) values of each PAH) [34,35]. The molar solubilization ratio (MSR) is the number of moles of the PAH solubilized per mole of the gemini present in the solution. MSR can be calculated by using following equation,

$$\mathrm{MSR} = \frac{(S_t - S_{cmc})}{(C_t - C_{cmc})} \quad (1)$$

where, S_t is the total PAH solubility in the mixture system at a particular total surfactant concentration C_t. S_{cmc} is the solubility of the PAH at the cmc of the mixture (C_{cmc}).

2.2.9. Extraction/adsorption experiment

A typical PAH (*e.g.*, Anthracene) has been extracted from the surfactant solution by standing it 20 °C above its CP (40 °C). The SRP has been separated and diluted to determine the extracted content of anthracene using spectrophotometry as given in the earlier section. The SRP is also used for adsorption experiment using $GZrO_2$-NC.

3. Results and discussion

3.1. Micellization behavior

3.1.1. Micellization of single 12-4-12A/TPeAB

Conductometry (Fig. 1) and Tensiometry (Fig. S1a see supplementary information) result almost similar *cmcs* (Table 1) which indicate the validity of the measurement. However, a little variation in *cmc* values is mainly due to the nature of the technique and its response to the micellization (surface tension is mainly sensitive to [monomeric] form as micelles are non-surface active while conductance depends on the mobilities of ionic species). TPeAB has much higher cmc than 12-4-12A. This may be due to four short n-pentyl chains which may hinder the packing in TPeAB micelles. The absence of minima in Fig. S1a ensures the purity of the 12-4-12A. In the solution, TPeAB furnishes $TPeA^+$ (+vely charged surface-active species) and Br^-. This can interact with anionic micelle (of 12-4-12A) and produces synergistic interactions (electrostatic interaction). In the next section, such interactions are studied by *cmc* measurements (conductometrically) at various mole fractions of 12-4-12A and TPeAB.

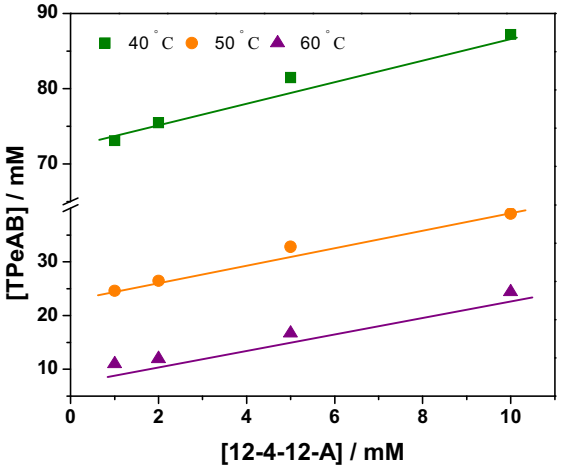

Fig. 7. Interplay between [12-4-12A] and [TPeAB] to obtain CP at 40, 50 or 60 °C.

Table 3
Average hydrodynamic data (<D_H>) and Zeta (ζ)-potential values for various mixed System at two different temperatures (*T*).

System	<D_H>		ζ-potential	
	30 °C	40 °C	30 °C	40 °C
2 mM 12-4-12A + 80 mM TPeAB	9.1, 461	19.8, 252	−2.6	−1.2
2 mM 12-4-12A + 38 mM TPeAB	3.7, 256	4.8, 295	−13.4	−9.2
2 mM 12-4-12A + 38 mM TPeAB + 7.3 mM β-CD	75.2, 328	101.5, 602	−14.3	−12.3

Table 4
Linear Regression data for conventional (SDS) and gemini (12-4-12A) surfactant for the interplay of [surfactant] – [TPeAB] to get CP at different temperature (40–70 °C).

CP (°C)	SDS[a]			12-4-12 A[b]		
	S	I	R	S	I	R
40	–	–	–	1.55	72.35	0.984
50	0.279	2.877	0.997	1.60	23.48	0.986
60	–	–	–	1.51	9.20	0.998
70	0.271	1.448	0.998	–	–	–

[a] Data taken from#8.
[b] Data taken from Fig. 8.

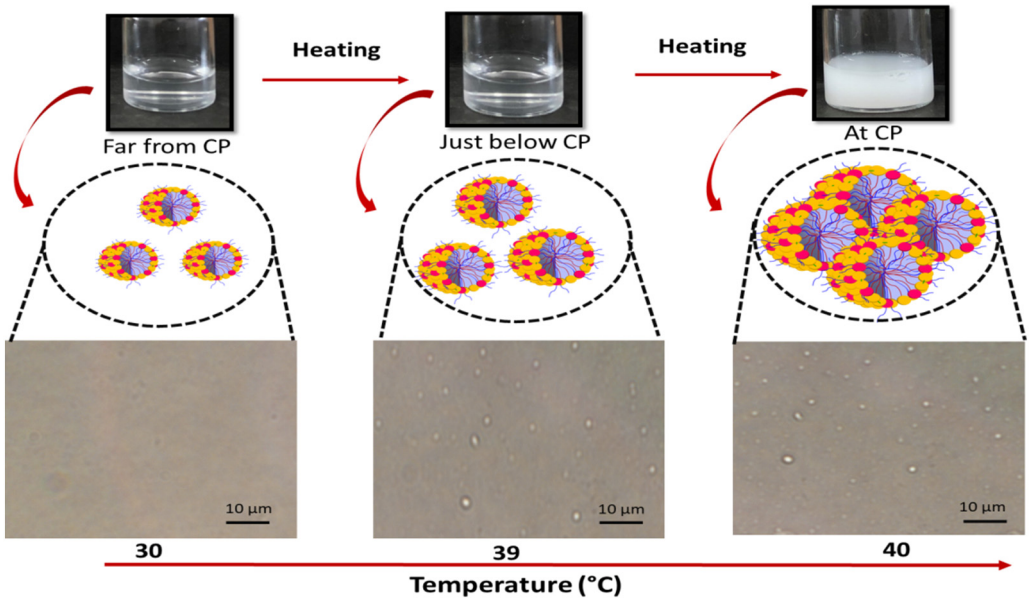

Fig. 8. Polarizing optical micrographs of 2 mM 12-4-12A + 80 mM TPeAB aqueous system at different temperatures.

3.1.2. Mixed Micellization of 12-4-12A with TPeAB

cmc measurements (Fig. 1) have also been performed in the mixed aqueous system (12-4-12A + TPeAB) at various mole fractions and data are compiled in Table 2. CMC variation with a mole fraction of added TPeAB, to12-4-12A, has been shown in Fig. 2. A pseudo phase separation model has been applied to evaluate how the *cmcs* of binary mixtures (12-4-12A + TPeAB) deviate from the ideal mixing [36]. The *cmc* values of the mixture (cmc_{exp}) are found lower than the individual components of the mixture (12-4-12A(cmc_1) or TPeAB (cmc_2)). For a mixture of oppositely charged surfactant and surface active ionic liquid (TPeAB), a relation (Eq. (2)) exists for ideal mixing [37].

$$\frac{1}{cmc_i} = \frac{x_1}{cmc_1} + \frac{x_2}{cmc_2} \tag{2}$$

where, x_1 and x_2 are mole fractions of 12-4-12A and TPeAB, respectively. The *cmc* for ideal mixing (cmc_i) of oppositely charged components can be determined using Eq. (1). The negative variation of cmc_{exp} from cmc_i (Fig. 2) indicates synergistic interaction in various mixtures (Table 2). Following expression (Eq. (3)) has been proposed based on regular solution theory [38].

$$\frac{\left[(X_1^m)^2 \ln\left(cmc_{exp}x_1/cmc_1X_1^m\right)\right]}{(1-X_1^m)^2\left[cmc_{exp}(1-x_1)/cmc_2(1-X_1^m)\right]} = 1 \tag{3}$$

X_1^m denotes the mole fraction of 12-4-12A in the mixed micelle. The Ideal micelle mole fraction of 12-4-12A (X_1^i) can be calculated using Motomura's approximation [39].

$$X_1^i = \frac{x_1 cmc_2}{x_1 cmc_2 + (1-x_1)cmc_1} \tag{4}$$

Mostly, the interaction parameter (β^m) has been used to understand the nature and strength of the interactions between different amphiphilic molecules (constituting the mixture) and can be obtained by applying following expression (Eq. (5)) [40],

$$\beta^m = \left[\ln\left(cmc_e p_1/cmc_1X_1^m\right)\right]/(1-X_1^m)^2 \tag{5}$$

As cmc_{exp} has been found lower than the cmc_i, β^mvalues are expected to be negative in each case (synergistic effect). This indeed was

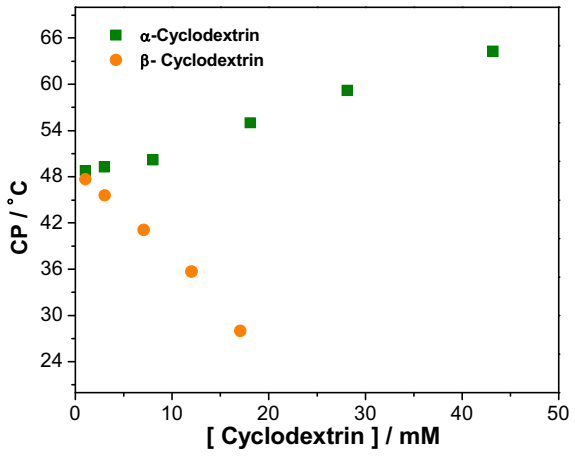

Fig. 9. Variations of Cloud point (CP) for 2 mM 12-4-12-A + 38 mM TPeAB aqueous system with [Cyclodextrin].

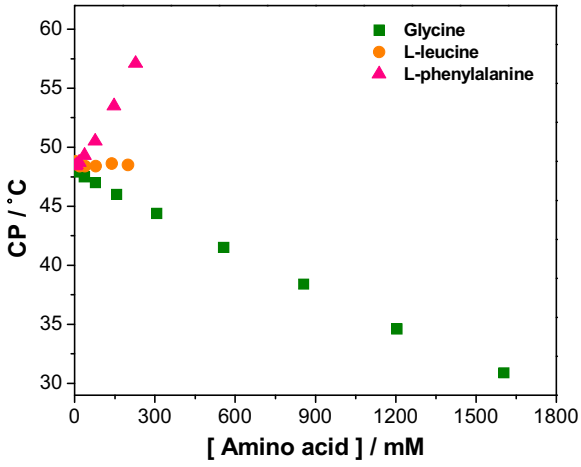

Fig. 10. Variation of Cloud point (CP) for 2 mM 12-4-12-A + 38 mM TPeAB aqueous system with [amino acid].

Table 5
Molar Solubilization Ratio (MSR) of PAHs in different aqueous single and mixed (12-4-12A + TPeAB) system at room temperature (30 °C) and near cloud point (39 °C).

Systems	MSR					
	Anthracene		Pyrene		Fluorene	
	30 °C	39 °C (~CP)	30 °C	39 °C (~CP)	30 °C	39 °C (~CP)
TPeAB (80 mM)	0.000042	0.000063	–	–	–	–
12-4-12A	0.0012	0.0024	0.0061	–	0.0205	–
12-4-12A (10 mM)	0.0261	0.0293	0.0381	–	0.0910	–
12-4-12A(1 mM) + TPeAB (80 mM)	0.0103	0.0115	–	–	–	–
12-4-12A (2 mM) + TPeAB (80 mM)	0.0119	0.0143	0.113	0.122	0.165	0.210
12-4-12A (5 mM) + TPeAB (80 mM)	0.0058	0.0066	–	–	–	–
12-4-12A(10 mM) + TPeAB (86 mM)	0.0032	0.0046	–	–	–	–
12-4-12A (2 mM) + TPeAB(38 mM) + β Cyclodextrine(7.3 mM)	0.0226	0.0264	0.0817	0.0896	–	–

observed (Table 2). The behavior is the result of the packing of TPeAB and 12-4-12A monomers in the mixed micelle (and the resultant cmc_{exp}). The data related to cmc_{exp}, cmc_i, cmc_1, cmc_2, X_1^m, X_1^i and β^m are tabulated in Table 2.

2D NOESY spectra of 12-4-12A + TPeAB solution have been shown in Fig. 3. Details of various peaks and respective protons for 12-4-12A and TPeAB are given (Fig. S2 see the supplementary information) in the spectra. Intermolecular interaction is clearly reflected from the cross peaks shown in 2D NOESY spectra. Cross peaks between N1-N3/N4, N1-N2, and GS1-N3/N4 protons show space interaction which indicates the intercalation of pentyl chain of $TPeA^+$ between gemini monomers of the micelle. Probably this interaction of the chains (pentyl and dodecyl of SAIL and gemini, respectively) is responsible for negative β_m (synergistic effect) as has been discussed above.

3.2. Clouding behavior

3.2.1. Clouding phenomenon in aqueous 12-4-12A with TPeAB

Many SAILs (quaternary salts) have been tried in combination with 12-4-12A to observe the appearance of the clouding phenomenon at elevated temperature. However, the phenomenon has been observed only with TPeAB. Fig. 4 shows the variation of CP, with the addition of TPeAB to solutions of 12-4-12A and sodium dodecylsulphate (SDS). A perusal of CP data shows that more amount of TPeAB is required to observe CP with 12-4-12A than SDS (for equal [surfactant], 10 mM). This may be due to the fact that 12-4-12A has two anionic $-PO_4^-$ head groups which require more SAIL (TPeAB) to neutralize the head group (s) charge. Further, nature of head group ($-PO_4^-$ or $-SO_4^-$) may also influence its interaction with the TPeA+ and may contribute in the requirement of higher concentration of TPeAB to produce clouding. [41] Above two interrelated factors seem responsible for the behavior shown in Fig. 4. A detailed mechanism of the appearance of clouding phenomenon in the ionic surfactant solution, with such quaternary salts, has been reported elsewhere [11,12]. The $TPeA^+$ contains four *n* pentyl chains, in addition to a positive charge on the central N-atom, therefore, the cation can interact with the negatively charged micellar surface (electrostatically) as well as interior part of the anionic micelle (hydrophobically). Due to above interactions, micelles would be of much lower charge (pseudo–nonionic) and larger size (with close interactions among them through pentyl chains). All these factors are responsible for dehydrated micelle and the observed clouding behavior. The mechanism is well supported by earlier findings [7,10,14,42]. DLS and zeta-potential data (Fig. 5 and Table 3) support the above proposition of increased micellar size and lowering of micellar charge as the system moves towards CP. Two morphologies have been shown by DLS results. NMR data discussed earlier show the intercalation of pentyl chain(s) A plausible explanation is the assumption that the two *n*-pentyl chains would embedded towards the micellar interior while the remaining two pointed towards the aqueous phase [10,13,14]. The latter pentyl chains may connect micellar aggregates. However, each micelle has not been expected to involve in the process of micellar linking and can be the cause of formation of two different morphologies near CP though they are formed by the same components. However, higher aggregate sizes are chosen to compile Table 3. This is due the fact that bigger aggregates are distinctly contribute towards clouding. The reasons are discussed in detail in earlier study [12]. Fig. 4 show that there exists a well-defined value of [TPeAB] for a particular [12-4-12A]. The exact relationship between [TPeAB] and [12-4-12A] is depicted in Fig. 6. From the fit of the straight-line plot (Fig. 7), one can obtain the linear regression data (Table 4) which can be used to determine concentrations of gemini surfactant and surface active ionic liquid to get CP at the desired temperature. To see the influence of temperature on micellar structures, POM micrographs (Fig. 8) were obtained at room temperature, just below and at the CP. This study shows that size of the aggregates increases as the system approaches the CP. This observation has been in consonance with DLS results discussed above. This may be due to dehydration of the micellar surface region and the *n*-pentyl chain mediated linking of aggregates [10–12,43].

3.2.2. Effect of biocompatible additive on clouding behavior

Fig. 9 shows the variation of CP with cyclodextrin (CD) addition. Anionic gemini surfactant is expected to form an inclusion complex with

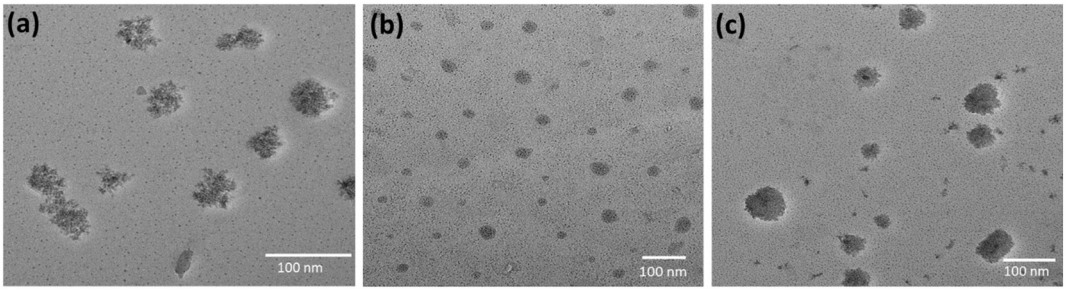

Fig. 11. Negative stained TEM images of aggregates of 2 mM 12-4-12-A with: (a) 80 mM TPeAB, (b) 38 mM TPeAB; (c) 38 mM TPeAB + 7.3 mM β-CD.

Table 6
PAHs solubilization parameters (molar solubilization ratio, MSR; micelle-aqueous phase partition coefficient, ln K_m) of 2 mM 12-4-12A + 80 mM TPeAB in aqueous solution at two different temperatures (T).

T (°C)	Anth	Anth-Pyr	Anth-Flu	Pyr	Pyr-Anth	Pyr-Flu	Flu	Flu-Anth	Flu-Pyr
MSR									
30.0	0.012	0.013	0.013	0.113	0.129	0.152	0.165	0.105	0.322
39.5	0.014	0.027	**0.031**	0.122	0.173	**0.203**	0.210	0.205	**0.388**
ln K_m									
30.0	8.08	8.07	8.17	10.4	10.14	10.12	10.88	10.49	10.37
39.5	8.27	8.24	9.18	10.3	10.16	10.15	11.13	10.62	10.50

CD's, affecting the aggregation process of the gemini itself [44]. For gemini surfactants, the stoichiometry of CD-surfactant complexes depends upon spacer chain length (of gemini) and cavity size (of CD) [45]. In a separate work, it has been shown that two-tailed surfactant interacts with CD *via* inclusion of one tail in the cavity [46]. These facts indicate that the two CDs behave differently when present in an aqueous surfactant solution. The CP behavior of 12-4-12A is also different (α-CD increases the CP while β-CD shows a reverse trend). Probably an extra –OH group together with large cavity size will bound more water and gemini monomers, respectively, and hence CP decreases with β-CD as can be seen in Fig. 9. Data hint towards the formation of a more hydrophobic complex with β-CD which can separate out at a lower temperature as indeed observed from the CP lowering effect. A similar type of CP decrease in presence of hydrophobic alkanols has been interpreted by taking hydrophobic interactions into consideration [47].

Fig. 10 shows the interplay of CP-[amino acid]. CP variation depends on the nature of amino acid. CP increases with a relatively hydrophobic amino acid (L phenylalanine), nearly constant with less hydrophobic (L leucine) and decreases with a hydrophilic amino acid (glycine). Each amino acid has similar functionalities with a structurally different side chain. In an earlier report, the rate of ninhydrin-amino acid reaction has been found to increase with the hydrophobicity of the amino acid [48]. Being a polar amino acid, glycine prefers headgroup region of the micelle and may replace head group region water with a concomitant decrease in CP. Contrary to this, other amino acids prefer micellar interior and can compete with the alkyl chains of surface active ionic liquid (TPeAB) present in the micellar interior. This would hinder the hydrophobic interaction of gemini alkyl chains and *n* pentyl chain of the TPeAB. Probably, this is responsible for constancy (with leucine) or increase in CP (with L phenylalanine).

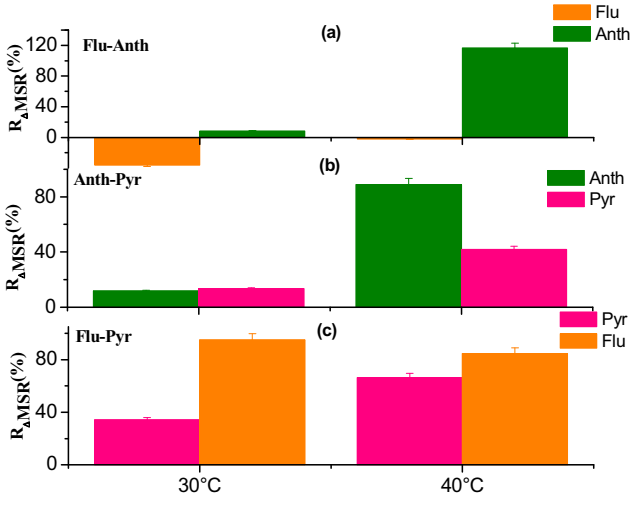

Fig. 12. Change in solubilization ($R_{\Delta MSR}$) % of individual PAH (in pair) at 30 °C and 40 °C (just below the CP) in 2 mM 12-4-12A+ 80 mM TPeAB system: (a) Anthracene (Anth) - Fluorene (Flu); (b) Anthracene (Anth) – Pyrene (Pyr); (c) Pyrene (Pyr) - Fluorene (Flu).

3.3. PAH solubilization studies in 12-4-12A + TPeAB with and without additives

3.3.1. Interplay of [12-4-12A], [TPeAB] and CP on single PAH solubilization

Based on CP variation (Fig. 6), sample (having CP at 40 °C) has been chosen for anthracene solubilization (Table 5) and to compare it at 30 °C (for the same system). Anthracene has been selected for solubilization as it has least aqueous solubility (among all the PAHs studied here) in aqueous, micellar and mixed micellar systems [22,49]. The idea behind this experiment (Table 5) was to exploit the advantages of the mixed system together with *clouding phenomenon* (and also temperature effect). It has been reported that hydrophobicity of the surfactant system has been found maximum just below the CP [11].

Data show that anthracene solubilization (MSR value) increases in the presence of TPeAB. MSR increases further as the system (1 mM 12-4-12A + 80 mM TPeAB) approaches the CP (40 °C). MSR, under the similar conditions (40 °C and 80 mM TPeAB), increases with [12-4-12A] to 2 mM. However, further increase of [12-4-12A] or [TPeAB] causes a decrease in anthracene MSR. This allows us to choose 2 mM 12-4-12A + 80 mM TPeAB system for the solubilization study of other PAHs at both the temperatures (30 °C and at just below CP (40 °C)). Again, pyrene and fluorene solubilization increases near CP as observed with anthracene. Therefore, CP has a distinct influence on solubilization phenomenon of PAHs which may be due to structural growth near CP as reported in our earlier studies [11,12].

3.3.2. Solubilization of PAHs in 12-4-12A + TPeAB + β cyclodextrin system

Recently, extraction of PAHs from soil has been reported in aqueous β cyclodextrin (β-CD). [30] Table 5 also shows MSR data related to solubilization of PAHs in the system, having CP 40 °C, adjusted by β-CD (which reduces the requirement of TPeAB to 38 mM). The system is greener (due to β-CD) and also showed better solubilization potential, for anthracene than the system containing 80 mM TPeAB, (Table 5). However, the system shows limitation towards pyrene solubilization. This may be due to different solubilization sites of anthracene and pyrene in the micellar system. Anthracene solubilizes in the outer region of the micellar interior while pyrene goes in the inner micellar core [50]. β-CD has several hydroxyl groups together with the hydrophobic region in the rim of the bucket type structure. Probably, due to above structural features, the β-CD system is more effective towards anthracene solubilization. To get insight about the morphologies present in the above two systems (with and without β-CD), TEM micrographs were acquired (Fig. 11). A system with β-CD shows more compact structures as compared to open fragmented/smaller structures seen in the sample without β-CD with 80 mM or 38 mM TPeAB. Probably these compact structures are responsible for higher MSR with anthracene. Moreover, such system may also find potential application for extracting thermo-responsive biological compounds such as vitamins, proteins, drugs, nucleotides *etc.* [51,52].

3.4. Co-solubilization of PAHs

Since PAH contaminated sites (*e.g.*, aquatic and soil matrix) contains a mixture of different PAHs, multiples PAHs solubilization can mimic the

situation for selective micellar solubilization from different PAHs. For the purpose, co-solubilization of three different pairs of PAHs selected and solubilization studies are performed in 2 mM 12-4-12A+ 80 mM TPeAB. The co-solubilization data are compiled in Table 6. Data show that solubilization of an individual PAH can increase or decrease on co-solubilization of another PAHs. As mentioned earlier, solubilization site of a particular PAH has a role to play in the co-solubilization of more than one PAH. If the solubilization site is common for the PAHs in the pair, the solubilization content of one of them may decrease. However, if the two PAHs has different micellar solubilization sites, their mutual presence may increase solubilization content due to increased hydrophobic interactions caused by the presence of PAHs (MSR mentioned in bold numbers). This indeed was observed in Table 6. Here, MSR values of anthracene increases in presence of pyrene and nearly remain constant in fluorene. However, fluorene MSR decreases in presence of anthracene than the without anthracene. Additionally, pyrene solubilization (singly or with other PAHs) shows a remarkable increase in presence of other PAHs. The increase was higher in case of fluorene than the anthracene. This may be due to higher MSR of fluorene in comparison of anthracene (single solubilization) which subsequently provide more hydrophobicity to the micelle and concomitant higher solubilization of pyrene. This indeed observed from our co-solubilization experiment (Table 6, and Fig. 12).

3.5. Extraction/adsorption of PAH

Anthracene solubilized systems with or without β-CD are used for the extraction process. Anthracene has been found to partition in SRP preferentially (Fig. 13) over surfactant lean phase (SLP). Almost all anthracene has been concentrated in SRP of the system without β-CD. The lower content of anthracene, in the β-CD containing system, may be due to the partitioning of β-CD both in SRP and SLP. β-CD in SLP can solubilized more anthracene and restrict it to go in SRP. This proposition may find support from the fact that β-CD contain several –OH groups which has certain preference for water and making it β-CD + water mixed solvent (probably less polar) and prefer to bind with anthracene as reported in a recent study. [30] SRP with extracted anthracene has been used to determine the adsorption potential of $GZrO_2$ nanocomposite. Fig. 13 show that no anthracene left in the diluted SRP solution indicating nearly complete adsorption on the composite. The information can be used for the possible degradation of anthracene from the adsorbed state (degradation data will be reported in the next communication). This may find support from a recent report in which graphene-Titanium oxide has been used to photodegrade polyaromatic hydrocarbon [53]. It is expected that present nanocomposite $GZrO_2$ exhibit advanced hybrid properties from both the constituent and have potential application in field of catalysis [54].

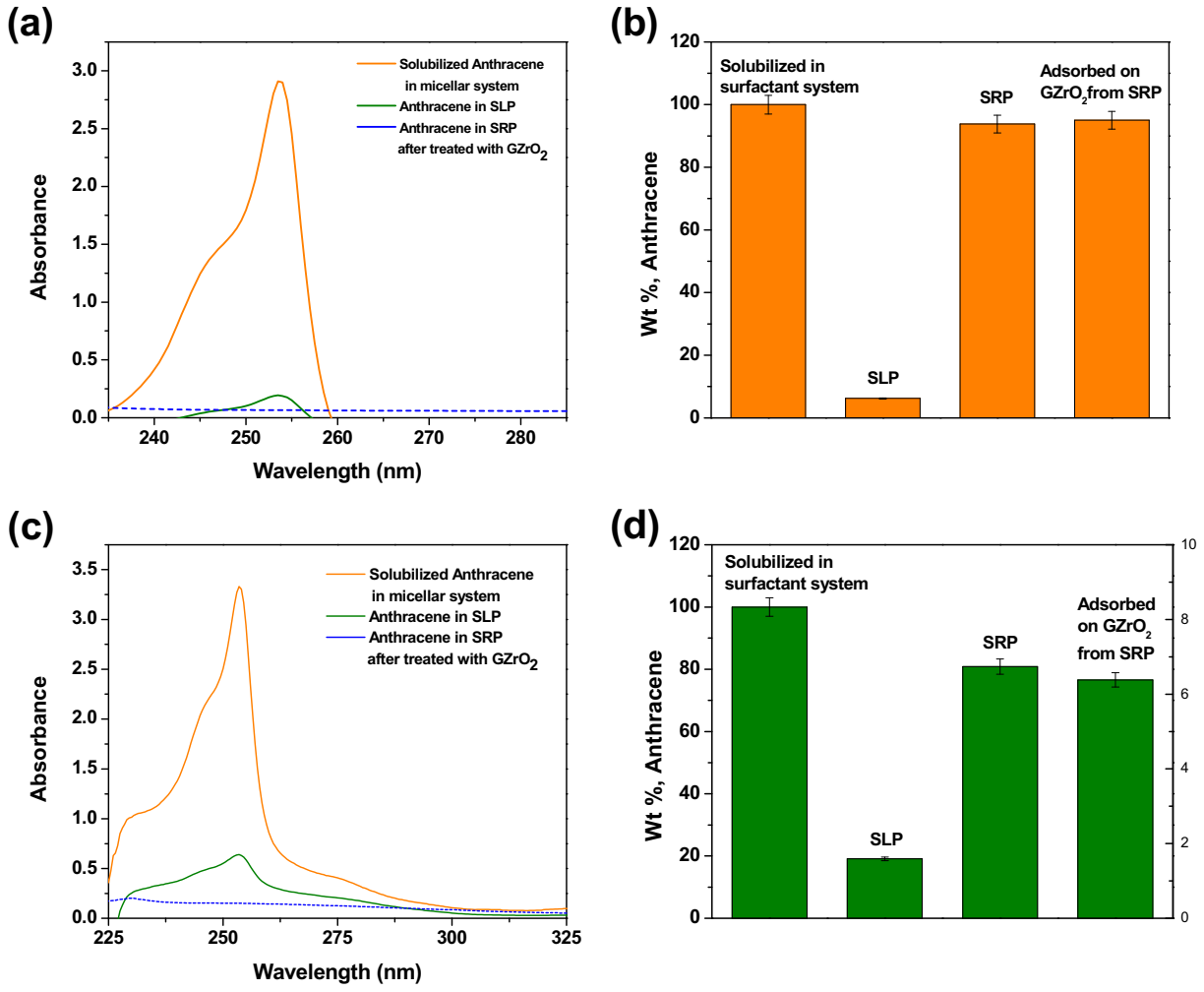

Fig. 13. UV spectra of Anthracene solubilization in: (a) 2 mM 12-4-12 A + 80 mM TPeAB and (b) 2 mM 12-4-12 A + 38 mM TPeAB + 7.3 mM β-CD; before (———), after phase separation in surfactant lean phase (———) and after adsorption on $GZrO_2$ nanocomposite from surfactant rich phase (·····).

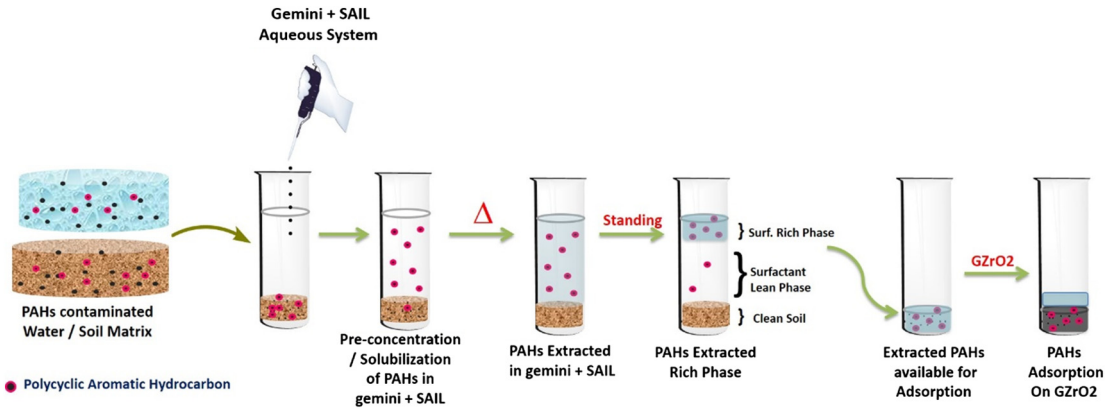

Scheme 1. Representation of extraction and degradation of PAHs.

4. Conclusion

This study was planned to exploit the positivity of the surfactant research such as (1) performance of gemini (anionic) over conventional surfactant, (2) synergism of mixed systems over individual ones, (3) CP observance with 12-4-12A (with a SAIL, TPeAB) (4) tuning of CP with biocompatible material (amino acid or cyclodextrine) (5) CP observance at ambient temperature (~40 °C) with lower [12-4-12 A] (2 mM) and [TPeAB] (38 mM, in presence of 7 mM β-CD) and (6) solubilization of PAHs at different temperatures. Interaction and morphologies of the aggregates are confirmed by ^{1}H NMR and POM/TEM studies. POM data show bigger aggregates near CP while TEM results show formation of compact aggregates in presence of β-CD. By adopting above strategies, it was possible to increase MSR for anthracene (least soluble PAH of the present study) from 0.012 to 0.031 (2.58 times). Similar increase was found with other PAHs. However, solubilization enhancement depends upon nature and site of solubilization of a particular PAH (singly or in mixture). The study may find potential applications in increasing the bioavailability of the hydrophobic material (PAHs, drugs, pesticides, organic pollutant *etc.*) and their subsequent biodegradation (Scheme 1) [55].

Acknowledgment

Authors are thankful to UGC-DAE CSR, Mumbai, India (CRS–M–204), for financial support. Ms. Sneha Singh is thankful for the project fellowship. The Head, Applied Chemistry Department, Faculty of Tech. & Engg., The Maharaja Sayajirao University of Baroda, Vadodara, India, is gratefully acknowledged for research facilities.

Conflict of interest

The authors declared that there is no conflict of interest.

Appendix A. Supplementary data

Supplementary data to this article can be found online at https://doi.org/10.1016/j.molliq.2018.09.022.

References

[1] Z. Liu, Y. Fan, M. Tian, R. Wang, Y. Han, Y. Wang, Surfactant selection principle for reducing critical micelle concentration in mixtures of oppositely charged gemini surfactants, Langmuir 30 (2014) 7968–7976.
[2] W.H. Ansari, N. Fatma, M. Panda, Solubilization of polycyclic aromatic hydrocarbons by novel biodegradable cationic gemini surfactant ethane 1, 2 diyl bis (N, N dimethyl N hexadecylammoniumacetoxy) dichloride and its binary mixtures with conventional surfactants, Soft Matter 9 (2013) 1478–1487.
[3] S. Kumar, D. Sharma, Kabir-ud-din, Micellization of sodium dodecyl benzenesulfonate in aqueous quaternary bromides, J. Surf. Sci. Technol. 18 (2002) 25–33.
[4] S. Kumar, H. Patel, S.R. Patil, Test of Hofmeister-like series of anionic headgroups: clouding and micellar growth, Colloid Polym. Sci. 291 (2013) 2069–2077.
[5] D. Xie, J. Zhao, Cloud point phenomena in aqueous solutions of an anionic gemini surfactant with a dibenzene spacer in the presence of tetra n propyl ammonium bromide, RSC Adv. 6 (2016) 27031–27038.
[6] F.A. Vicente, I.S. Cardoso, T.E. Sintra, J. Lemus, E.F. Marques, S.P. Ventura, J.A. Coutinho, Impact of surface active ionic liquids on the cloud points of nonionic surfactants and the formation of aqueous micellar two-phase systems, J. Phys. Chem. B 121 (2017) 8742–8755.
[7] P. Mukherjee, S.K. Padhan, S. Dash, S. Patel, B.K. Mishra, Clouding behaviour in surfactant systems, Adv. Colloid Interf. Sci. 162 (2011) 59–79.
[8] S. Kumar, D. Sharma, Kabir-ud-Din, Temperature−[salt] compensation for clouding in ionic micellar systems containing sodium dodecyl sulfate and symmetrical quaternary bromides, Langmuir 19 (2003) 3539–3541.
[9] A. Klaus, G.J. Tiddy, R. Rachel, A.P. Trinh, E. Maurer, D. Touraud, W. Kunz, Hydrotrope-induced inversion of salt effects on the cloud point of an extended surfactant, Langmuir 27 (2011) 4403–4411.
[10] B.L. Bales, R. Zana, Cloud point of aqueous solutions of tetrabutylammonium dodecyl sulfate is a function of the concentration of counterions in the aqueous phase, Langmuir 20 (2004) 1579–1581.
[11] S. Kumar, A. Bhadoria, H. Patel, V.K. Aswal, Morphologies near cloud point in aqueous ionic surfactant: scattering and NMR studies, J. Phys. Chem. B 116 (2012) 3699–3703.
[12] A. Bhadoria, S. Kumar, V.K. Aswal, S. Kumar, Mechanistic approach on heat induced growth of anionic surfactants: a clouding phenomenon, RSC Adv. 5 (2015) 23778–23786.
[13] S. Kumar, D. Sharma, Kabir-ud-Din, Cloud point phenomenon in anionic surfactant + quaternary bromide systems and its variation with additives, Langmuir 16 (2000) 6821–6824.
[14] M. Almgren, S. Swarup, Size of sodium dodecyl sulfate micelles in the presence of additives. 3. Multivalent and hydrophobic counterions, cationic and nonionic surfactants, J. Phys. Chem. B 87 (1983) 876–881.
[15] S. Kumar, A.Z. Naqvi, Kabir-ud-Din, Micellar morphology in the presence of salts and organic additives, Langmuir 16 (2000) 5252–5256.
[16] S. Kumar, A.Z. Naqvi, Kabir-ud-Din, Solubilization-site-dependent micellar morphology: effect of organic additives and quaternary ammonium bromides, Langmuir 17 (2001) 4787–4792.
[17] T. Pantsyrnaya, S. Delaunay, J.-L. Goergen, E. Guseva, J. Boudrant, Solubilization of phenanthrene above cloud point of Brij 30: a new application in biodegradation, Chemosphere 92 (2013) 192–195.
[18] F.A. Vicente, L.P. Malpiedi, F.A. Silva, A. Pessoa, J.A. Coutinho, S.P. Ventura, Design of novel aqueous micellar two-phase systems using ionic liquids as co-surfactants for the selective extraction of (bio) molecules, Sep. Purif. Technol. 135 (2014) 259–267.
[19] S. Liu, C. Guo, X. Liang, F. Wu, Z. Dang, Nonionic surfactants induced changes in cell characteristics and phenanthrene degradation ability of *Sphingomonas* sp. GY2B, Ecotoxicol. Environ. Saf. 129 (2016) 210–218.
[20] S. Lamichhane, K.B. Krishna, R. Sarukkalige, Surfactant-enhanced remediation of polycyclic aromatic hydrocarbons: a review, J. Environ. Manag. 199 (2017) 46–61.
[21] S.K. Yadav, K. Parikh, S. Kumar, Mixed micelle formation of cationic gemini surfactant with anionic bile salt: a PAH solubilization study, Colloids Surf. A Physicochem. Eng. Asp. 522 (2017) 105–112.
[22] S.K. Yadav, K. Parikh, S. Kumar, Solubilization potentials of single and mixed oppositely charged gemini surfactants: a case of polycyclic aromatic hydrocarbons, Colloids Surf. A Physicochem. Eng. Asp. 514 (2017) 47–55.
[23] S. Singh, A. Bhadoria, K. Parikh, S.K. Yadav, S. Kumar, V.K. Aswal, S. Kumar, Self-assembly in aqueous oppositely charged gemini surfactants: a correlation between morphology and solubilization efficacy, J. Phys. Chem. B 121 (2017) 8756–8766.
[24] X. Liang, M. Zhang, C. Guo, S. Abel, X. Yi, G. Lu, C. Yang, Z. Dang, Competitive solubilization of low-molecular-weight polycyclic aromatic hydrocarbons mixtures in single and binary surfactant micelles, Chem. Eng. J. 244 (2014) 522–530.

[25] R. Oda, I. Huc, M. Schmutz, S. Candau, F. MacKintosh, Tuning bilayer twist using chiral counterions, Nature 399 (1999) 566.
[26] G.C. Kalur, S.R. Raghavan, Anionic wormlike micellar fluids that display cloud points: rheology and phase behavior, J. Phys. Chem. B 109 (2005) 8599–8604.
[27] X. Ji, M. Tian, Y. Wang, Temperature-induced aggregate transitions in mixtures of cationic ammonium gemini surfactant with anionic glutamic acid surfactant in aqueous solution, Langmuir 32 (2016) 972–981.
[28] K. Parikh, B. Mistry, S. Jana, S. Gupta, R.V. Devkar, S. Kumar, Physico-biochemical studies on cationic gemini surfactants: role of spacer, J. Mol. Liq. 206 (2015) 19–28.
[29] M. Jansson, A. Jönsson, P. Li, P. Stilbs, Aggregation in tetraalkylammonium dodecanoate systems, Colloids Surf. A Physicochem. Eng. Asp. 59 (1991) 387–397.
[30] M. Sánchez-Trujillo, E. Morillo, J. Villaverde, S. Lacorte, Comparative effects of several cyclodextrins on the extraction of PAHs from an aged contaminated soil, Environ. Pollut. 178 (2013) 52–58.
[31] F.A. Vicente, L.D. Lario, A. Pessoa Jr., S.P. Ventura, Recovery of bromelain from pineapple stem residues using aqueous micellar two-phase systems with ionic liquids as co-surfactants, Process Biochem. 51 (2016) 528–534.
[32] K. Materna, E. Goralska, A. Sobczynska, J. Szymanowski, Recovery of various phenols and phenylamines by micellar enhanced ultrafiltration and cloud point separation, Green Chem. 6 (2004) 176–182.
[33] R.A.K. Rao, S. Singh, B.R. Singh, W. Khan, A. Naqvi, Synthesis and characterization of surface modified graphene–zirconium oxide nanocomposite and its possible use for the removal of chlorophenol from aqueous solution, J. Environ. Chem. Eng. 2 (2014) 199–210.
[34] Y. Moroi, K. Mitsunobu, T. Morisue, Y. Kadobayashi, M. Sakai, Solubilization of benzene, naphthalene, anthracene, and pyrene in 1 dodecanesulfonic acid micelle, J. Phys. Chem. 99 (1995) 2372–2376.
[35] R.A. Friedel, M. Orchin, Ultraviolet Spectra of Aromatic Compounds, Wiley, New York, 1951.
[36] P. Holland, D. Rubingh, Nonideal multicomponent mixed micelle model, J. Phys. Chem. 87 (1983) 1984–1990.
[37] J.H. Clint, Micellization of mixed nonionic surface active agents, J. Chem. Soc., Faraday Trans. 1 Phys. Chem. Condens. Phases 71 (1975) 1327–1334.
[38] D. Rubingh, K.L. Mittal, Solution Chemistry of Surfactants, Plenum Press, New York, 1979.
[39] K. Motomura, M. Yamanaka, M. Aratono, Thermodynamic consideration of the mixed micelle of surfactants, Colloid Polym. Sci. 262 (1984) 948–955.
[40] L. Liu, M.J. Rosen, The interaction of some novel diquaternary gemini surfactants with anionic surfactants, J. Colloid Interface Sci. 179 (1996) 454–459.
[41] Z.M. He, P.J. O'Connor, L.S. Romsted, D. Zanette, Specific counterion effects on indicator equilibria in micellar solutions of decyl phosphate and lauryl sulfate surfactants, J. Phys. Chem. 93 (1989) 4219–4226.
[42] U. Thapa, J. Dey, S. Kumar, P. Hassan, V. Aswal, K. Ismail, Tetraalkylammonium ion induced micelle-to-vesicle transition in aqueous sodium dioctylsulfosuccinate solutions, Soft Matter 9 (2013) 11225–11232.
[43] D. Sharma, Z.A. Khan, V. Aswal, S. Kumar, Clouding phenomenon and SANS studies on tetra n butylammonium dodecylsulfate micellar solutions in the absence and presence of salts, J. Colloid Interface Sci. 302 (2006) 315–321.
[44] E. Junquera, G. Tardajos, E. Aicart, Effect of the presence of beta.-cyclodextrin on the micellization process of sodium dodecyl sulfate or sodium perfluorooctanoate in water, Langmuir 9 (1993) 1213–1219.
[45] A.J. Valente, O. Söderman, The formation of host–guest complexes between surfactants and cyclodextrins, Adv. Colloid Interf. Sci. 205 (2014) 156–176.
[46] R. Palepu, J.E. Richardson, V.C. Reinsborough, Binding constants of. Beta.-cyclodextrin/surfactant inclusion by conductivity measurements, Langmuir 5 (1989) 218–221.
[47] T. Ahmad, S. Kumar, Z.A. Khan, Additives as CP modifiers in an anionic micellar solution, Colloids Surf. A Physicochem. Eng. Asp. 294 (2007) 130–136.
[48] A. Kabir-ud-Din, J.K. Salem, S. Kumar, Z. Khan, Effect of cationic surfactants on the addition-elimination type interaction between aspartic acid and ninhydrin, Colloids Surf. A Physicochem. Eng. Asp. 168 (2000) 241–250.
[49] J. Lakra, D. Tikariha, T. Yadav, S. Das, S. Ghosh, M.L. Satnami, K.K. Ghosh, Mixed micellization of gemini and cationic surfactants: physicochemical properties and solubilization of polycyclic aromatic hydrocarbons, Colloids Surf. A Physicochem. Eng. Asp. 451 (2014) 56–65.
[50] N. Fatma, M. Panda, W.H. Ansari, Solubility enhancement of anthracene and pyrene in the mixtures of a cleavable cationic gemini surfactant with conventional surfactants of different polarities, Colloids Surf. A Physicochem. Eng. Asp. 467 (2015) 9–17.
[51] S. Kumar, M.S. Alam, N. Parveen, Influence of additives on the clouding behavior of amphiphilic drug solutions, Colloid Polym. Sci. 284 (2006) 1459–1463.
[52] A.S. Yazdi, Surfactant-based extraction methods, Trends Anal. Chem. 30 (2011) 918–929.
[53] H. Bai, J. Zhou, H. Zhang, G. Tang, Enhanced adsorbability and photocatalytic activity of TiO2-graphene composite for polycyclic aromatic hydrocarbons removal in aqueous phase, Colloids Surf. B: Biointerfaces 150 (2017) 68–77.
[54] B.R. Singh, M. Shoeb, W. Khan, A.H. Naqvi, Synthesis of graphene/zirconium oxide nanocomposite photocatalyst for the removal of rhodamineB dye from aqueous environment, J. Alloys Compd. 651 (2015) 598–607.
[55] A. Rodrigues, R. Nogueira, L.F. Melo, A.G. Brito, Effect of low concentrations of synthetic surfactants on polycyclic aromatic hydrocarbons (PAH) biodegradation, Int. Biodeterior. Biodegrad. 83 (2013) 48–55.